Master Thesis

Flame extension for pool fires under ceiling at various heights

Mats Flo

Masteroppgave i prosessteknologi
Institutt for fysikk og teknologi
Universitetet i Bergen

2015

Abstract

Spill and ignition of flammable fuel can occur. The following fire can be free burning or affected by nearby objects, such as overlying ceiling (or similar) that do not let flames through. When a flame impinges on a ceiling, the gases will spread out radially (1) and establish extending flames under the ceiling. Heat distribution is dissimilar to free burning fires.

How do flame extension length, mass flux, heat flux on the side of the fuel bed, rim temperature and liquid temperature correlate to the ceiling height above pool fires? Results give correlations useful in estimating mentioned parameters in the future.

It is constructed an apparatus assigned pool fires with constant surface area of burning heptane and methanol liquid under a height adjustable ceiling. It is performed experiments by two squared burners with sizes of 0.25 and 0.40 m. Supply of fuel into the burner is equal to the fuel evaporated, which give constant liquid height related to both ceiling and burner rim. Flame images processed in MatLab is used to obtain flame lengths.

Result contains obtained flame length, mass flux, heat flux and temperatures from various ceiling heights. The conclusion come out with an equation for estimating length of an extending flame under a ceiling.

Summery

It is constructed apparatus to perform pool fire experiments from burning heptane and methanol at steady state. The length of extending flames under ceiling is investigated and the work is focused on finding a correlation between flame length and ceiling height. The following aspects are looked at:

- The highest ceiling level where flame extends horizontally.
- The length of extending flame under ceiling.
- Heat flux.
- Mass flux.
- Liquid and burner rim temperature.

Heptane pool fire from a squared burner with size 0.25 m give result of flame extension lengths under ceiling at various heights. An equation is developed to estimate flame extension lengths from pool fires under ceiling in the future.

Foreword

This thesis is compiled on the college Stord / Haugesund through a masters issued by the university in Bergen. The fire laboratory in Haugesund has been the working area for many weeks where the design and building have taken place. Thanks to the good help from the laboratory staff, and the access and quality of all the equipment.

A great thanks to:

- Bjarne Christian Hagen for great supervising and feedback on my work.
- Fredrik Hemmingson for letting me use his camera equipment.
- David Johansen for great supervising regarding image processing in Matlab.
- Arjen Kraijeveld for assistance and preparations in the laboratory.
- Ingunn Haraldseid for motivation and feedback on my work.

Definitions

Plume – When a mass of hot gases is surrounded by colder gases, the hotter and less dense mass will rise upward due to the density difference, or rather, due to buoyancy. This is what happens above a burning fuel source, and the buoyant flow, including any flames, is referred to as a fire plume (2).

Flame impingement – The striking of flame against an object, in this work the ceiling.

Register

1. Introduction

1.1. Background

It is developed equations that allow us to predict the flame height of free burning pool fires. One of the most useful equations is presented by Heskestad (2). In many situations, free burning fires is not the occurring situation, but fires affected by nearby objects, such as an overlying ceiling (or similar) that does not let the flame through.

When a flame impinges on a ceiling, the gases will spread out radially and entrain air for combustion, and a circular flame will be established under the ceiling (2). There is limited research conducted on flame extension under ceilings regarding pool fires. More research is needed.

The phenomenon of flame extension was first investigated by Hinkley *et. al.* (1968) (3), who studied the deflection of diffusion flames (4). Heskestad & Hamada (5) and You and Faeth (6) carried out flame extension experiments. Finding work implementing flame extension under ceiling performed by pure liquid as fuel, is difficult. Most of the work is performed by gas as fuel where the desired burning rate is set by the gas flow. You and Faeth used liquid as fuel in some of their experiments. The fire source was simulated by burning wicks soaked with liquid fuel (methanol, ethanol, l-propanol and n-pentane) (1), not pure liquid.

In this work it is used pure liquid as fuel, where the burning rate is defined by the size of the burner and steady state.

1.2. Objectives

Pool fire experiments are performed to investigate the affection of mounting a ceiling at variable heights above the fire. The following aspects will be looked at:

- The highest ceiling height where flame extends horizontally.
- The length of extending flame under ceiling.
- Mass flux.
- Liquid and burner rim temperature.
- Heat radiation.

The main goal is to:

- Build necessary apparatus, which enables an adjustable ceiling height and a constant liquid surface height to achieve steady state.
- Find a correlation between flame height and flame extension length.
- Find a correlation between flame extension and heat flux.

1.3. Intensions

The intension is to investigate the flame extension under the ceiling, and the interactions between the mentioned parameters (see section 1.2) when the ceiling is mounted at various heights, using liquid as fuel. Parameters are measured at the same time. The liquid surface height relative to the rim of the burner is kept constant; meaning that the fuel supply is equal to the fuel evaporated.

1.4. Limitations

The thesis is limited to experiments performed with heptane and methanol liquid burning in two burners with sizes 0.25 x 0.25 and 0.40 x 0.40 m. The heat release from the fires is within 10 and 100 kW. Ceiling is incombustible and made of an insulating material.

2. Pool fires

2.1. Character and structure of pool fires

Accidental spills of liquid fuels in industrial process and power plant systems can pose a serious fire hazard. Once ignited, very rapid flame spread will occur over the liquid spill surface. In free burn conditions, the burning rate will quickly reach a constant value, depending on the diameter of the spill (2).

Many common fire scenarios can be classified as pool fires. These include fires ranging in size from a cigarette lighter, where D is approximately 10^{-3}m, to a forest fire, where D can be as large as 10^{5}m. A pool fire is defined as a buoyant diffusion flame in which the fuel is configured horizontally. Although the name implies that the fuel is a liquid it may be a gas or a solid. The fuel bed may be of an arbitrary geometry, but for simplicity, most studies consider a circular configuration characterized by a single geometrical scale, the pool diameter (D) (7).

Beyond obvious differences in length scale, fire hazard can be characterized in terms of the combustion kinetics of a fuel such as resistance to suppression, flash point temperature, or lower flammability limits, or in terms of heat transfer during combustion, which can be characterized by the total heat release rate, the flame spread rate, or the power radiated to the surroundings (7).

Fire hazard can be modified by ambient conditions such as the absence or presence of an enclosure, a hot surface, wind, currents, or ventilation. These conditions play a role in governing both the detailed structure and the overall hazard of a fire (7).

2.2. Flame characteristics and shape

2.2.1. Flame definition

In most fire safety engineering applications we are concerned with the so-called buoyant, turbulent diffusion flame (2).

Diffusion flames refer to the case where fuel and oxygen are initially separated, and mix through the process of diffusion. Burning and flaming occur where the concentration of the mixture is favorable to combustion. Although the fuel and the oxidant may come together through turbulent mixing, the underlying mechanism is molecular diffusion. This is the process in which molecules are transported from a high to low concentration. Flames in accidental fires are nearly always characterized as diffusion flames. Very small diffusion flames can be laminar, such as the flame on a candle (2).

When a mass of hot gases is surrounded by colder gases, the hotter and less dense mass will rise upward due to the density difference, or rather, due to buoyancy. The upward velocity of the flow within a flame will be dominated by the buoyancy force if the velocity at which the fuel is injected is not exceptionally high (2).

2.2.2. Fluctuation

Larger diffusion flames are turbulent and will fluctuate with periodic oscillations with large eddies shedding at the flame edge, as shown in Figure 2.1Figure 2.2.

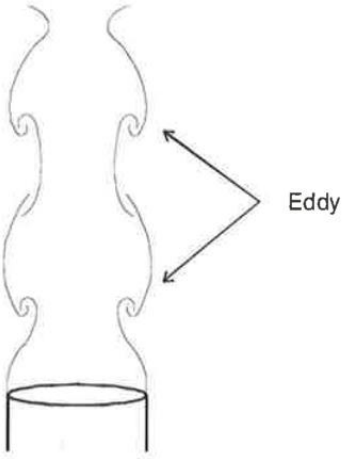

Figure 2.1: Flame fluctuations due to eddy shedding.

The eddies, which are visible in turbulent plumes (more so in momentum-driven plumes than in buoyancy driven ones), roll up along the outside of the plume and are a result of the instability between the hot flame and the cold air (2).

These random fluctuations, which are characteristic of turbulence, will give rise to periodic flame height (and shape) fluctuations. The fluctuations normally have a frequency of the order of 1-3 Hz, i.e., will occur between one and three times per second; in general, this shedding depends on fire diameter. Figure 2.2 shows a characteristic sketch of this phenomenon where L_f is the visible flame height as a function of time (2).

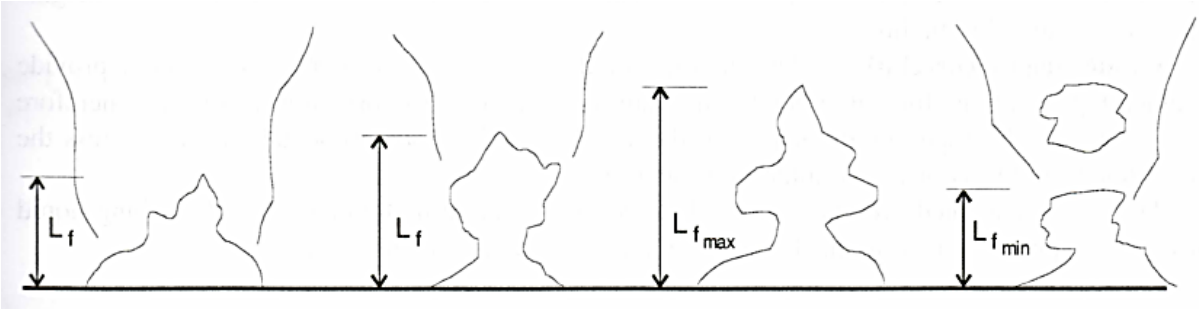

Figure 2.2 Fluctuation influences on the free burning flame height, L_f.

2.2.3. Flame height and length

The flame height is generally defined as the height at which the flame is observed at or above that height 50% of the time. Visual observation tends to yield slight overestimates of flame heights (8).

In order to provide engineering equations allowing calculation of the flame height, we must first define the mean flame height. This is most conveniently done by averaging the visible flame height over time. The luminosity of the lower part of the flaming region appears fairly steady. The upper part fluctuates or, in other words, is intermittent (2).

The graph in

Figure 2.3 is generally used to define the mean flame height (2).

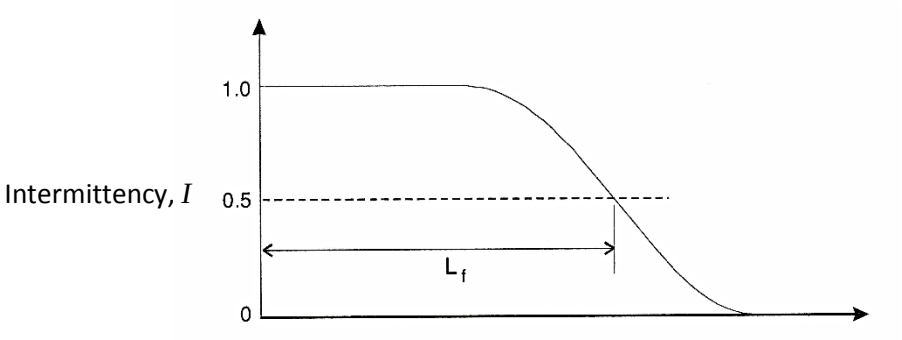

Figure 2.3 Definition of mean flame height.

The intermittency, denoted I, is shown on the vertical axis, where a value of 1 indicates the appearance of the flame at all times. The horizontal axis shows the distance above the fire source, z. The height at which the intermittency is 0.5, i.e., the height above which flame appears half the time, is defined as the mean flame height, *L* (2).

Videotape analysis seems to provide the best estimates, though averaging a number of one-second-exposure photographs seems to work acceptably (8).

In this work it is only considered time-mean results. The mean flame height, denoted L_f, is given in meters and refers to the vertical length for free burning fires (no ceiling). The flame length, r_f, is referring to the horizontal, radial flame length when the flame is deflected under a ceiling. Flame probability plots conducted by using Matlab, handles the time-mean results. It is assumed that the time-mean flame height, or length, appears where the flame probability is 0.5. It is given more information about this method in section 3.3.6.

2.2.4. Flame shape

Rasbash *et al.* (1956) made a detailed study of the flames above 30 cm diameter pools of alchohol, benzene, kerosene, and petrol. Their apparatus is shown in Figure 2.4 (4).

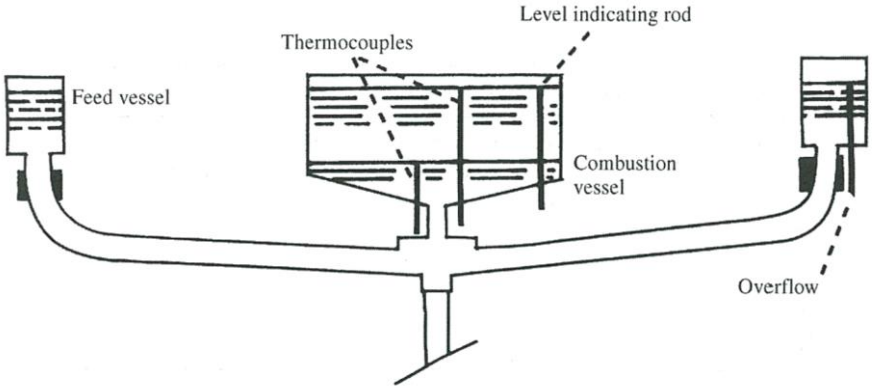

Figure 2.4: Details of the apparatus used by Rasbash *et* al. in 1956 to study liquid pool fires (4).

The pale blue alcohol flame burns very close to the surface, apparently touching it as shown in Figure 2.5, while with other fuels there is a discernible vapor zone immediately above the liquid (3). Heptane flame is more similar to the shape shown in Figure 2.6 further down on this page.

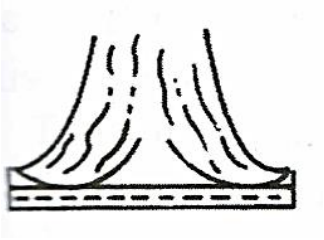

Figure 2.5 Shape of the blue alcohol flame (like methanol) immediately above the liquid surface (Rasbash et al. 1956) (4).

A buoyant axisymmetric plume will form above a fire. Along with the vertical centerline of the plume, it is assumed an axis of symmetry (2). In order to sustain an axisymmetric plume, there must be no interferences of the flame by for example close obstacles, moving air, nearby walls, ceilings etc.

The axisymmetric fire plume is conventionally divided into the three zones as shown below:

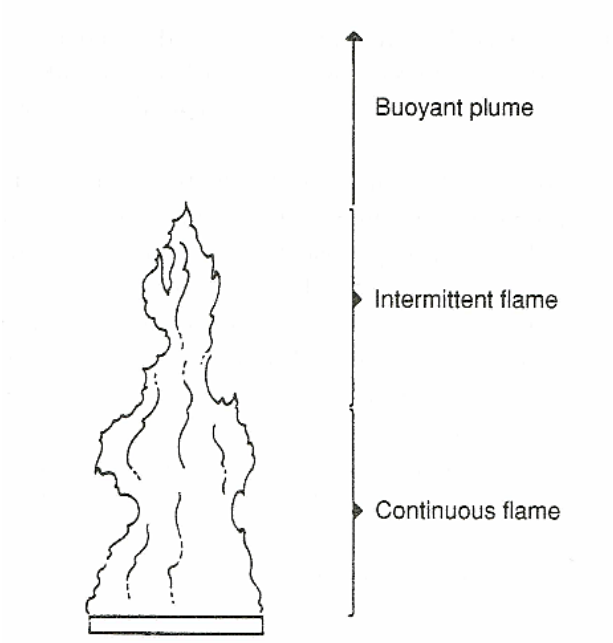

Figure 2.6 The three zones of the axisymmetric buoyant plume (adapted from McCaffrey) (2).

In the continuous flame zone the upward velocity is near zero at the base and increases with height. In the intermittent flame zone the velocity is relatively constant, and in the far field zone the velocity decreases with height (2).

2.2.5. Free burning and burning under ceilings

A free burning flame rises upwards by thermal buoyancy forces. The heat dissipates in the upwards direction with no obstructions. Burning under ceilings gives significant different flames.

When a flame impinges on a ceiling, the gases will spread out radially and entrain air for combustion, and a circular flame will be established under the ceiling (2). See Figure 2.7.

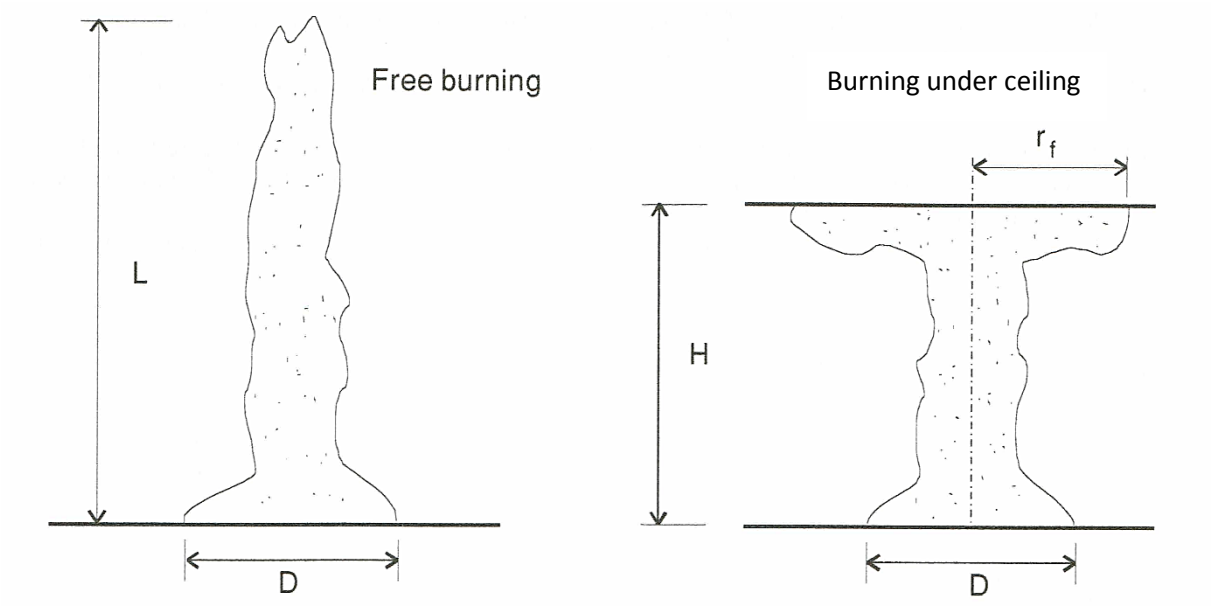

Figure 2.7 Sketch of the radial flame extension when burning under a ceiling (b), compared with free burning (a) (2).

Figure 2.7 gives a picture of important variables to be considered in research on flames happening under ceilings:

- D is the diameter of the liquid surface [m].
- r_f is the radial flame extension under the ceiling [m].
- H is the vertical height from the liquid surface to the ceiling [m].
- L is the vertical flame height during free burning.

Heskestad developed an equation for the ratio between mean flame height and liquid diameter (9):

$$\frac{L}{D} = 3.7\dot{Q}^{*2/5} - 1.02 \qquad \text{Eq. 2.1}$$

Where $\dot{Q}^*$ is a non-dimensional energy release rate, used to control the geometry of fire plumes. This equation can be used in determining a free-burning mean flame height (L), written in the form:

$$L = 3.7\dot{Q}^{2/5} - 1.02D \qquad \text{Eq. 2.2}$$

Where $\dot{Q}$ is the energy release given in kilowatts [kW].
You and Faeth carried out, through their experiments and analysis, an approximate expression for the radial flame extension under a ceiling, divided by the diameter of the fuel source diameter (6):

$$\frac{r_f}{D} = 0.5\left(\frac{L-H}{D}\right)^{0.96} \qquad \text{Eq. 2.3}$$

The equation is intended only for very rough estimates since the experiments it is based on were carried out with small flames, small heights, and low energy release rates. The exponent is close to one. A simplified way of thinking to get a clearer picture of the context, gives:

$$r_f < 0.5(L - H)$$ Eq. 2.4

The fire was fueled by natural gas, flowing from a cylindrical burner tube. The natural gas was largely methane. The burner tube had an inside diameter of 55 mm and was packed with stainless steel wool and screens in order to provide a uniform exit velocity. The test flames attached naturally at the exit of the burner. A water-cooled ceiling, 1000 mm in diameter, was positioned concentrically with the burner tube, 400 mm above it's exit (6).

Heskestad and Hamada investigated ceiling jets of strong fire plumes by using propane burners of three different sizes (D=0.30, 0.15 and 0.61m). Experiments were within energy release rates between 93 – 760 kW (5). An average flame extension was found:

$$r_f = 0.95(L - H)$$ Eq. 2.5

The constant 0.95 is an average of values between 0.88 – 1.05. The number of experiments carried out are 15, but only seven corresponded to cases where flames touch and flare out under the ceiling (5). This calls for more research on this topic.

2.3. Heat transfer

Within a pool fire there is a heat source, which is generated in the flame itself. The heat is transferred to the surroundings by three different modes; conduction, convection and radiation. Part of the heat produced by the flame will be transported back to the fuel by these three modes. It is given more information about these three aspects shown in Figure 2.9:

The heat flux from the flame to the fuel surface ($\dot{Q}''_F$) is the sum of three terms (4):

$$\dot{Q}''_F = \dot{Q}''_{conduction} + \dot{Q}''_{convection} + \dot{Q}''_{radiation} \quad \textbf{Eq. 2.6}$$

Where:
$\dot{Q}''_{conduction}$ is the heat flux through conduction.
$\dot{Q}''_{convection}$ is the heat flux through convection.
$\dot{Q}''_{radiation}$ is the heat flux through radiation.

$\dot{Q}''_{radiation}$ takes into account surface re-radiation, which would normally be considered as part of $\dot{Q}''_L$ (see section 0).

2.3.1. Conduction

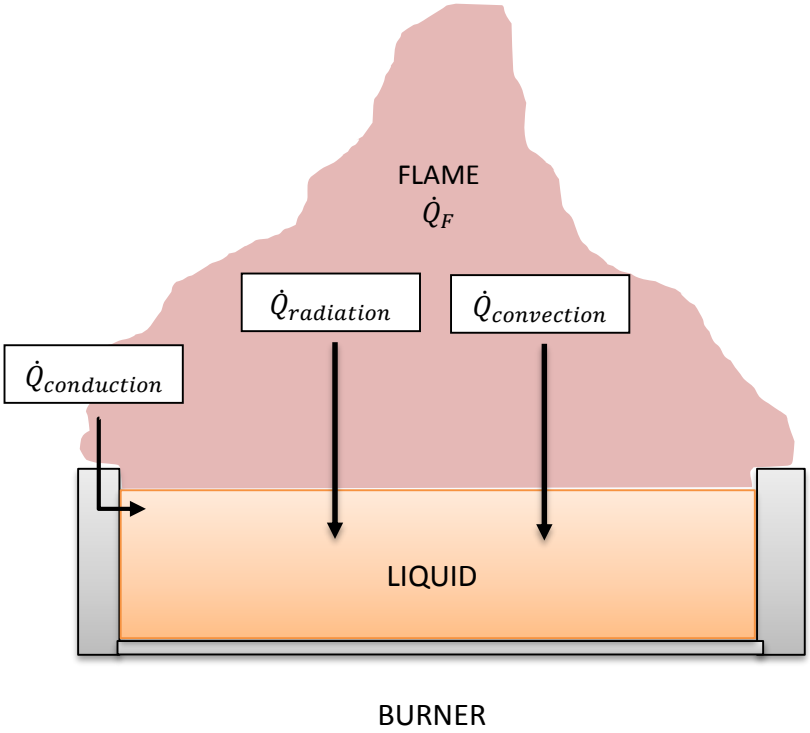

Figure 2.8 Illustration on how some of the energy produced by the flame is transported back to the fuel.

In pool fires, conductive heat transfer is mostly represented within the solids, which the containment of the liquid is made of; the rim, sidewall and bottom of the burner. In the case where a liquid is spilled on the ground, the ground will represent the solid which heat is conducted trough. The thermal conductivity of the solid material defines how well the heat is conducted.

One directional conductive heat flux, denoted $\dot{q}''_x$, is given by (4):

$$\dot{q}_x'' = -k\frac{\Delta T}{\Delta x}$$ **Eq. 2.7**

Where:
ΔT is the temperature over the distance [K]
Δx is the distance between temperature differences [m].
k is the thermal conductivity [$W/m \cdot K$]

Hottel *et* al. represented conductive heat transfer to the pool surface in terms of global flame properties as (10):

$$\dot{Q}_{s,conduction} = k'\pi D(T_f - T_s)$$ **Eq. 2.8**

Where:
k' is a conduction coefficient. (A constant, which incorporates a number of heat transfer, terms (4)).
D is the pool diameter.
T_f is the flame temperature.
T_s is the pool surface temperature.

2.3.2. Convection

Convection is associated with the transfer of heat by motion of a liquid. In a free burning fire, most of the heat released is carried away from the burning surfaces by buoyancy-induced convective flows (4).

The empirical relationship first discussed by Newton is (4):

$$\dot{q}'' = h\Delta T \text{ [W/m}^2\text{]}$$ **Eq. 2.9**

where:
h is the convective heat transfer coefficient [W/m·K]

This equation defines *h,* which, unlike thermal conductivity, is not a material constant. It depends on the characteristics of the system, the geometry and orientation of the solid and the properties of the fluid, including the flow parameters. In addition, it is also a function of *ΔT* (4).

Hottel *et* al. represented convective heat transfer to the pool surface in terms of global flame properties as (10):

$$\dot{Q}_{s,convection} = hA_s(T_f - T_s)$$ **Eq. 2.10**

Where:
A_s is the pool surface area.
T_f is the flame temperature.
T_s is the pool surface temperature.

2.3.3. Radiation

Radiation is a term given to the transfer of energy trough space by electromagnetic waves. If radiation is passing through empty space, it is not transformed to heat or any other form of energy, nor is it diverted from its path. If, however, the matter appears in its path, the radiation will be transmitted, reflected, or absorbed. It is only the absorbed energy that appears as heat, and this transformation is quantitative (11).

The properties of reflectivity, absorptivity, and transmissivity represent the fractions of incident energy reflected, absorbed, and transmitted, respectively. All of these properties depend on the material, the wavelength of the incident energy, and the materials temperature (2).

Emissivity (ε) is a measure of the efficiency of the surface as a radiator. The perfect emitter – the black body – has an emissivity of unity. The intensity of radiant energy ($\dot{q}''$) falling on a surface remote from the emitter can be found by using the appropriate 'configuration factor' (ϕ), which takes into account the geometrical relationship between the emitter and the receiver (4).

According to the Stefan-Boltzmann equation, the total energy emitted by a body is proportional to T^4, where T is the temperature in Kelvin. The total emissive power is expressed as (4)

$$E = \varepsilon\sigma T^4 \qquad \textbf{Eq. 2.11}$$

where:
σ is the Stefan-Boltzmann constant ($5.67 \cdot 10^{-8}$ W/m^{2}K^4)
ε is the emissivity.

Combined with the configuration factor there is:

$$\dot{q}'' = \phi\varepsilon\sigma T^4 \qquad \textbf{Eq. 2.12}$$

This equation gives the total radiation emitted by unit area of grey surface into the hemisphere above it (4), which represent an external energy transfer, (R_0 in figure Figure 2.10).

Hottel *et* al. represented radiative heat transfer to the pool surface in terms of global flame properties as (10):

$$\dot{Q}_{s,radiation} = \sigma V A_s({T_f}^4 - {T_s}^4)(1 - \exp(-\Gamma D)) \qquad \textbf{Eq. 2.13}$$

Where:
σ is the Stefan-Boltzmann constant ($5.67 \cdot 10^{-8}$ W/m^{2}K^4)
V is a dimensionless volume flame-pool surface radiative configuration factor.
Γ is a radiative extinction coefficient (m^{-1}).

Figure 2.9 shows the radiated power from burning different fuels.

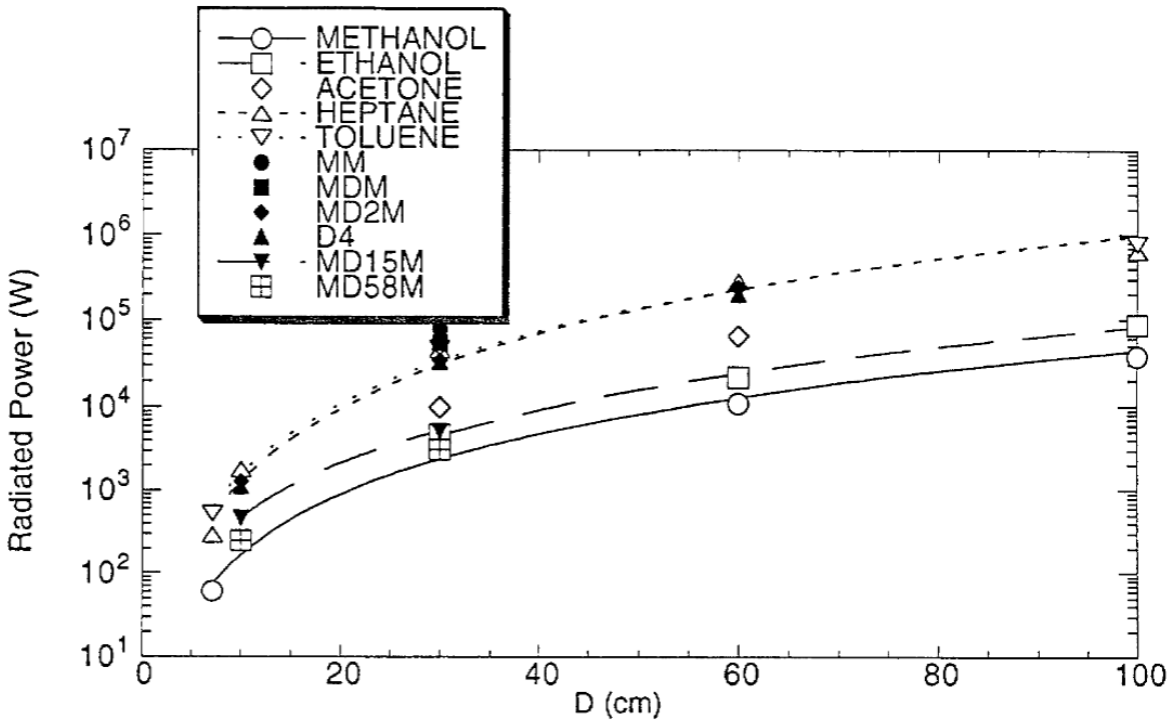

Figure 2.9 Measurements of $\dot{Q}_{radiation}$ as a function of pool diameter for fires burning a number of liquid fuels (12).

Figure 2.9 shows that a fuel diameter of 30 cm gives about 12 kW of global radiated power for heptane fuel, and about 2 kW for Methanol.

2.3.1.Internal and external radiation

There are two aspects of radiation in fires. One is flame radiation, in which radiative transfer can be divided into internal (R_i) and external (R_0) energy transfers. Of the internal transfers, radiation feedback to the fuel surface is most significant (2). Radiation plays an important if not dominant role in the heat feedback to 0.30 m pool fires for both luminous and non-luminous fuels (12).

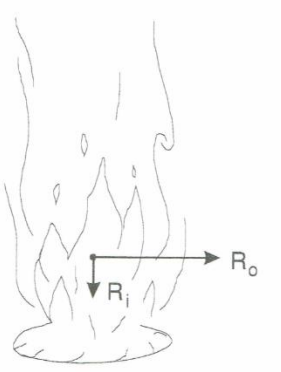

Figure 2.10 Illustrates the difference between internal energy radiation (R_i), and the external energy radiation (R_0) within a pool fire (2).

Further it is focused on the internal radiation. In other words the heat radiating on the fuel surface. The absorbed radiative heat flux normalized by the net heat flux as a function of location on the surface is shown in Figure 2.11.

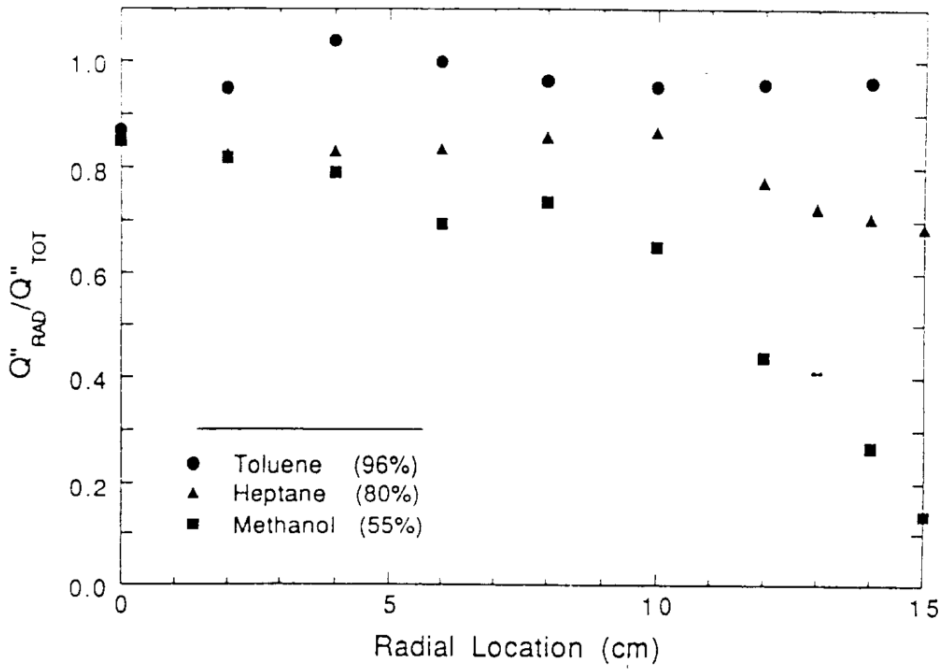

Figure 2.11: The absorbed radiative heat flux normalized by the local net heat flux as a function of location on the surface of 0.30m pool fires burning toluene, heptane and methanol. Numbers in parenthesis indicate the percentage of heat feedback, which was due to radiation (12).

The radiative heat intensity is greatest in the middle of the burner and drops when moving radially away from the center. From the heptane results, radiative heat seems to cease at around 10 cm from the center. Heptane results reveals a slightly decrease already from center, and gets steeper when going further away than 7 cm from center. From the heptane and the methanol fire, 80% and 55% of the heat feedback, respectively, was due to radiation.

2.4. Burning rate

Burning rate or mass loss rate is the mass rate of liquid fuel vaporized and burned. It is expressed as mass flow per unit time, typically in kg/s or g/s, and is here denoted $\dot{m}$. It can also be expressed as mass flux or mass burning rate per unit area, typically in kg/(m^2 s). In this case denoted $\dot{m}''$ (2).

It should be noted that the term "burning rate" is really a misnomer for the mass loss rate, because all of the fuel volatilized may not burn when there is insufficient oxygen available. Most textbooks equate the two terms. In a compartment fire where there is insufficient oxygen, all of the mass loss from the fuel will not burn (2). In this work, regarding pool fires, the two terms are assumed as identical.

In addition to the heat flux from the flame to the liquid surface ($\dot{Q}_F''$), there is also a heat flux loss throughout the liquid surface, denoted $\dot{Q}_L''$. Another transfer of heat loss is through the energy required to produce the volatiles. Figure 2.12 shows a schematic representation of the heat and mass transfer processes of a burning fuel surface.

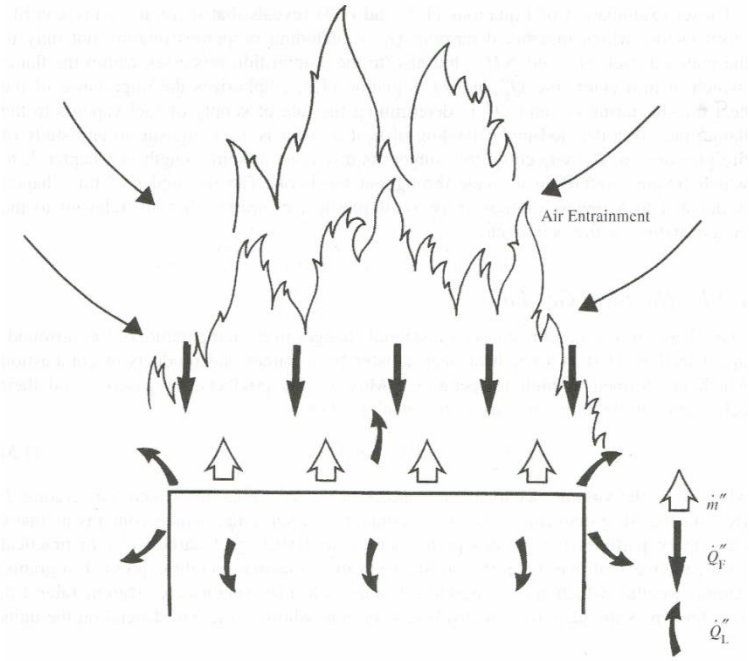

Figure 2.12: Schematic representation of the heat and mass transfer processes of a burning surface (4).

The rate of supply of volatiles from the fuel surface is directly linked to the rate of heat transfer from the flame to the fuel Figure 2.12). The rate of burning ($\dot{m}''$) can be expressed quite generally as (4):

$$\dot{m}'' = \frac{\dot{Q}_F'' - \dot{Q}_L''}{L_v}\ g/m^2 s \qquad \textbf{Eq. 2.14}$$

Where:
$\dot{m}''$is the mass loss rate [g/m^{2}s]
$\dot{Q}_F''$ is the heat flux supplied by the flame [kJ/m^2]
$\dot{Q}_L''$ is the heat flux loss through the fuel surface [kJ/m^2]
L_v is the latent heat of evaporation [kJ/g]

2.4.1. Diameter and rim

Through extensive pool fire experiments it is found that the burning rate is depending on the diameter of the pool fire and the rim of the burner:

Hottel *et* al. noted that D when D is small (D<<1), conduction dominates the heat feedback because convection are proportional to D^2 and conduction is proportional to D. When D is large, the importance of conduction diminishes and radiation eventually dominates convection. This is because *ΓD* in Eq. 2.13 becomes large and radiation is proportional to T_f^4 (10).

Burgess and Hertzberg determined that radiative transfer becomes dominant over convection for pool diameters from 0.1 to 0.5 m, depending on fuel type. Below these sizes, convection was found to be important (13).

Blinov and Khudiakov (1957) studied the burning rates of pools of hydrocarbon liquids with diameters ranging from 0.0037 to 22.9 meters. They found that the rate of burning expressed as a "regression rate" was high for small-scale laboratory pools (0.01 m diameter and less), and exhibited a minimum at around 0.1 m (4). This is shown in Figure 2.13.

Regression rate, R, is measured in mm/min and is equivalent to the volumetric loss of liquid per unit area. This rate is convenient for some purposes, but the mass flux (kg/m^{2}s) is a more logical measure of the burning rate (4).

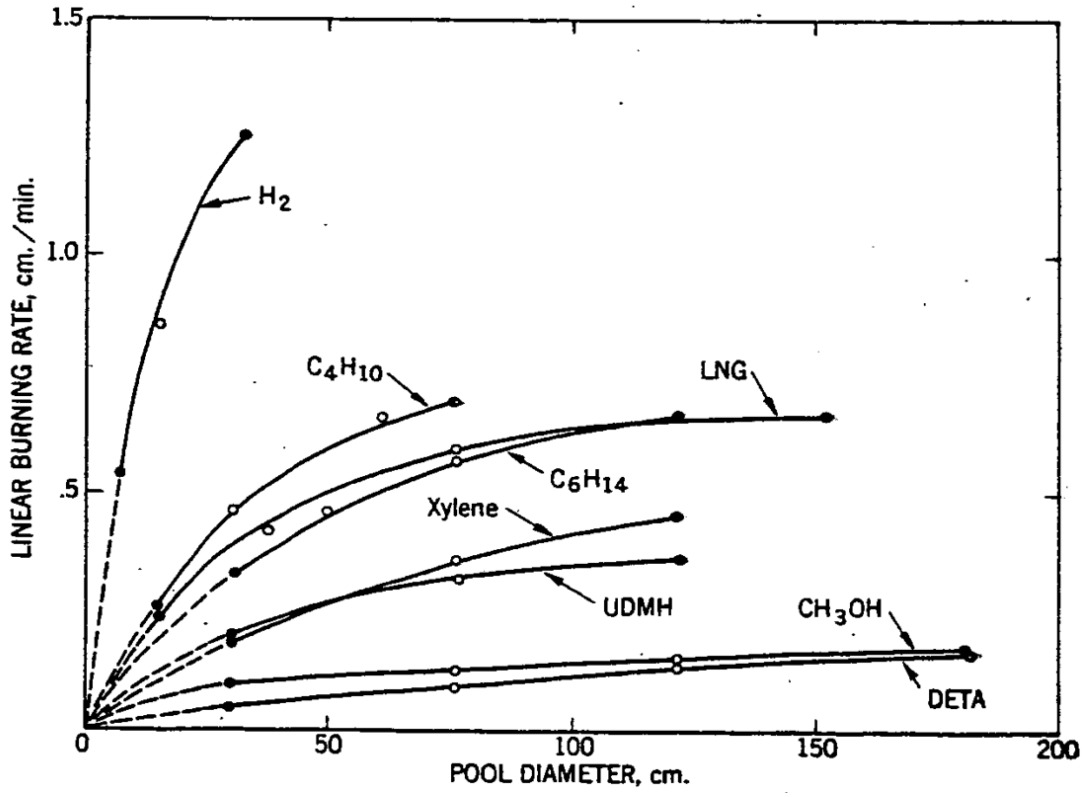

Figure 2.13: Dependence of liquid burning rate on pool diameter (14).

Figure 2.14 shows the dependence of liquid burning rate on pool diameter. The vertical axis refers to the regression rate in cm per minute. When burning methanol (CH_3OH) in a diameter of 0.3 meter, the fuel surface will sink about 0.1 cm/min at the rim.

Using the formula:

$$\dot{m}'' = \frac{R\rho}{60\ sec} \qquad \textbf{Eq. 2.15}$$

Gives a mass flux of 13.3 grams of methanol. The further increase of mass flux with diameter is weak.

For alcohols, effect of the diameter is negligible. The flames from alcohols contain little soot and are nearly invisible to the human eye, so radiation to the surface is much less than that for sootier flames. The mass loss rate is therefore a relatively constant for almost all diameters larger than 0.2 m. In addition, the combustion efficiency for alcohols is close to unity for the same reason (2).

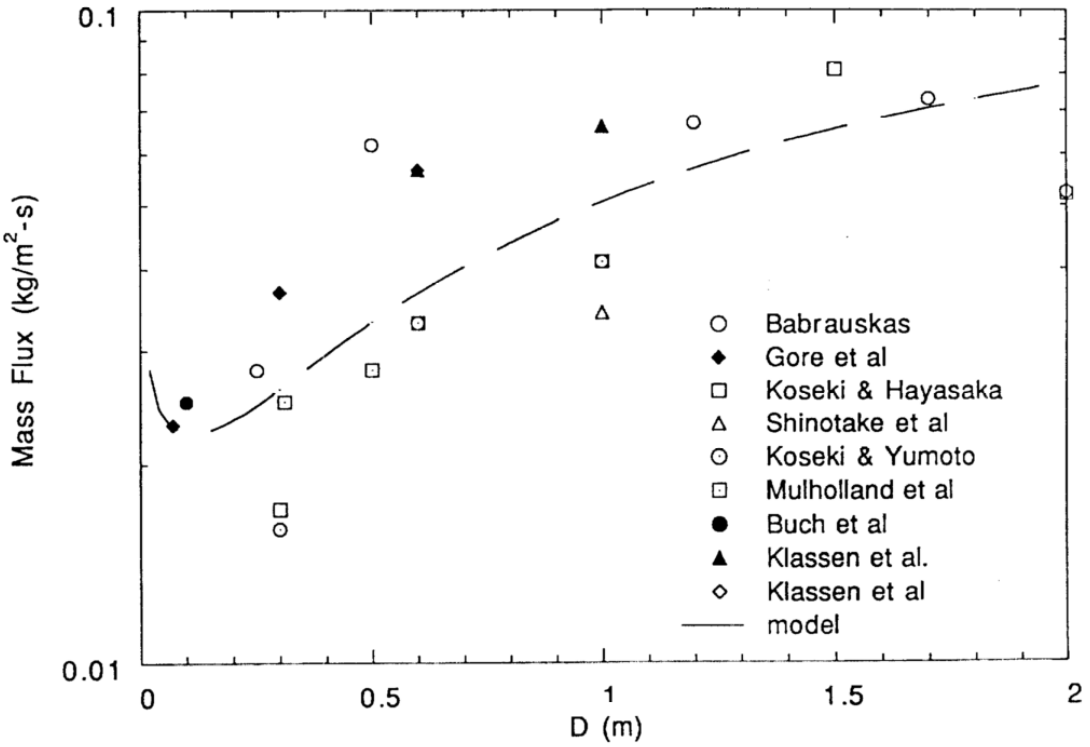

Figure 2.14: Comparison of experimentally measured burning rates for those predicted by the model for heptane as a function of pool diameter. Filled symbols represent measurements where the lip height was maintained at a constant value. Open symbols represent measurements where the lip height was varying (15).

National Institute of Standards and Technology (1999) developed a g*lobal model for predicting the burning rates of liquid pool fires* (15). The curve in Figure 2.14 reveals a modeled mass flux of $3.0 \cdot 10^{-2}$ kg of heptane fuel with 0.4 m in diameter. Results from other measurements is shown in the figure.

If there is an exposed rim above the liquid surface, the flame characteristics are altered (Corlett, 1968; Hall, 1973; Orloff and de Ris, 1982; Brosmer and Tien, 1987; Bouhafid et al., 1988) due to the turbulence induced by the entrainment of air around the perimeter of the container. This causes an increase in the rate of convective heat transfer to the fuel surface, which in turn affects the rate of burning significantly (de Ris, 1979) (4).

If the diameter is less than 0.03 m, the flames are laminar and the rate of mass loss is reduced with increasing diameter. For diameters larger than 1 m, the flames are fully turbulent and the regression rate becomes independent of diameter (4).

In the range 0.03m < D < 1.0m, transitional behavior between laminar and turbulent is observed (4).

Fairly extensive pool fire experiments have been carried out for a wide range of liquids. It has been found that for diameters larger than 0.2 meters, the burning rate increases with diameter up to a certain value, which is called the asymptotic diameter mass loss rate, or mass flux, denoted $\dot{m}''_{\infty}$ (4). It is listed a range of asymptotic mass loss rates for different types of liquids in Table 2.1.

2.4.2. Burning rate estimates

Zabetakis and Burgess recommended that the following expression is used to predict the burning rate (kg/m^2 s) of liquid pools of diameters greater than 0.2 m (4):

$$\dot{m}'' = \dot{m}''_{\infty} \left(1 - \exp(-k\beta D)\right) \qquad \textbf{Eq. 2.16}$$

Where $k\beta$ consists of an extinction coefficient (k) and a "mean beam length corrector" (β), given in Table 2.1. For pool fire calculation purposes it is not necessary to determine these two constants separately, only their product. The diameter (D) is assumed circular. Square and similar configurations can be treated as a pool of equivalent circular area (2). In this work, the 25cm and the 45cm squared burners have an equivalent diameter of 27.3cm and 49.2cm, respectively.

Table 2.1: Data for large pool (D > 0.2m) Burning rate estimates (16).

Liquid	Density (kg/m^3)	$\dot{m}''_{\infty}$ (kg/m^{2}s)	ΔH_c (MJ/kg)	kβ (m^{-1})
Methanol (CH_3OH)	796	0.017	20.0	[a]
Heptane (C_7H_{16})	675	0.101	44.6	1.1

[a] **Value independent of diameter in turbulent regime.**

2.4.3. Latent heat of evaporation, L_v

L_v is the heat required to produce the volatiles (kJ/g, which for a liquid, is simply the latent heat of evaporation in Table 2.2. Table 2.1shows that the limiting burning rates for the simple alcohols methanol and ethanol are much less than that of the hydrocarbons. This is partly due to the grater values of L_v (4).

Table 2.2: Boiling points and latent heats of evaporation for heptane and methanol (17).

Liquid	*Boiling point (°C)*	*L_v (kJ/g)*[a]
Methanol	64.6	1.100
Heptane	98.5	0.318

[a]The latent heat of evaporation refers to the boiling point at normal atmospheric pressure.

2.4.4. Boiling point

Boiling point represent the temperature at which the liquid starts to boil under atmospheric pressure. Boiling point temperatures for heptane and methanol are given in Table 2.2.

3. Experimental setup

3.1. Fuel

The apparatus is mainly designed for burning heptane and methanol liquid. The flame of burning these fuels are different due to the chemical composition. Heptane fire is identified with a red, yellow and orange composed flame and yields heavy, black smoke. The methanol flame is clear blue, yields nearly no smoke, and emits much less radiative heat than heptane fires. Some properties and hazards are listed in Table 3.1 and Table 3.2.

Table 3.1: Properties of heptane and methanol (18).

Liquid	*Air and water reactions*	*Vapor densities*	*Color*
Methanol	Highly flammable. Soluble in water in all proportions.	Slightly heavier than air.	colorless
Heptane	Highly flammable. Insoluble in water.	Havier than air.	colorless

Table 3.2: Hazards regarding heptane and methanol (18).

Liquid	*Fire Hazard*	*Health hazard*
Methanol	FLAMMABLE. Containers may explode.	Exposure to excessive vapor causes eye irritation, head- ache, fatigue and drowsiness. High concentrations can produce central nervous system depression and optic nerve damage. 50,000 ppm will probably cause death in 1 to 2 hrs. Can be absorbed through skin. Swallowing may cause death or eye damage.
Heptane	FLAMMABLE. Flashback along vapor trail may occur. Vapor may explode if ignited in an enclosed area.	VAPOR: Not irritating to eyes, nose or throat. If inhaled, will cause coughing or difficult breathing. LIQUID: Irritating to skin and eyes. If swallowed, will cause nausea or vomiting.

3.2. Apparatus

The apparatus used in the experiments is built as shown in Figure 3.1 and Figure 3.2.

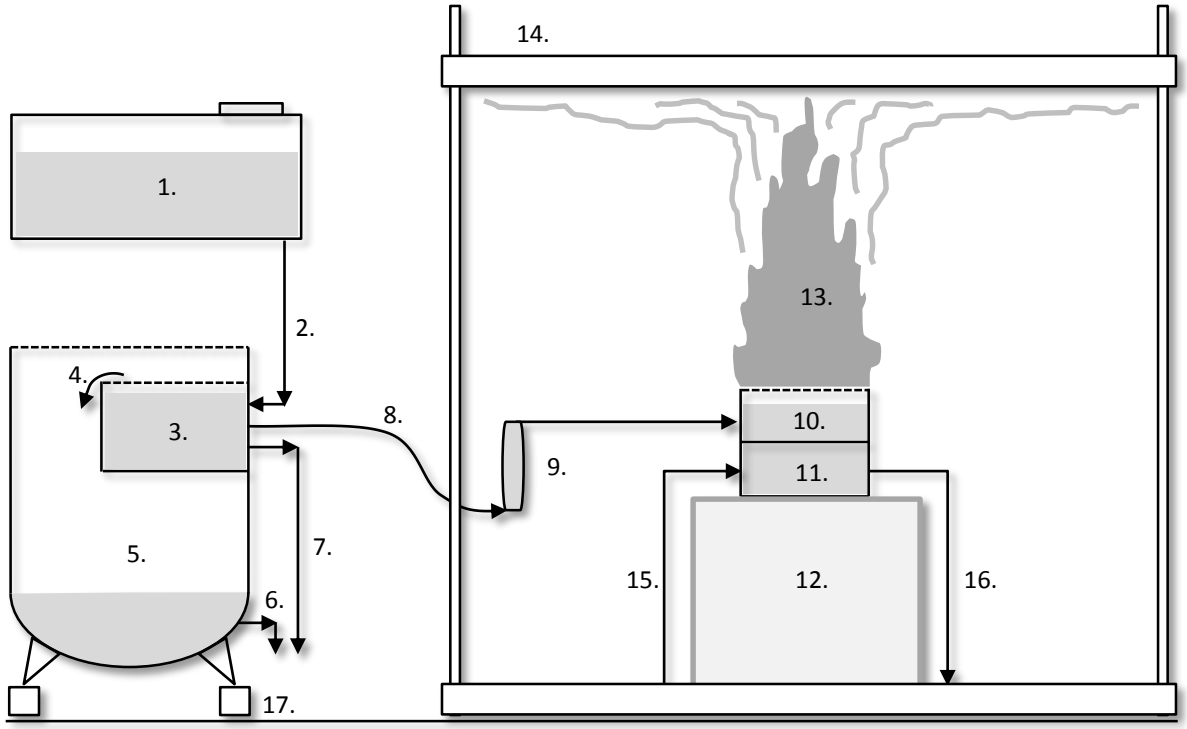

1. Elevated fuel tank.
2. Fuel flow pipes.
3. Corresponding tank.
4. Overflow edge.
5. Overflow tank.
6. Overflow tank drain.
7. Corresponding tank drain.
8. Fuel supply elastic pipe.
9. Flowmeter.
10. Burner.
11. Burner cooling chamber.
12. Burner support.
13. Flame.
14. Height adjustable ceiling.
15. Water flow inlet.
16. Water flow outlet.
17. Height adjustable legs.

Figure 3.1: Schematic vertical presentation of apparatus structure for experiments burning heptane and methanol liquid under an adjustable ceiling.

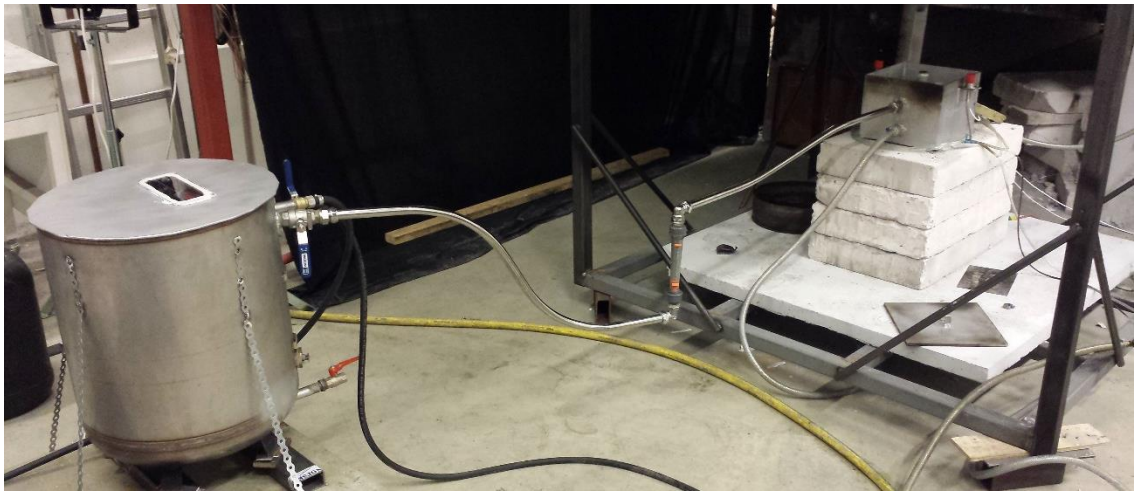

Picture 3.1: Picture of the apparatus used showing the tank system on the left (not the fuel tank) and the piping connected to the 25cm burner to the right. The overlaying ceiling is not shown. The flow meter is located in the middle.

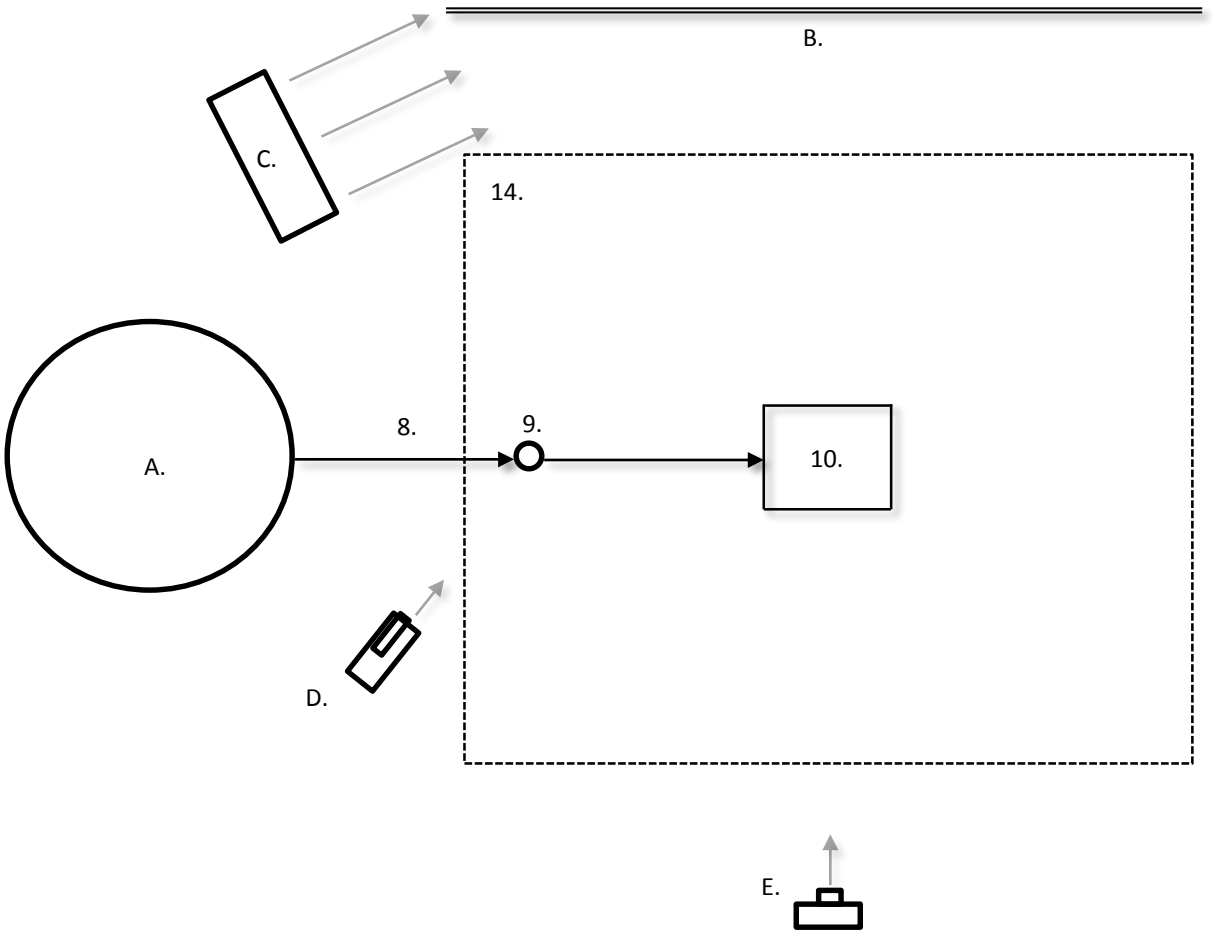

A. Tank system.
B. Background; black curtain.
C. Strong light fixture.
D. Video camera.
E. Photo camera.
8. Fuel supply pipe.
9. Flowmeter.
10. Burner.
14. Height adjustable ceiling.

Figure 3.2: Schematic horizontal presentation of apparatus structure for experiments burning heptane and methanol liquid under an adjustable ceiling.

3.3. Method

This chapter explains the background to the apparatus design.

3.3.1. Burner

Burner (Figure 3.1 point 10) is centered under the ceiling on supporting blocks of incombustible material. Two different sizes is applied. One with a 25x25 cm inside length, and one 40x40 cm. The burners are made of 4 mm thick steel plates. The inside depth is 9.5 cm in both burners.

It is manufactured a lid to each burner, which is put on when it is desired to extinguish the fire. An arm with a hook is applied to outdistance radiative heat, and prevent burns.

3.3.2. Fuel surface height

As previously written in section 2.4.1, the height from the fuel surface to the rim of the burner affects the burning rate. If the surface height is kept constant, steady state should be established and sustained. A corresponding tank (Figure 3.1 point 3) is applied instead of height adjusting instruments or solenoid valves, which would occupy area required to present fuel surface. The tank has an overflow edge (Figure 3.1 point 4) to ensure the fuel level does not rise. In addition, the overflow edge must also ensure that spill during experiments is impossible. Burning spill can cause severe consequences.

Fuel supply is provided from a fuel tank (Figure 3.1 point 1) leveled in a certain height to perform the desired flow. Excess fuel runs over the overflow edge and is collected in a tank beneath (Figure 3.1 point 5). When the overflow tank gets full it is easily drained of fuel (Figure 3.1 point 6), which is poured back into the fuel tank. A lid is covering the open top of the overflow tank to avoid release of fuel vapor. The lid has a window of Plexiglas, making it possible to monitor the overflow is always present. Halted overflow will corrupt the experiment.

3.3.3. Mass flux measurement

A fire requires supply of fuel to sustain. The rate of fuel burned every second is measured by a flowmeter (Figure 3.1 point 9), mounted on the fuel supply pipe (Figure 3.1 point 8). It is used a variable area flowmeter, also called rotameter. It consists of a vertically oriented plastic tube with a larger end at the top, and a metering float that is free to move within the tube. Pictures of the flowmeter is shown in Picture 3.2.

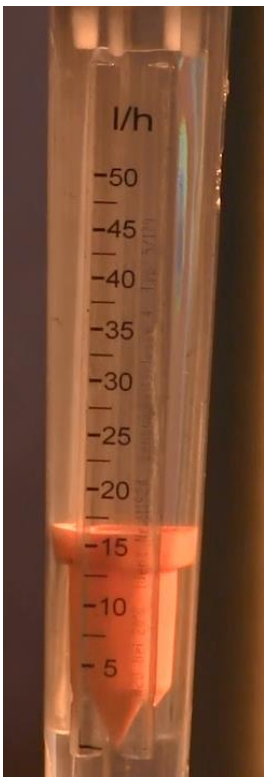

Picture 3.2: Flowmeter with a measure scale of 5 - 50 l/h.

Fluid flow causes the float to rise in the tube as the upward pressure differential and buoyancy of the fluid overcome the effect of gravity. When the float is at the bottom, almost no liquid flows through. As there is no sensors reading the float's position, the rotameter is recorded by a video camera (Figure 3.2 point D). A disadvantage is the time consuming work by viewing all the videos afterwards to register the results. Flow values were taken out manually for every 5th second and saved on a data sheet. The measure scale of the flowmeter is 5 to 50 liters per hour, dimensioned to handle heptane fires in both burners and methanol fires in the 40x40 cm burner.

The flowmeter is by manufacturer calibrated for water. Instead of calculating coefficients handling density and viscosity of heptane and methanol, which is complicated and not necessarily the most accurate, it is performed tests with a constant flow into a container at a given time. Weight calculated into volume and divided by the time of flow, gives a transfer coefficient used to obtain the actual heptane and methanol flow. See calculations in Appendix 1.

3.3.1. Flow friction

Heptane and methanol densities are different, which gives height variations in the configured flow system. The corresponding tank is mounted on height-adjustable legs (Figure 3.1 point 17). The intension is to level the corresponding tank slightly higher than the burner to compensate flow friction in the fuel supply pipe (Figure 3.1 point 8). The fuel supply pipe is made of a soft metal that is bendable by hand. In addition, it is designed to reduce flow friction by performing the following:

- Reduce distance between the corresponding container and the burner. It must still be far enough to prevent fire spread.
- Using pipes with a large diameter and a low surface roughness on the inside.
- Using as few elbows, couplings and fittings as possible.

Once the liquid vapor is ignited, the liquid level starts to drop. The pressure difference exceeds the pressure due to pipe friction, and the liquid starts to flow. It is expected some inertia within flow velocity, but will eventually stabilize once started.

3.3.2. Ceiling height

Experiments with variable ceiling heights can be performed by either adjusting the height of the burner or the height of the ceiling. The burner is positioned relative to the corresponding tank. If raised, the entire fuel supply system must be raised evenly, which is difficultly practicable by hand. Adjusting the ceiling is more simple. The ceiling can be designed light enough to be lifted by hand.

The height given in the results is measured from the burner rim to the lower edge of the ceiling, added with 1.5 cm. This represent the exact height from the fuel surface to the ceiling in the heptane experiment with the 40X40 cm burner. If the ceiling height is given to be 0.65 meter, it is 0.635 m above the rim (0.65 – 0.015 m). Since the fuel surface in this experiment is 0.015 m below the rim, according to Table 3.3, the height between ceiling and fuel surface is 0.65 m (0.635 + 0.015 m). For the heptane experiment with the 25x25 cm burner, this height is exactly 0.648 m (0.635 + 0.013 m).

When the length of the ceiling is fully utilized by the flame length underneath, there is no point in lowering the ceiling further without increasing it’s length. The ceiling can be adjusted as low as 0.30m

above the liquid. This height limit is set by the calibration plate, which is 0.3m high and has to be placed between the ceiling and the burner during calibration.

3.3.3. Test similarity

If the tests with the same burner and fuel were divided up and performed on different days, it is expected ambient conditions not the same. To ensure that tests are as similar as possible to each other, the tests are performed continuously by only adjusting the height of the ceiling.

3.3.4. Air flow

The extractor fan, mounted on top of the smoke collecting steel cabinet, prevents the laboratory to be filled with smoke. The air suction is powerful, which leads to turbulent air flow conditions. In addition, there is only one air inlet. One directional airflow gives an uneven air entrainment into the fire. Before steady state burning is achieved, the fan power is adjusted to balance between smoke filling and extraction, entailing no more turbulence than necessary. Once steady state is reached, the fan is switched off. The room is being filled with smoke while recordings are made. When the recordings are finished, the fan is turned on again.

3.3.5. Height from liquid surface to burner rim

The height from the liquid surface to the rim of the burner is shown below, and is the result from several attempts trying to find as small height as possible.

Reference:	Burner size:	Liquid:	Height from liquid surface to rim:
B25/heptane	0.25 x 0.25 m	Heptane	13mm
B40/heptane	0.25 x 0.25 m	Heptane	6 mm
B25/methanol	0.40 x 0.40 m	Methanol	15 mm
B25/methanol	0.40 x 0.40 m	Methanol	8 mm

Table 3.3: Height from liquid surface to rim of the burner for each experiment.

The heptane liquid was boiling during experiments, which caused some liquid to spill over the rim even when burner is mounted completely horizontally. This increases the liquid surface area increased evaporation, which is undesired. The height from liquid surface to rim was set to a point where the liquid do not run over, plus a couple of millimeters as a safety margin. The methanol liquid does not boil, giving no bobbles at all. This gives the opportunity to have a higher liquid surface for this experiment. A highest possible surface level is desired. The reason is that the rim is cooled by the liquid, which is cooled by the water in the chamber underneath. When the liquid level drops, less of the rim surface is in contact with the liquid. Instead, more steel surface is exposed to the radiative heat, which causes the rim temperature to increase. This also increases the mass loss near the rim due to a higher temperature of the liquid close to it. This leads to unsteady heat release.

Height from rim to liquid surface was measured while liquid was pouring into the burner. This is important, as it is interesting to know the liquid height during flow (burning). When the flowmeter was showing between 20 and 30 liters per hour (middle of the scale), a ruler was used to measure the height at the edge,

The reason why measurements are performed during flow, is that the corresponding tank is leveled slightly higher to make buoyancy forces great enough to compensate flow friction, mentioned

previously in section 3.3.1. In the heptane experiments, the height difference was measured to be 31 millimeters. For methanol experiments a little lower. This is due to differences in density.

The height from rim to liquid surface is different by a few millimeters between the two burners, even when using the same liquid. This is due to flow friction. There is a higher flow rate when using the biggest burner. Increased flow velocity gives increased flow friction.

When the float in the flowmeter reaches the bottom, it shuts the flow. This is an important feature to prevent spill when the fire is out.

3.3.6. Flame image capture and processing

A single-lens reflex photo camera (NIKON D90) is used to capture images of the flame at two frames per second (Figure 3.2 point E). The camera is able to capture up to 100 images, which afterwards are imported to Photoshop for editing. Light from the flame is reflected by parts of the equipment. Reflection spots are removed from images by brightness adjustments and cutting, without affecting the flame.

Picture 3.3: Image of flame before editing. Arrows points at reflections.

Picture 3.4: Cut and edited version of Picture 3.3.

Afterwards images are imported to MatLab and processed into flame probability plots. More information about image processing can be found in the appendix, section 0. The method is an appropriate way of finding the mean-time flame height and length (see section 2.2.3).

Note the following: The photo camera is leveled equally to the underneath surface of the ceiling. This is in order to get realistic measures of the horizontal flame length. This has a disadvantage to the vertical length scale. The input image is cut at the nearest rim of the burner, which make the vertical axis start it's measure scale from a point that is lower than the fuel source. Meaning that the scale on the vertical axis is showing a greater height than actually appear. The vertical scale must be elevated to the backside rim of the burner, as shown in an example of a flame probability plot in Figure 3.3.This means that the height representing the burner in the plot, must be subtracted.

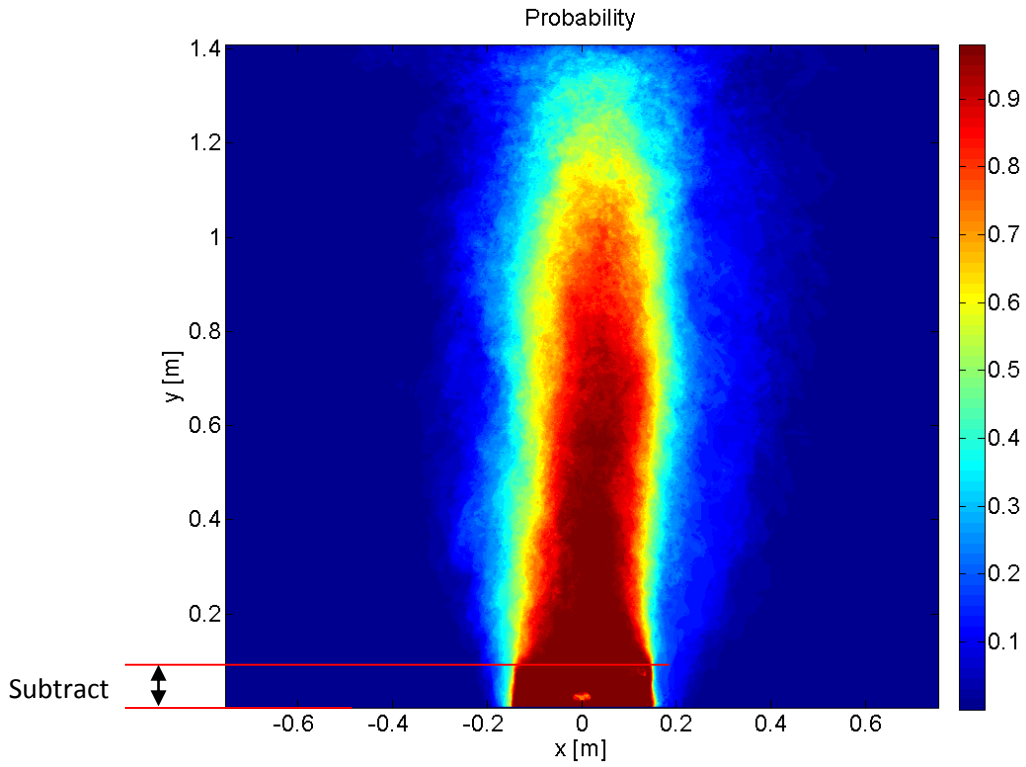

Figure 3.3 Example of Flame probability plot.

MatLab is programmed to find the flame height and length, but struggles to find the correct flame origin from the inputs. When the origin is tweaked to one side, the flame length on one side gets smaller or bigger than the other. However, the average flame length found by MatLab is used to ensure that the average length found manually, is not far away. The average length is not affected by flame leaning and does not take the location of the fuel source into account. Note that there is a distinction between the averages calculated. “Average flame length” is an average of the flame lengths sorted out from the probability plots visually. “MatLab average flame length” is the average result carried out by MatLab.

In order to capture sharp and clear images of the methanol flame, the lights were turned off during methanol fire experiments. The methane flame is blue and difficult to see in bright light. Because the video camera (recording the flowmeter) needs more or less a daylight environment, the flow is recorded after images of the flame were taken. The methanol flow sustains quite steady, which give this opportunity. During the experiments, it is checked regularly that the flow is steady and sustains at an equal flow.

Behind the apparatus (from the camera point of view) it is mounted a black curtain made of fabric (Figure 3.2 point B) which is illuminated by a strong light from a fixture (Figure 3.2 point C). The purpose is to prevent shadows that could interfere with the image processing in Matlab. Therefore, the fixture is located on the side to prevent lightning up the equipment under the ceiling. Lights was not used in the methanol fire tests as described above.

3.3.7. Burner cooling

A fire releases heat that gradually warms up the burner and the liquid inside. As the evaporation rate is temperature dependent, the heat release increases to the level where heat dissipation is equal to heat generation. The burner is cooled by water flow in a separate chamber underneath the fuel chamber (Figure 3.1 point 11). The main approach is to reduce time until steady state is obtained. The cooling prevents the bottom of the burner and the support beneath to gain heat. It is expected that heat transfer this way require longer time until equilibrium is reached, than using the cooling system. The sooner the steady state is established, the better. An illustration of the cooling system is shown in Figure 3.4.

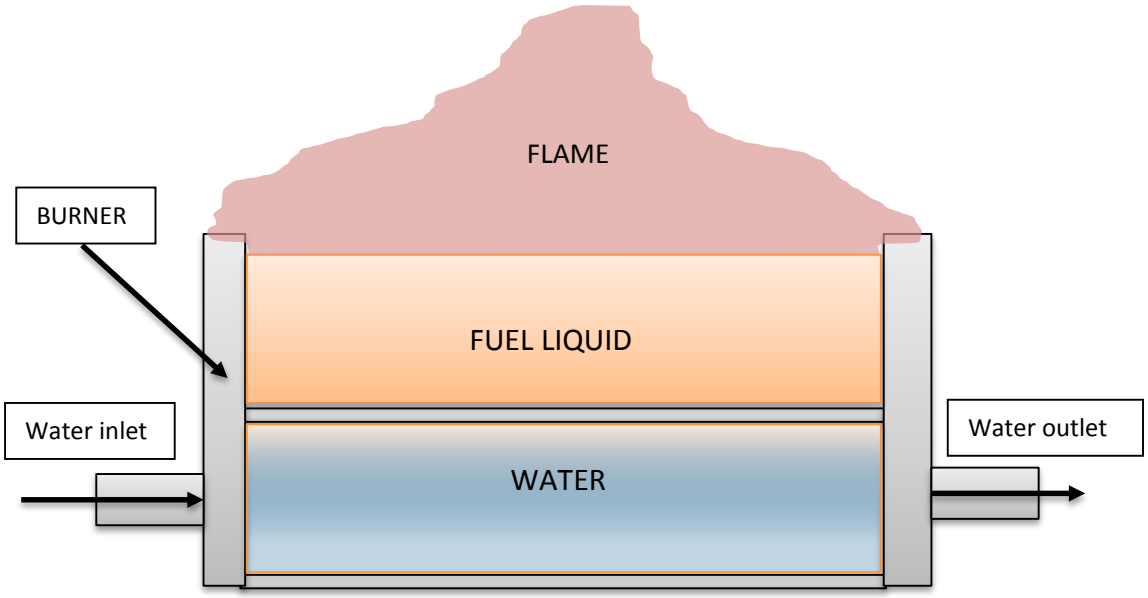

Figure 3.4 Illustration of the water-cooling chamber in the burner.

In most cases it is used a layer of water just underneath the heptane liquid to prevent the heptane to be heated. Water have higher density than heptane, and will locate at the bottom by itself. A water layer will also have temperature increase that brings uncertainties. The main issue with using water is it's density, which forces water to flow into the flowmeter, displacing heptane liquid. The flow system will fail completely.

3.3.8. Heat flux measurements

It is located heat flux meters on both sides of the burner. They are mounted at the horizontal centerline 65mm from the outside of, and 5 mm lower than the edge. A radiation flux meter is located at the same height in the middle of the burner, within the liquid. See Picture 3.5. The flux meters are cooled by water.

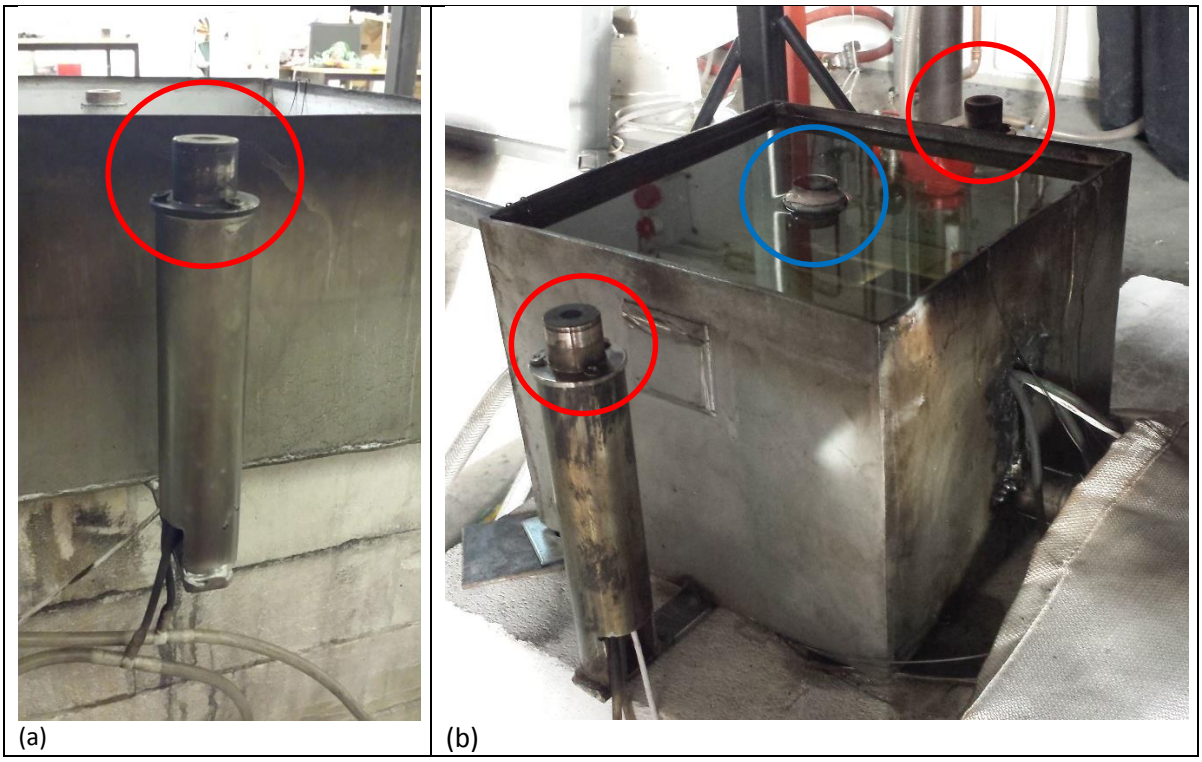

Picture 3.5: Picture (a) and (b) shows the heat flux meters located on each side of the burner (red circles). Picture (b) also shows the radiation flux meter in the middle (blue circle).

It is desired to locate the flux meters as close to the rim as possible, as their main purpose is to give a measurement of the heat close to the rim at various ceiling heights. Difficulties followed when the flux meters was located too close. Because the density of heptane vapor is heavier than air, the vapor flows down at the sidewall of the burner. The flux meters got exposed to flames on the sidewall and gave measurements that did not reveal pool fire realistic results. The flux meters had to be replaced as far as 6.5cm from the rim in order to completely prevent heptane vapor flow down the sidewall. Cables attached to the flux meter needed protection from radiative heat. The metal cylinder beneath (shown in Picture 3.5 (a) and (b)) is for cable protection as well as flux meter support.

A radiative heat flux meter is located in the middle of the burner as shown in Picture 3.5 (b), leveled equally to the rim. The purpose is to measure the radiative heat feedback on the fuel bed. The flux meter has a circular glass on top that allows penetration of radiative heat. Soot makes the glass dirty. To avoid absorption of radiation, the glass maintains clean by flushing nitrogen from a very thin gap around the glass.

3.3.9. Temperature measurements

There are tree temperatures measured with thermocouples: the rim, the liquid surface and the liquid bottom. Two thermocouples are attached on the outside of the rim on both sides of the burner, 5 mm from the top, and with a heat conduction paste to ensure contact. Two thermocouples is laid over the rim on both sides to measure liquid surface temperature. Equally is done for the thermocouple in the bottom. The dual measurements for each location is performed to calculate an average. Average measurements are used to give better accuracy and reliability.

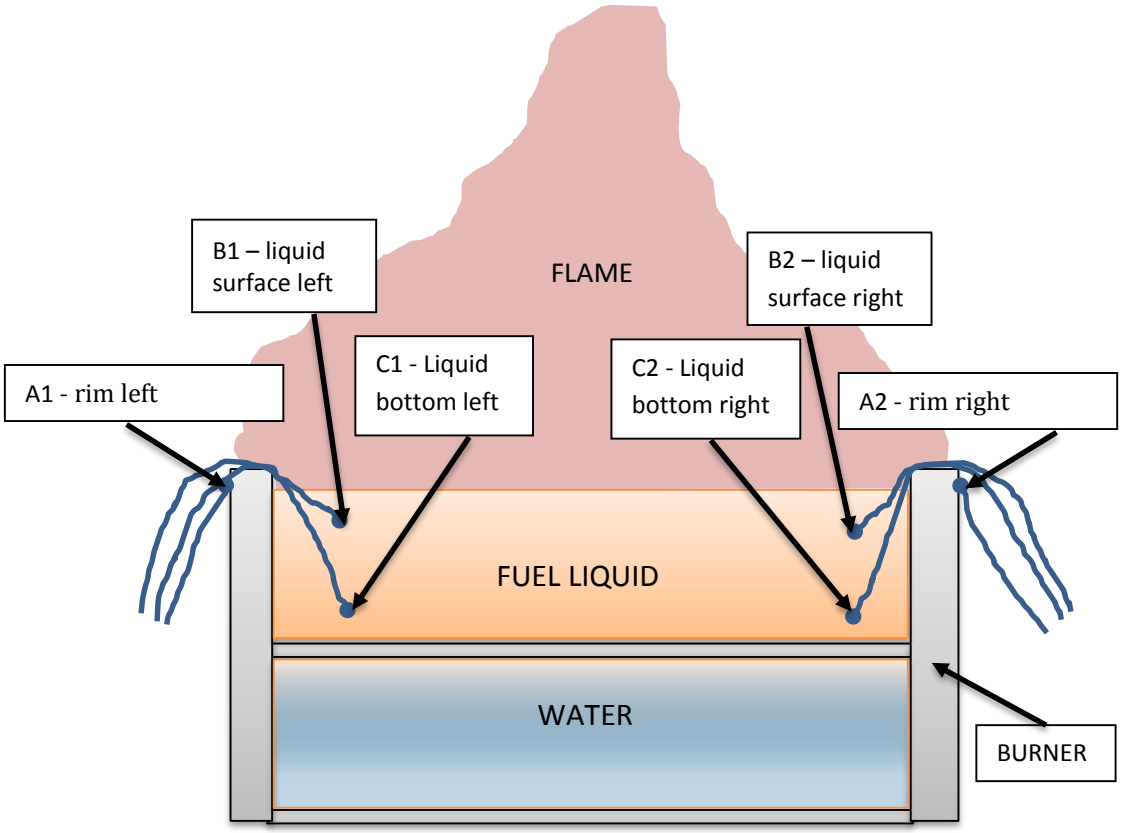

Figure 3.5 Illustration of location of the thermocouples in the burner.

Thermocouples in the surface is located at least 2 cm from the sidewall and 1 cm deep.
Thermocouples at the bottom is located at least 2 cm from the side wall and 1 cm from the bottom.

3.3.10. Number of experiments

It is performed experiments according to Table 3.4.

Reference:	Burner:	Liquid:	Test no:	Ceiling height:
B25/heptane	25x25 cm	Heptane	1 – 3	0.65m
			4 – 6	0.75m
			7 – 9	0.85m
			10 – 12	0.95m
			13 – 15	1.05m
			16 – 18	1.15m
			19 – 21	1.25m
			22 – 24	absent
B40/heptane	40x40 cm	Heptane	25	1.35m
B25/methanol	25x25 cm	Methanol	26 – 28	0.35m
			29 – 31	0.45m
			32 – 34	0.55m
			35 – 37	0.65m
			38 – 40	0.75m
			41 – 43	1.25m
B40/methanol	40x40 cm	Methanol	44 – 46	0.35m
			47 – 49	0.45m
			50 – 52	0.55m
			53 – 55	0.65m
			56 - 58	0.75m
			59 - 61	1.35m

Table 3.4: List of experiments and tests.

3.4. Limitations and uncertainties

3.4.1. Air flow

Above the area, where the experiments are performed, there is a 3-meter square steel cabinet in purpose of smoke extraction. The smoke is transported to the outside by the fan and prevents the lab from being filled with smoke. There are also vents installed in the wall just beneath the roof to ensure incoming airflow. The vents opens automatically when the fan switches on and causes air from the outside to enter the room from one direction only. Air flows towards the flame and causes it to lean to the side. A sliding gate is possible to keep open, but is placed beside the vents. The airflow still approaches from the same direction. An open gate will not only gain poor effect. Calm wind conditions outside are also required.

3.4.2. Combustible background

The adjustable ceiling cannot be placed too close to the black curtain in the background. The curtain is made of fabric and the heat radiation could make it catch fire. Since the curtain is hanging on the wall, the fire may spread to other installations. The steel frame is therefore not placed symmetrically beneath the extractor fan cabinet, but half a meter to one side, away from the fabric. This causes the air flow around the ceiling to become uneven when the extractor fan above is on.

4. Results

4.1. General

Results from experiments are presented in this chapter. It used own references to each experiment according to Table 4.1:

Experiment:	Reference:	Burner size:	Liquid:
1	B25/heptane	0.25 x 0.25 m	Heptane
2	B40/heptane	0.25 x 0.25 m	Heptane
3	B25/methanol	0.40 x 0.40 m	Methanol
4	B25/methanol	0.40 x 0.40 m	Methanol

Table 4.1: references to experiments performed.

Axes in the flame probability plots have equal dimensions to reflect the realistic proportion between height and length. Green color in the plots represent probability of 0.5 and is where the time-mean flame length is measured in this work.

Visually and simple considerations are made about the centerline axis symmetry of the flames in the probability plots. If there are deviations within 0.05m, the symmetry is characterized as good. Deviations between 0.05 and 0.1m is fear, and more than 0.1m is poor. It is used

In graphs representing results from experiments with a true impinging flame, linear trend lines inserted reflects correlation between measurements and ceiling heights. However, ceiling able to gain temperature reflects heat to the fuel bed. Results from free burning fires is not included in the trend lines due to absence of ceiling.

4.2. Radiative heat measurements

The radiative heat flux meter suffered from losing nitrogen supply during the experiment due to an empty tank. The loss of nitrogen caused heptane vapor to condensate around the flux meter cooled by water. Heptane liquid flowed inside the flux meter through the gap intended for flushing of nitrogen, causing incorrect measurements in further testing. The discovery was done too late to perform tests over again.

4.3. Experiment B25/heptane

The results from burning heptane in the 0.25 m squared burner are presented. It is performed experiments with free burning, and burning under a ceiling at variable heights. The experiment was completed, giving following results.

At the ceiling height at 0.65 m, the length of the ceiling was fully utilized by the flame length. This was the lowest ceiling height possible to perform due to radiant heat that did a great strain on the equipment. It required heat shields to be mounted to protect the cables. A thin, transparent hose with water flow (to cool the flux meters), started to melt and got punctured at the first test.

The time-mean flame is hard to predict visually during the experiments. When the ceiling was set to a height of 1.25 m, it was quite certain that the mean-time flame was not in contact with the ceiling. The ceiling was after this experiment taken completely off.

4.3.1. Flame height and length

0.65 m ceiling height:

Figure 4.1 shows a flame extension length under the ceiling of 0.73m at the left side, and 0.75m at the right. This is from test 1, which came out with a good centerline axis symmetry.

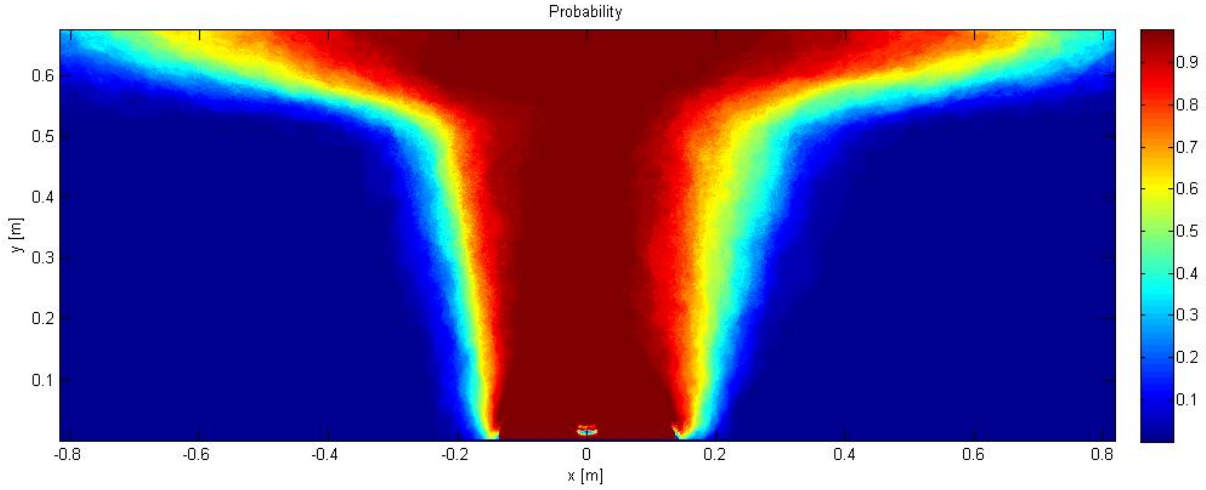

Figure 4.1: Flame probability plot at 0.65m ceiling height (test 1) (B25/heptane).

The flame length result from each test are listed in Figure 4.1

Test	r_f left:	r_f right:	Average:	MatLab average:
1	0.73	0.75	0.74	0.73
2	0.80	0.53	0.67	0.66
3	0.50	0.63	0.57	0.54

Values given in meter.

Table 4.2: Flame length results from burning heptane in a 25cm squared burner with 0.65 m ceiling height.

Test 2 and 3 suffered from turbulent air conditions, which resulted in a leaning flame. This was significant in test 3, which have the shortest average length of these 3 tests. A leaning flame is significant in test 2, where the r_f length clearly shortens on the right side and extends on the left. Test 1 shows that good axis symmetry contributes to equal flame lengths and an increased length. MatLab average lengths have acceptable deviations at maximum 0.03m, but all of them are shorter than the manually sorted average.

0.75 m ceiling height:

Figure 4.2 shows a flame extension length under the ceiling of 0.62m at the left side, and 0.65m at the right. This is from test 5, which came out with a good centerline axis symmetry.

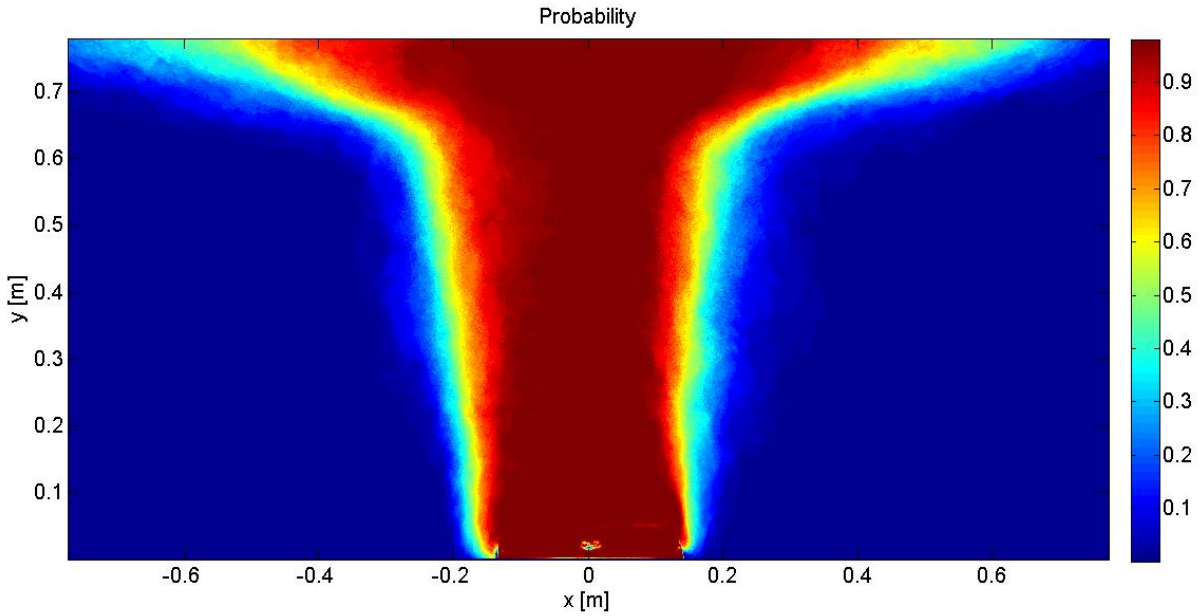

Figure 4.2: Flame probability plot at 0.75m ceiling height (test 5) (B25/heptane).

The flame length results from each test are listed in Table 4.3:

Test	r_f left:	r_f right:	Average:	MatLab average:
4	0.67	0.49	0.58	0.58
5	0.62	0.65	0.64	0.61
6	0.64	0.55	0.60	0.59

Values given in meter.

Table 4.3: Flame length results from burning heptane in a 25cm squared burner with 0.75 m ceiling height.

Test 4 and 6 suffered from a leaning flame and have the most dissimilar flame lengths on each side. Test 5 shows that good axis symmetry contributes to equal flame lengths and an increased length. MatLab average lengths have acceptable deviations at maximum 0.03m, but all of them are shorter than the manually sorted average.

0.85 m ceiling height:

Figure 4.3 shows a flame extension length under the ceiling of 0.33m to the left side, and 0.43m to the right. This is from test 9, where the flame is leaning more than in the other two experiments. The centerline axis symmetry in this test is poor.

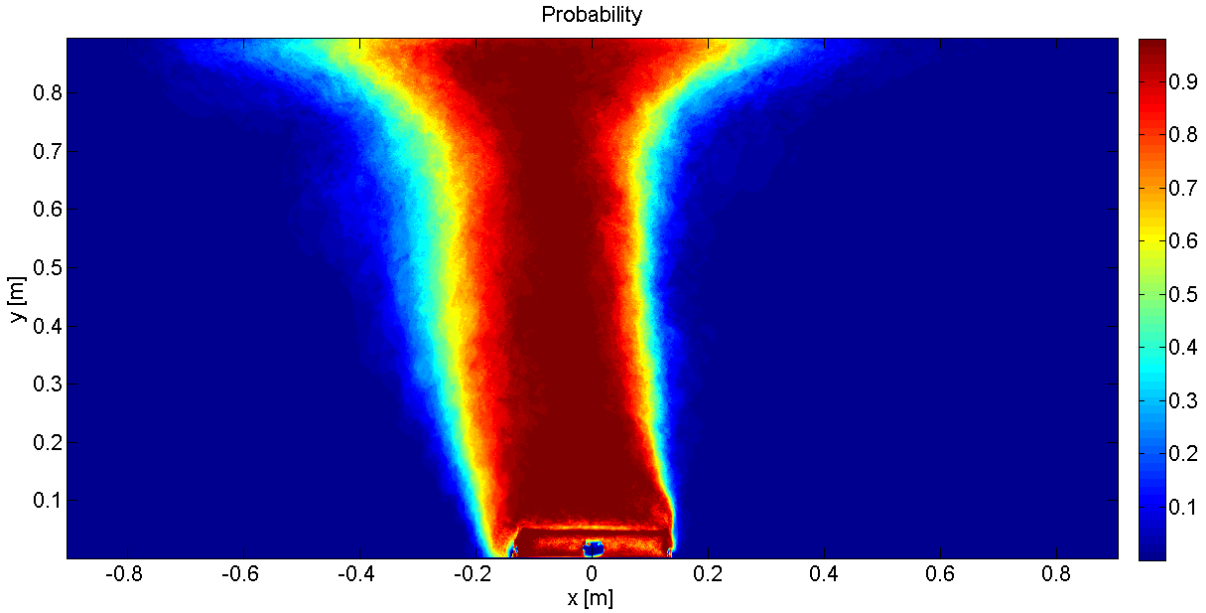

Figure 4.3: Flame probability plot at 0.85m ceiling height (test 9) (B25/heptane).

The flame length results from each test are listed in Table 4.4:

Test	r_f left:	r_f right:	Average:	MatLab average:
7	0.33	0.43	0.38	0.36
8	0.32	0.45	0.39	0.37
9	0.47	0.27	0.37	0.37

Values given in meter.

Table 4.4: Flame length results from burning heptane in a 25cm squared burner with 0.85 m ceiling height.

0.95 m ceiling height:

Figure 4.4 shows a flame extension length under the ceiling of 0.33m to the left side, and 0.43m to the right. This is from test 12 where the flame is leaning, but came out with a fair centerline axis symmetry.

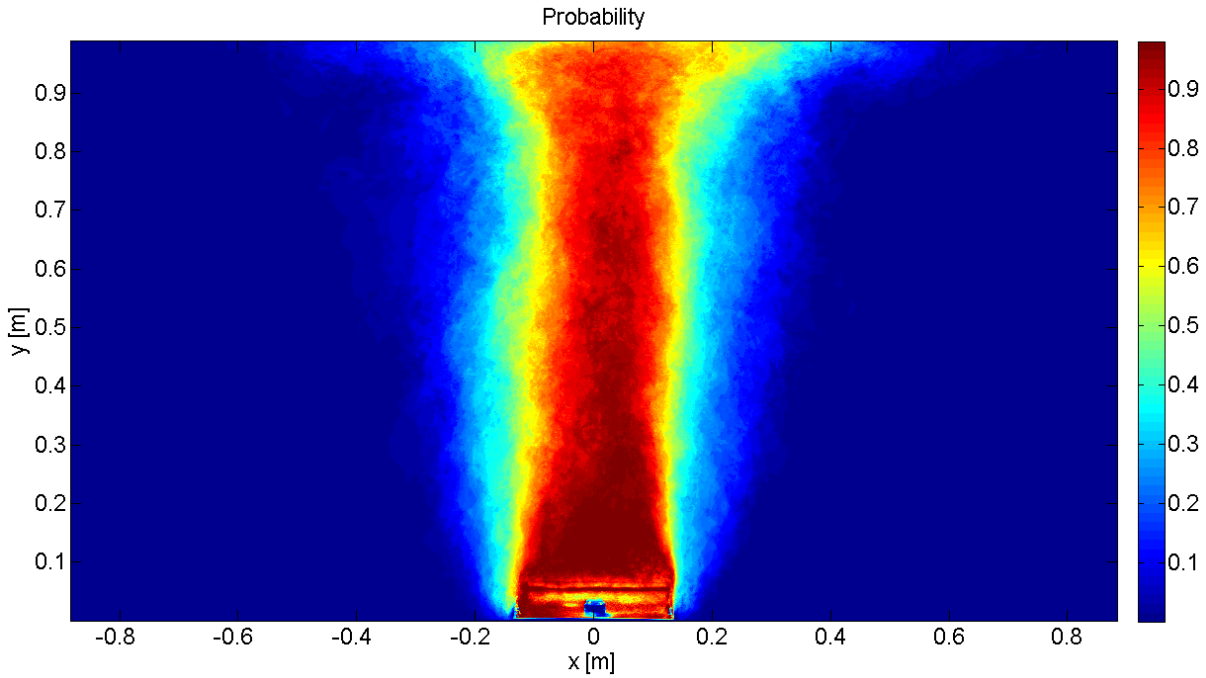

Figure 4.4: Flame probability plot at 0.95m ceiling height (test 12) (B25/heptane).

The flame length results from each test are listed in Table 4.5:

Test	r_f left:	r_f right:	Average:	MatLab average:
10	0.20	0.32	0.26	0.26
11	0.17	0.29	0.23	0.23
12	0.18	0.32	0.25	0.25

Values given in meter.

Table 4.5: Flame length results from burning heptane in a 25cm squared burner with 0.95 m ceiling height

1.05 m ceiling height

Figure 4.5 shows a flame extension length under the ceiling of 0.33m to the left side, and 0.43m to the right. This is from test 12 where the flame is leaning, but came out with a fair centerline axis symmetry.

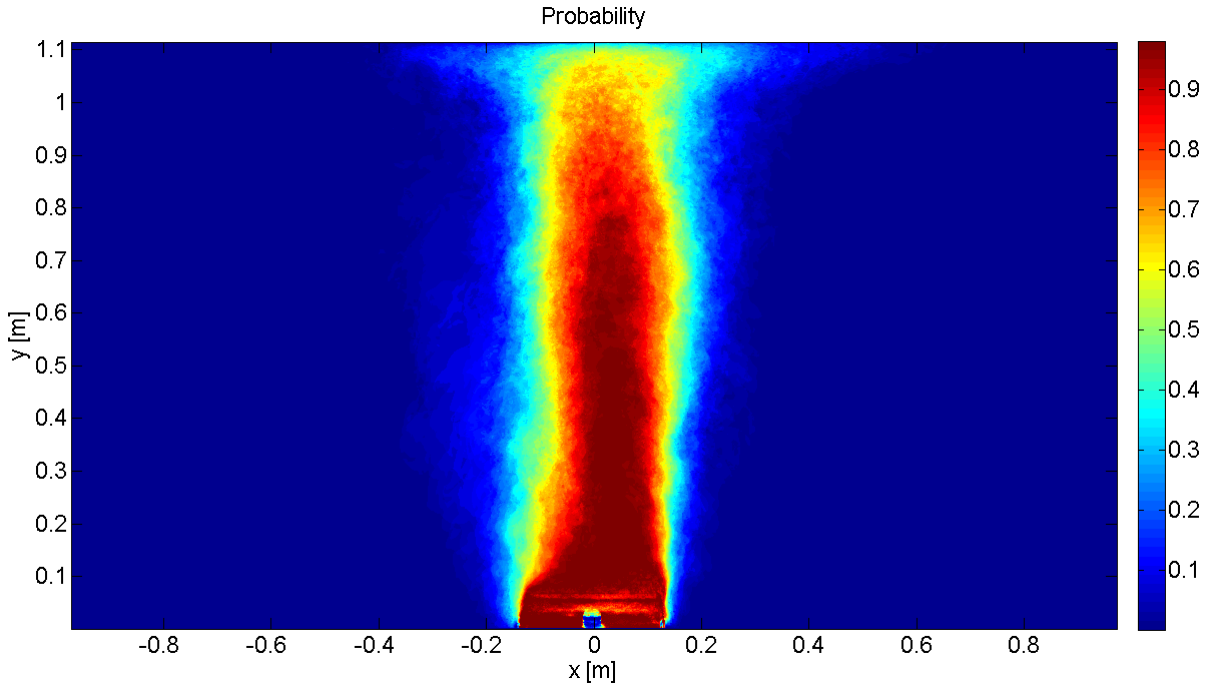

Figure 4.5: Flame probability plot at 1.05m ceiling height (test 13) (B25/heptane).

The flame length results from each test are listed in Table 4.6:

Test	r_f left:	r_f right:	Average:
13	0.10	0.18	0.14
14	0.08	0.21	0.15
15	0.05	0.23	0.14

Values given in meter.

Table 4.6: Flame length results from burning heptane in a 25cm squared burner with 1.05 m ceiling height

MatLab average is not supported because the flame is not widest where the flame impinges on the ceiling.

1.15 m ceiling height:

Figure 4.6 shows the probability plots from test 17 (a) and 18 (b). The flame in test 17 have an extending flame under the ceiling with a flame length of 0.08m to the left and 0.17 to the right. The flame in test 18 do not impinge on the ceiling and give instead flame height of 0.75m. The flame is leaning in both tests, giving poor centerline axis symmetry.

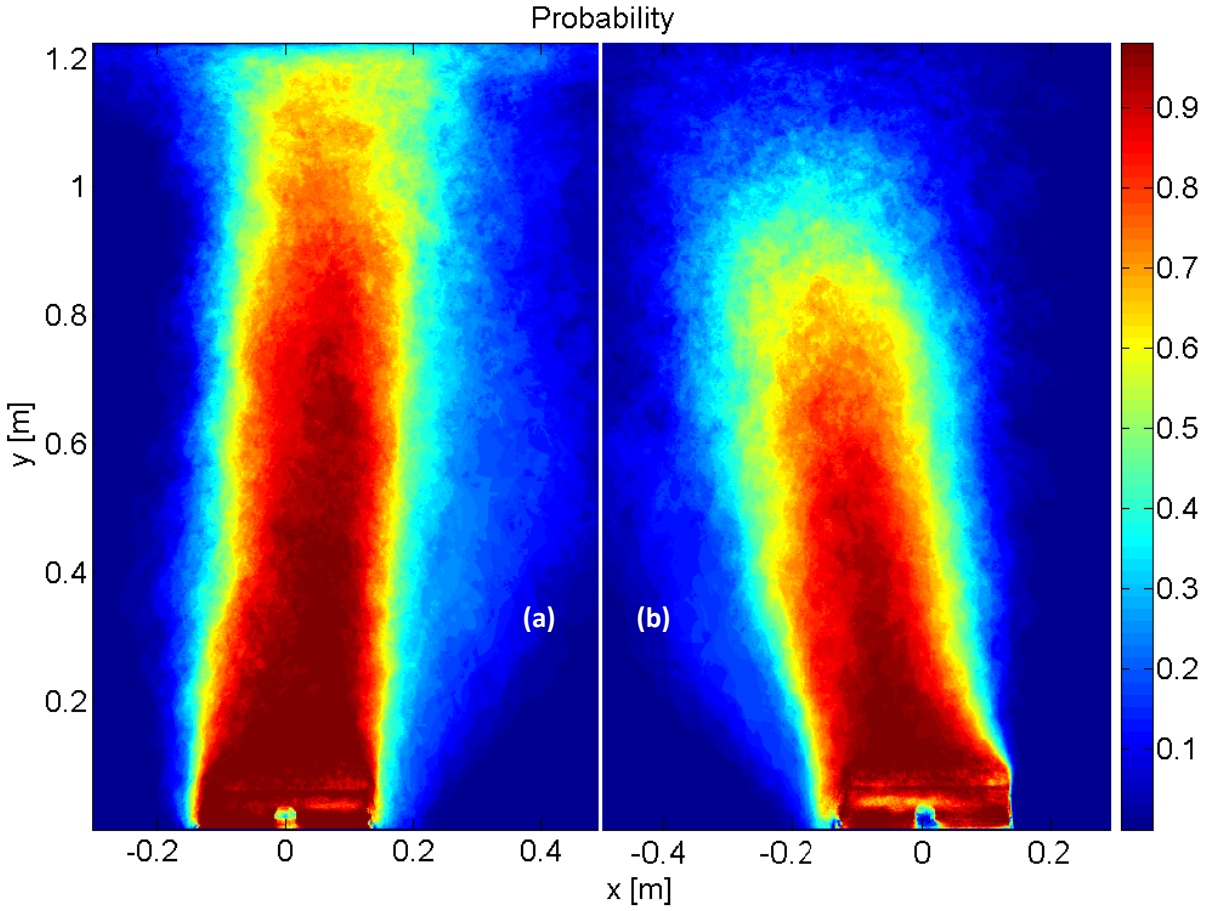

Figure 4.6: Flame probability plot at 1.15m ceiling height (B25/heptane). Test 17 (a) and test 18 (b).

The flame length results from each test are listed in Table 4.7:

Test	r_f left:	r_f right:	Average:	
16	0.08m	0.17m	0.13m	
17	0.08m	0.21m	0.15m	
Test	Flame height in plot:		Subtraction:	Actual flame height:
18	1.00		-0.07	0.93

Values given in meter.

Table 4.7: Flame length and height results (B25/heptane) with 1.15 m ceiling height.

MatLab average is not used because the flame is not widest in the impinging area, but at the middle of the flame.

1.25 m ceiling height:

Figure 4.7 shows the probability plot from test 20. The flame did not impinge at the ceiling, and resulted in a flame height of 0.87m. The centerline axis symmetry is fair.

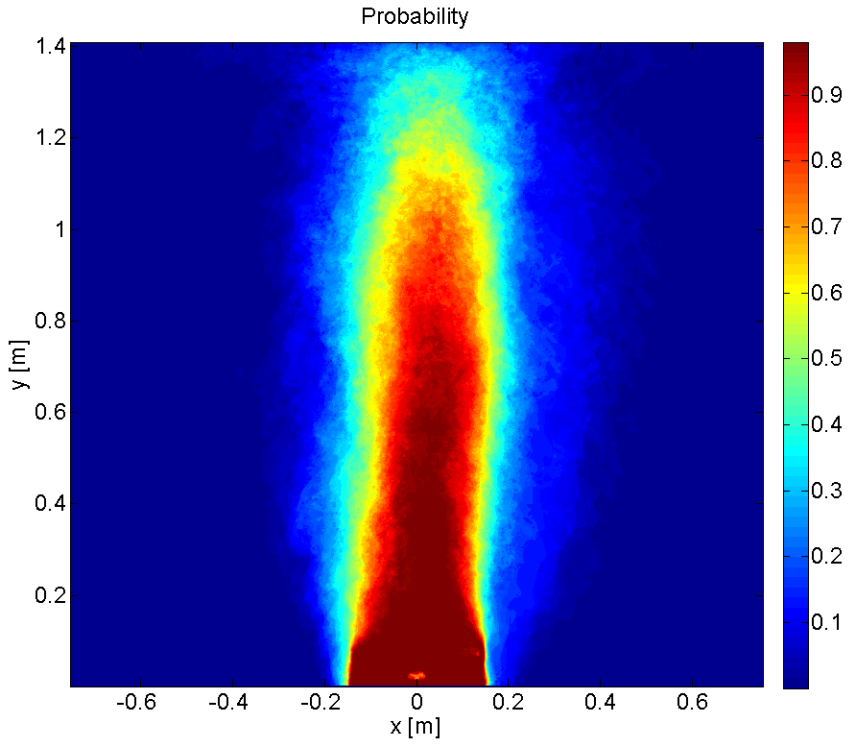

Figure 4.7: Flame probability plot at 1.25m ceiling height (test 20) (B25/heptane).

The flame height results from each test are listed in Table 4.8:

Test	Flame height in plot:	Subtraction:	Actual flame height:
19	1.19	-0.09	1.10
20	1.21	-0.09	1.12
21	1.27	-0.09	1.18

Values given in meter.

Table 4.8: Flame height results from burning heptane in a 25cm squared burner with 1.25 m ceiling height.

None of the flames from experiments with ceiling height 1.25 have probability of 0.5 or less impinging on the ceiling. Figure 4.7

No ceiling:

Figure 4.8 shows the probability plot from test 22. The flame did not impinge at the ceiling, and resulted in a flame height of 0.87m. The centerline axis symmetry is fair.

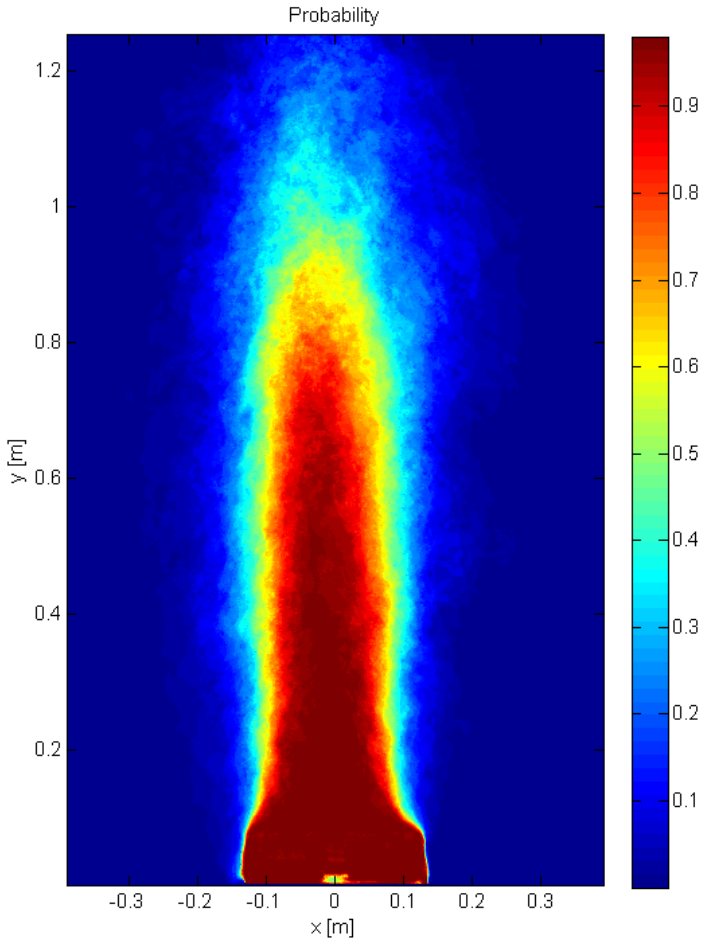

Figure 4.8: Flame probability plot without ceiling (test 22) (B25/heptane).

The flame height results from each test are listed in Table 4.9.

Test	Flame height in plot:	Subtraction:	Actual flame height:
22	1.01	-0.08	0.93
23	1.01	-0.08	0.93
24	1.16	-0.08	1.08

Values given in meter.

Table 4.9: Flame height results from burning heptane in a 25cm squared burner without ceiling.

Flame length overview:

Flame lengths and the corresponding ceiling heights are plotted in Figure 4.9 to make a clear overview. The last test from the experiment with a 1.15m ceiling height did not impinge on the ceiling. It is assumed that the flame is sensitive to turbulence at this ceiling height. Test results from the 1.15 m ceiling height are not included in Figure 4.9 due to the one test with no flame impingement.

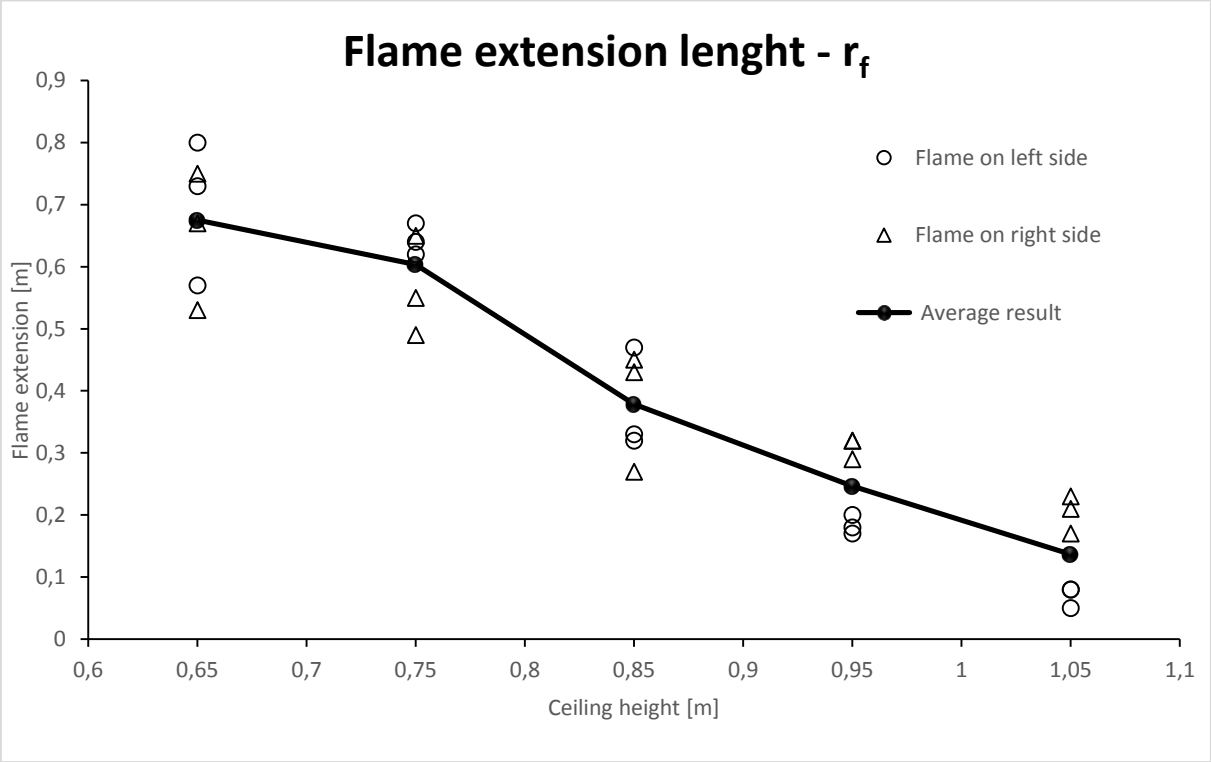

Figure 4.9: Plot of flame length results with various ceiling heights from experiment B25/heptane.

In Figure 4.9 the triangle symbol represent the flame extension lengths at the right side, and the circular symbols the left side. The whole line with black dots represent an average from the results at the same ceiling height.

The ideal situation for performing such experiments is completely quiescent air conditions in the laboratory. This experiment suffered from non-quiescent conditions, which is the main explanation to the deviation from the average-line in the figure. Particularly from one of the experiments with ceiling height at 0.65m, where the flame extension resulted above 0.8 m. This is outside the ceiling of the apparatus.

The average flame lengths do not take the location of the fuel surface into account. Typically, if the flame length is further to one side, it shortens more or less equivalently on the other. Average flame length is still the same, even if the flame is leaning.

4.3.2. Liquid and rim temperatures

Temperatures of the rim of the burner, the liquid surface, and the liquid bottom, are presented in Figure 4.10.

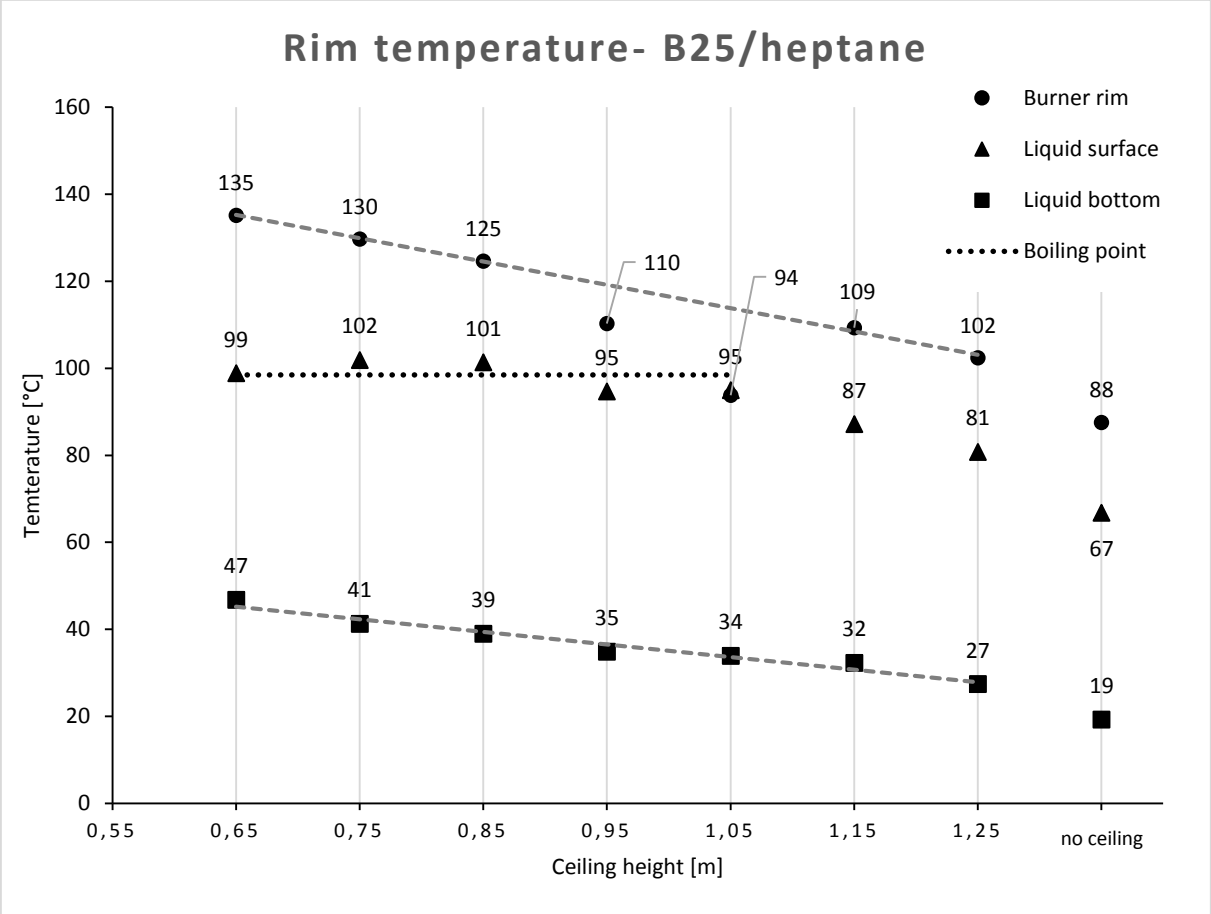

Figure 4.10: Temperatures of the rim of the burner, the liquid surface and the liquid bottom with various ceiling heights (B25/heptane).

The stability of the underlying measurements of liquid temperatures was good, which is considered out of the more or less straight lines shown in Figure 0.1: Liquid bottom temperatures measured by time, sorted by ceiling height (B25/heptane).Figure 0.1 and Figure 0.2 in the appendix (section 9.1). This confirms that equilibrium between heat loss to the lower chamber of the burner and heat supply from the flame is achieved.

Note the gap between experiment with ceiling height 1.25 m and without ceiling. Ceiling absence results in rim temperature 14 °C lower than ceiling height of 1.25m (102 - 88 °C). The liquid surface temperature is also 14 °C lower (81 - 67 °C), and the liquid bottom 8 °C lower (27 – 19 °C).

Temperatures of the liquid surface from the experiments with ceiling heights 0.65, 0.75 and 0.85 m are 99, 102 and 101 °C respectively. As heptane has a boiling point of 98.5 °C, there is a logical reason why the temperatures do not rise further. The highest temperature of 102 °C is represented by the experiment with a ceiling height of 0.75m. This is 3.5 °C above the boiling point. Experiments with ceiling heights of 0.95 and 1.05 m both have temperature measurements of 95 °C, which is 3.5 °C below the boiling point. Taken into account 5% tolerance in temperature measurement, which is 5

°C, reveals that experiments with ceiling heights of 0.95 and 1.05 m also have a boiling liquid. This is also supported by the observations made. These experiments represent a true flame extension under the ceiling.

The liquid surface was boiling in the interface between liquid and rim in every experiment, except the one without ceiling. Liquid temperatures increases linearly with a decreasing ceiling height (up to the boiling point).

However, the burner rim temperature was more unsteady. This is shown in Figure 4.11, which represent the underlying temperatures to the averaged results in Figure 4.10.

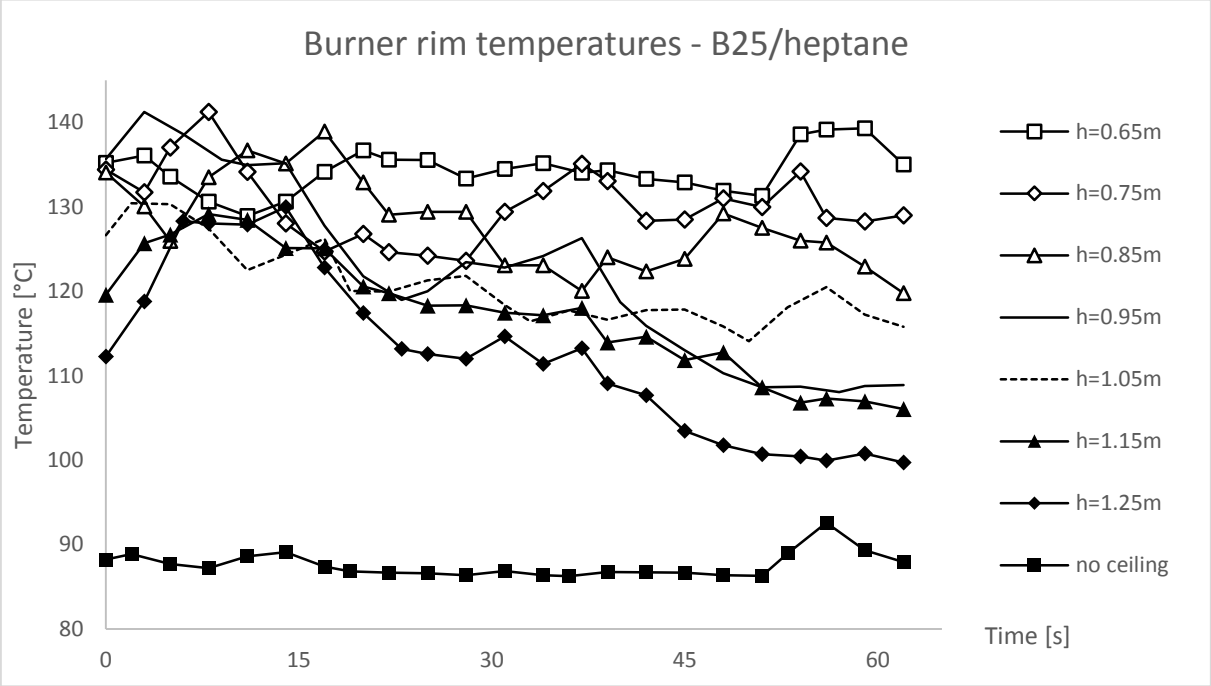

Figure 4.11: Temperature of the rim of the burner over time with various ceiling heights (B25/heptane).

In the beginning, experiments with ceiling heights 1.25, 1.15, 0.95 and 0.85 m increases to temperatures between 120 to 140 °C, and reduces after 15 seconds towards steady state. The last 15 seconds shows temperatures closer to steady state, except the temperature from ceiling heights 0.95 and 1.05 m. Ceiling height 1.05 m give a higher temperature of the rim than from ceiling height 0.95 m. Underlying reasons is discussed further in section 5.5.

Because of the misleading events, the upper trend line in Figure 4.10 does not take into account the temperature from experiments with ceiling heights of 0.95 and 1.05m.

4.3.3. Mass flux

Figure 4.12 shows result of mass flux, which is the flow rate measured by the flowmeter divided by the liquid surface area.

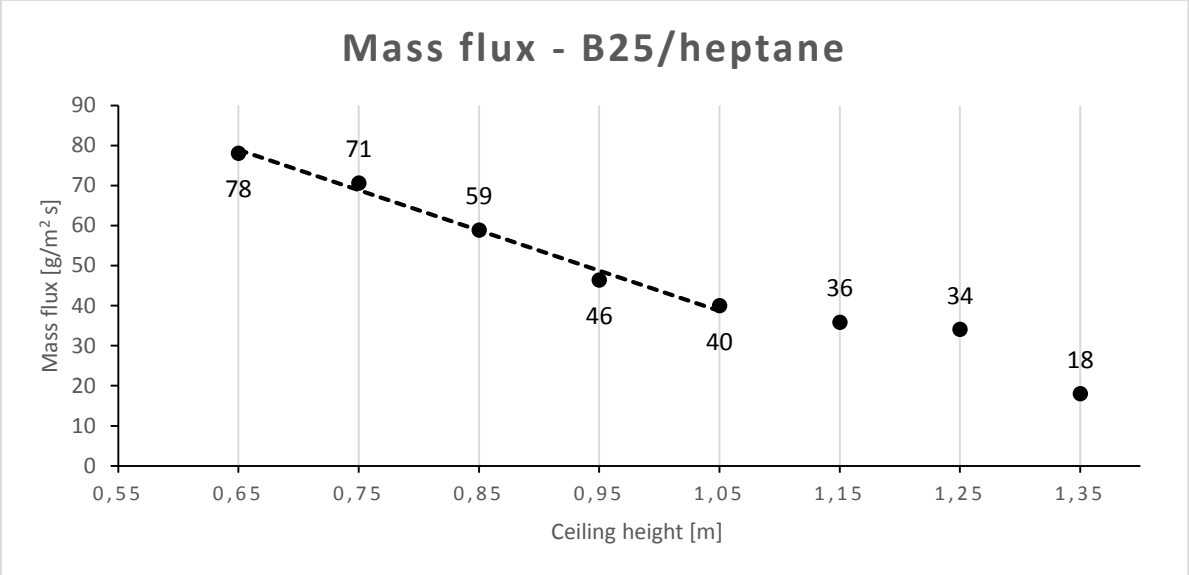

Figure 4.12: Mass flux at different ceiling heights (B25/heptane).

Note: Underlying measurements of mass flux by time is located in Appendix 2 (Figure 0.4).

Figure 4.12 shows a mass flux increasing with decreasing ceiling height, without exceptions. A trend line is plotted for results from ceiling heights with a true flame extension (ceiling height 0.65 - 1.05 m), which shows that mass flux have a linear correlation to the ceiling height.

There is a very small decrease in mass flux of 2 g/m^{2}s from ceiling height 1.15 to 1.25 m (34 – 36 g/m^{2}s). The difference of mass flux between experiment with ceiling height of 1.25 m and experiment without ceiling is 16 g/m^{2}s. The mass flux is primarily ruled by the temperature of the liquid, which also decreases according to Figure 4.10.

4.3.4. Heat flux

The heat flux results given in kilowatts are presented in Figure 4.13.

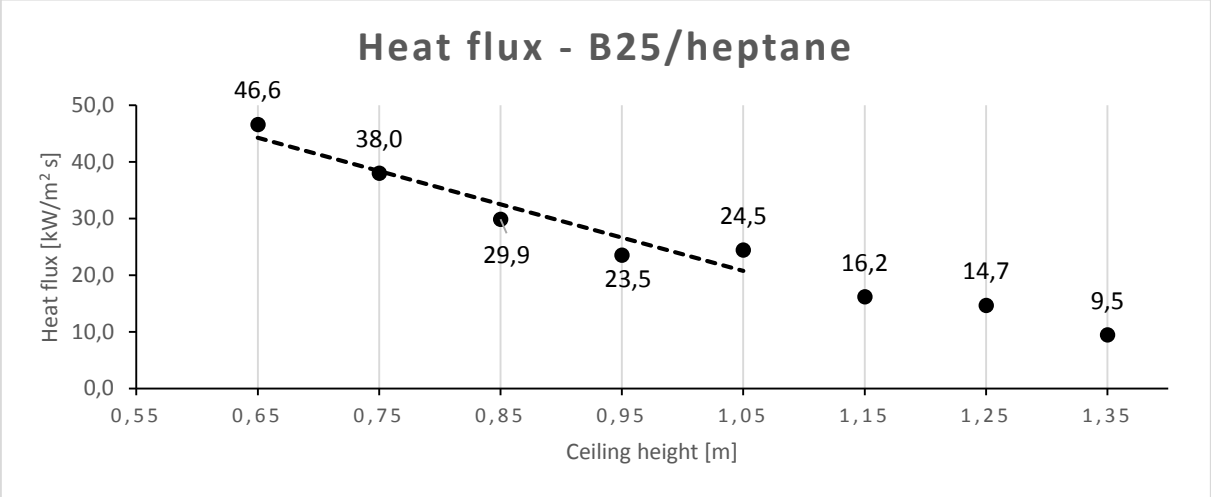

Figure 4.13: Heat flux with various ceiling heights (B25/heptane).

The heat flux is measured on both sides of the burner, exactly 65 mm from the rim. The heat flux resulted in 9.5 kW without the ceiling and 46.6 kW with the lowest ceiling height (0.65 m). The result from experiment with ceiling height of 1.05 m deviates from what is expected. The result is 1 kW more than the ceiling height next step below. If the trend line plotted exclude the result from ceiling height 1.05 m, all results from lower ceilings lay within a straight line.

Underlying measurements of mass flux by time is located in Appendix 2 (Figure 0.4).

4.3.1.Observations

An unexpected observation revealed during the experiments, was the rapidly increase of heat release when the heptane liquid level dropped unintendedly during testing. The fuel supply valve was closed when it should have been open. Unfortunately, there were no measurements done of the liquid temperature or radiation during this incident. The human body felt the remarkable increase in radiative heat, as the liquid level dropped just a couple of centimeters. It was clearly observed an escalation of the boiling within the liquid. It was the increased heat release that caught the attention to something was wrong.

4.1. Experiment B40/heptane

The experiment B40/heptane was unsuccessful. The apparatus worked as intended, but the intense heat release give an unacceptable risk of fire spread in performing further experiments with lower ceiling heights. A lower ceiling give even higher heat release.

The power of the extractor fan and the distance from the fire to other objects in the lab is inadequate. As the heavy smoke yield from the fire requires more power from the extractor fan, even heavier turbulence appear, forcing the flame to lean even more. The extractor fan stayed on until steady state was obtained, which took a while. During this time, risk of igniting the black curtain in the background and the supply system increased. The situation became unpleasant and the experiment was canceled due to safety. The first test was successful and is presented here.

Since there is only one successful experiment, the reliability of the result is poor.

4.1.1. Flame heights and lengths

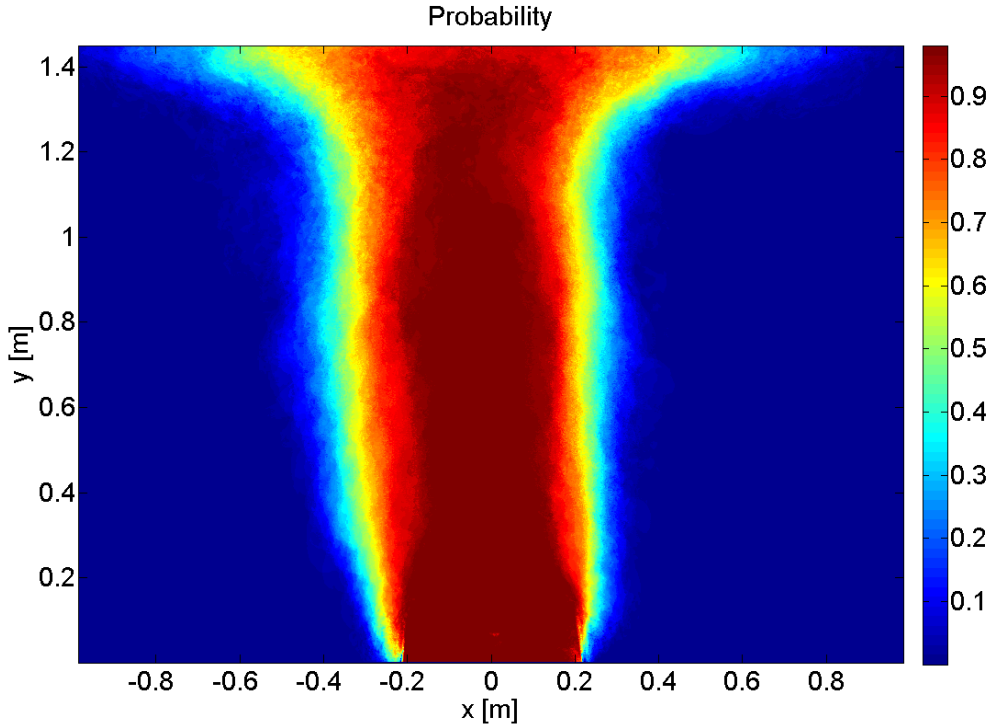

Figure 4.14: Flame probability plot at 1.35m ceiling height, burning heptane in a 0.4 m squared burner. Green color represent 50 percent time presence of the flame.

In Figure 4.14, the vertical axis starts measuring 10 cm lower than the mid-point of the burner, making it necessary to subtract 10 cm from the scale. The horizontal scale is correct. The flame is extending horizontally with length of 0.61 m on the right side, and 0.57 m on the left.

This ceiling height is a good starting point for further experiments. It is expected a longer flame extension length when lowering the ceiling. Until then, a laboratory customized for such heat release is required.

4.1.2. Liquid and rim temperatures

Rim, liquid surface, and liquid bottom temperatures by time, burning heptane in a 40 cm squared burner with a 1.35m ceiling height is shown in Figure 4.15.

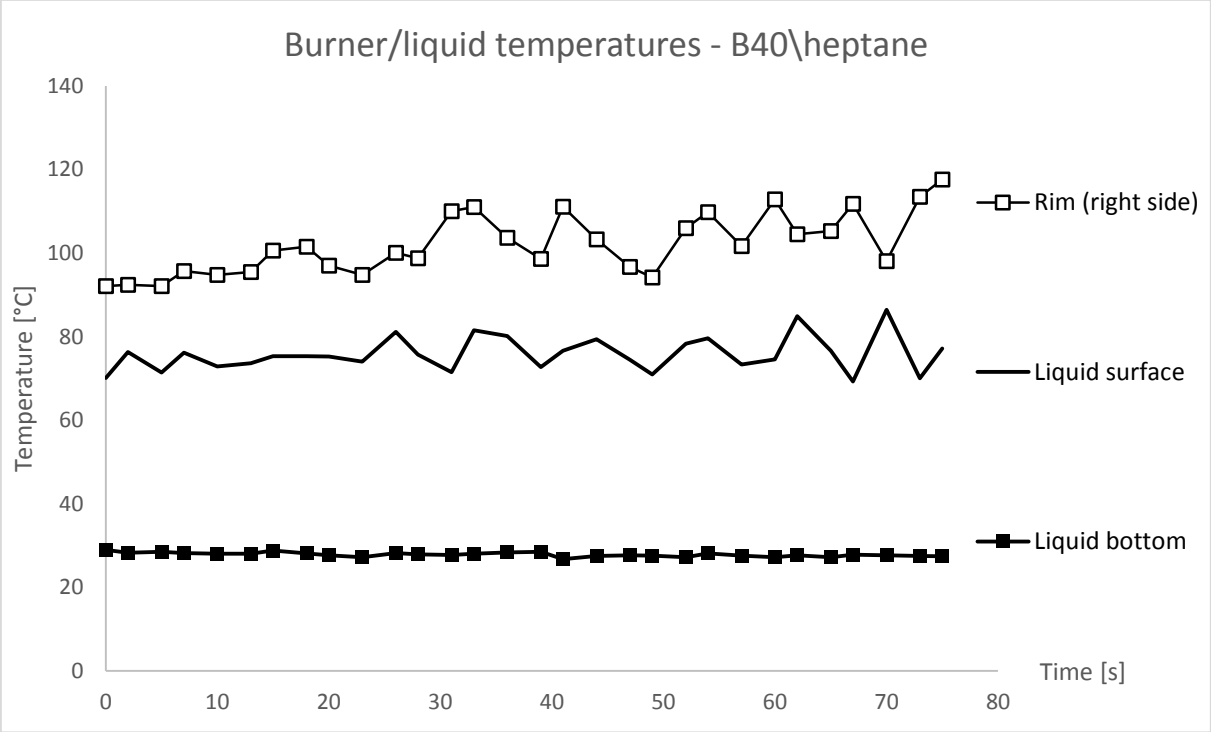

Figure 4.15: Rim, liquid surface, and liquid bottom temperatures from burning heptane in a 0.4 m squared burner with a 1.35 m ceiling height (rim temp. not averaged).

The thermocouple attached to the rim on the left side of the burner lost connection just before steady state was obtained. This was probably due to the intense heat. The thermocouple reconnected itself after the fire was extinguished. Due to this incident, result is not average.

The figure shows rim temperature at the heptane boiling point. After 30 seconds the temperature varies up and down, pending between 95 and 110 °C. The flame struck down on the side of the burner, but this is probably not the reason why. The phenomena also affect the liquid surface temperature, starting at the same time. An explanation can be pulsation.

The liquid bottom is at a steady temperature just below 30 °C.

4.1.3. Mass flux

Figure 4.16 reveals results from the flowmeter divided by the area of the liquid surface inside the burner, giving mass flux.

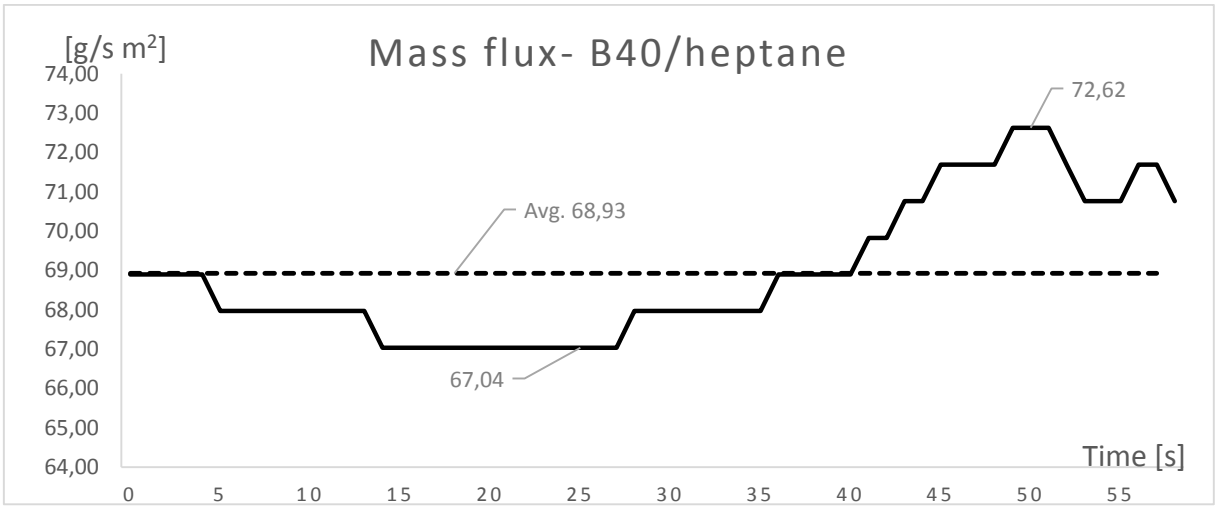

Figure 4.16: Mass flux results from experiment B40/heptane.

The lowest mass flux is 67.04 g/m²s and the highest is 72.62 m²s, which give an average of 68.93 g/m²s. The average mass flux is 69 g/m²s.

4.1.4. Heat flux

The heat flux results given in kilowatts are presented in Figure 4.17.

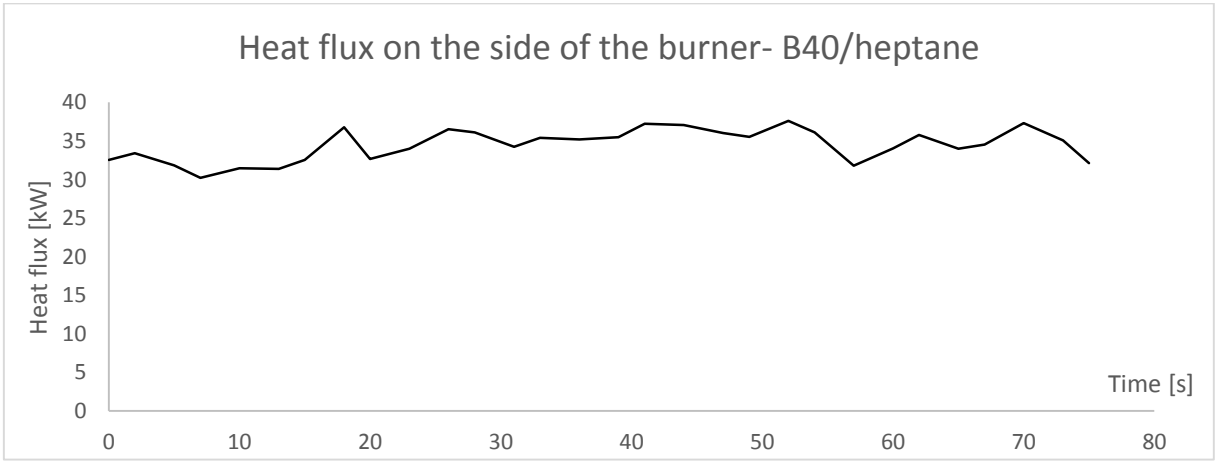

Figure 4.17: Heat flux on the side of the burner.

Results reveals an average heat flux on the side of the burner of 34.5 kW.

4.2. Experiment B25/methanol

4.2.1. Flame height and extension lengths

Flame probability plots from burning methanol in a 0.25 m squared burner is shown in Figure 4.18.

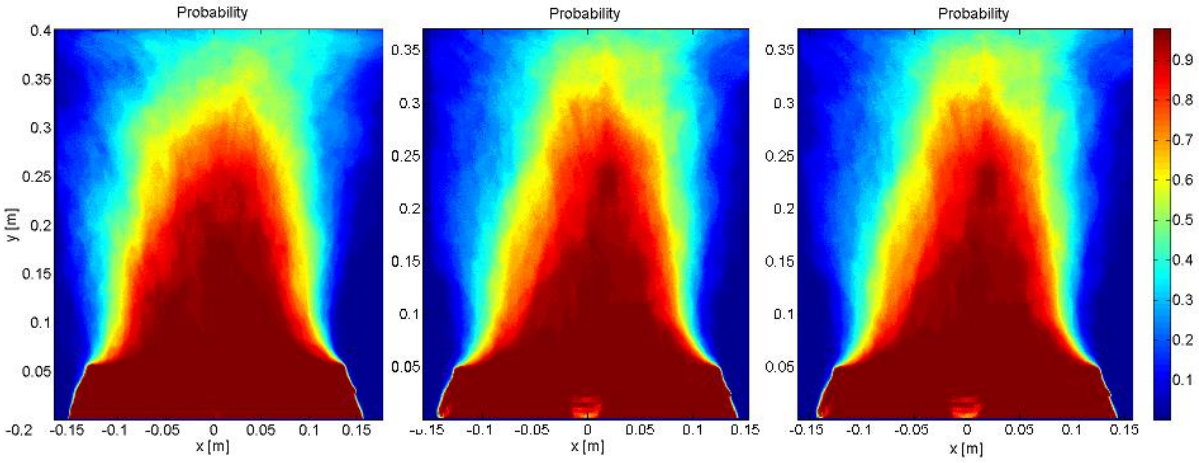

Figure 4.18: Flame probability plots from experiment B25/methanol with ceiling height of 0.35 m.

The flame is barely touching the ceiling with a ceiling height of 0.35 m, leaving the only experiment with flame in contact with the ceiling in experiment B25/methanol. The flame extension is 0.10 m, 0.12m and 0.11 m, giving average flame extension length of 0.11 m.

4.2.2. Liquid and burner rim temperature

Temperatures of the rim of the burner, the liquid surface, and the liquid bottom, are presented in Figure 4.19.

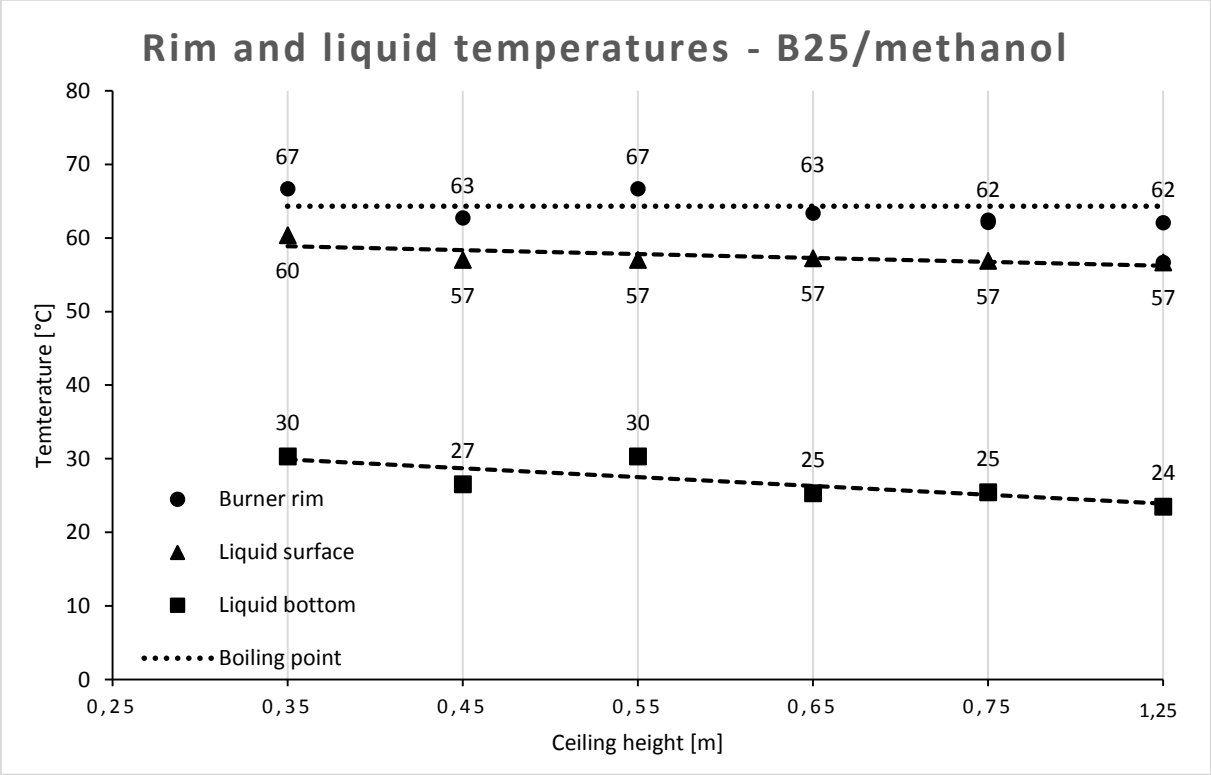

Figure 4.19: Temperatures of the rim of the burner, the liquid surface and the liquid bottom with various ceiling heights (B25/methanol).

Temperatures measured are steady. The boiling point of methanol is 64.6 °C. The liquid temperature is just below the boiling point with all ceiling heights. The changes in temperature from one ceiling height to another are very small.

Note: The last value on the horizontal axis is 1.25 m, not 0.85 m. Ceiling height of 1.25 m is assumed to give very similar results as without ceiling in this experiment.

4.2.3. Heat flux

The heat flux results given in kilowatts are presented in Figure 4.20.

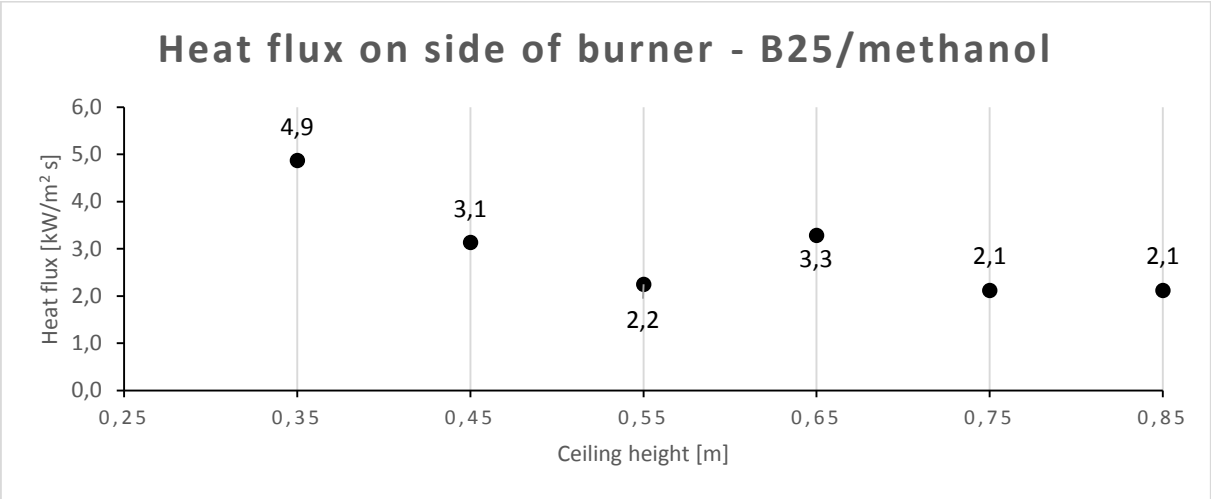

Figure 4.20: Heat flux with various ceiling heights (B25/methanol)

The figure shows that the only ceiling height where flame extension occurred, have a heat flux which is 1.8 kW more than from the ceiling one step higher.

4.3. Experiment B40/methanol

Results from burning methane in the 0.40 m squared burner are presented. It is performed experiments with free burning, and burning under a ceiling at variable heights. The experiment was completed, giving following results.

MatLab failed to find the correct average flame lengths. All lengths read out of the plots manually.

4.3.1. Flame height and extension length

0.35 m ceiling height:

Flame probability plots from burning methanol in a 0.40 m squared burner under a ceiling at 0.35 m height is shown in Figure 4.21Figure 4.18.

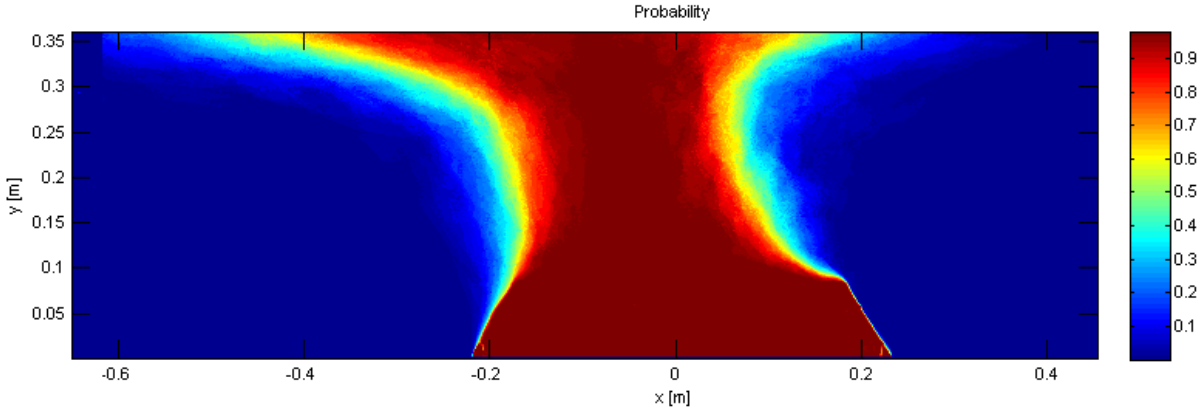

Figure 4.21: Flame probability plot at 0.35 m ceiling height (test 44) (B40/methanol).

The flame length result from each test are listed in Table 4.10.

Test	r_f left:	r_f right:	Average:
44	0.44	0.18	0.31
45	0.47	0.20	0.34
46	0.51	0.18	0.35

Values given in meter.

Table 4.10: Flame length results from burning methanol in a 0.40 m squared burner with 0.35 m ceiling height.

All of the probability plots shows a leaning flame.

Axis symmetry is poor.

0.45 m ceiling height:

Flame probability plots from burning methanol in a 0.40 m squared burner under a ceiling at 0.35 m height is shown in Figure 4.22Figure 4.18.

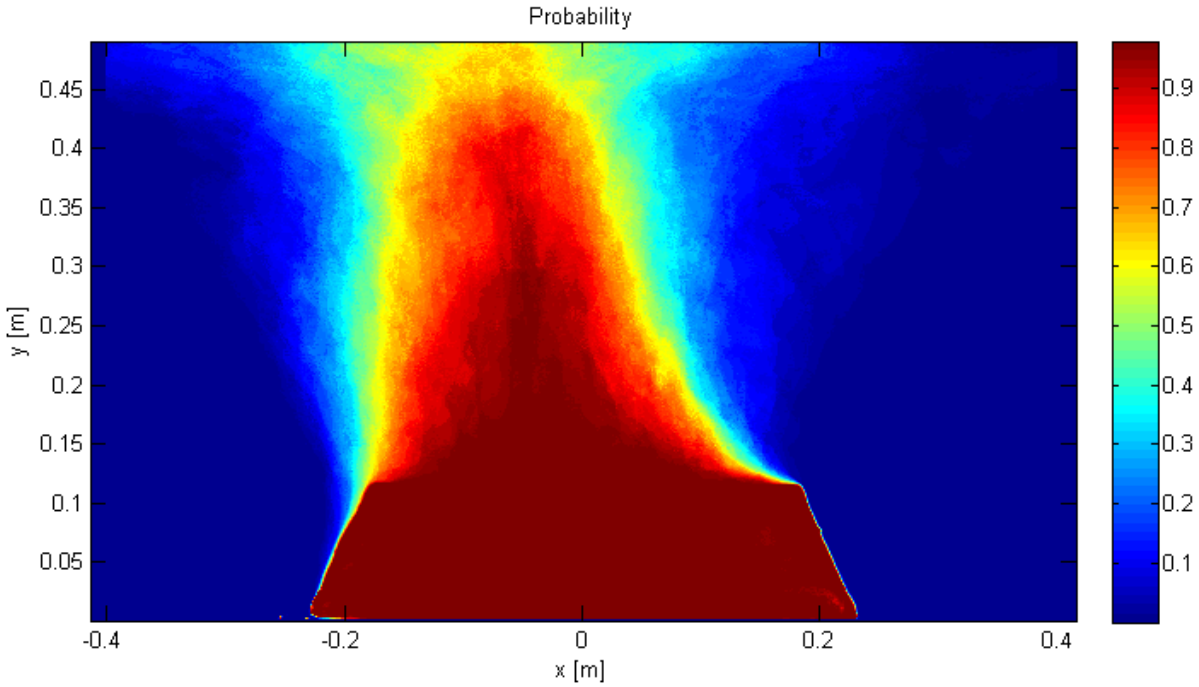

Figure 4.22: Flame probability plot at 0.45 m ceiling height (B40/methanol)

The flame length result from each test are listed in Table 4.11.

Test	r_f left:	r_f right:	Average:
47	0.20	0.01	0.11
48	0.20	0.09	0.15
49	0.23	0.10	0.17

Values given in meter.

Table 4.11: Flame length results from burning methanol in a 0.40 m squared burner with 0.45 m ceiling height.

Flame length is measured to an average of 0.14 m.

Axis symmetry is poor in all tests.

0.55 m ceiling height:

Flame probability plots from burning methanol in a 0.40 m squared burner under a ceiling at 0.55 m height is shown in Figure 4.23.

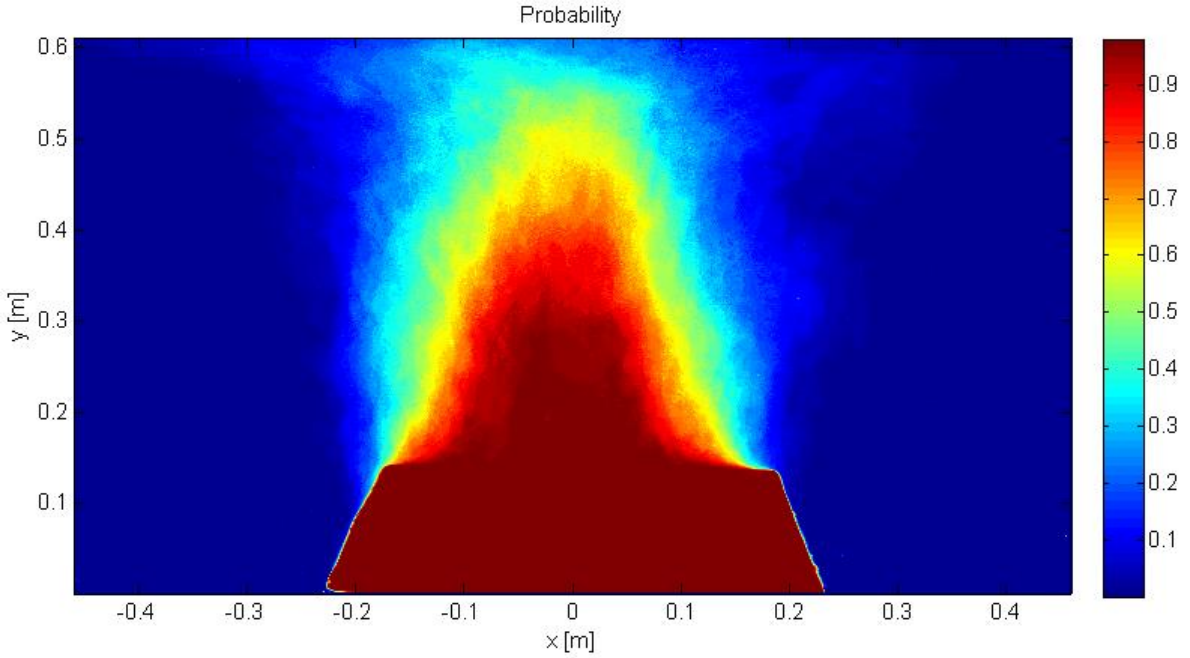

Figure 4.23: Flame probability plot at 0.55 m ceiling height (B40/methanol)

The flame length result from each test are listed in Table 4.12.

Test	Flame height in plot:	Subtraction:	Actual flame height:
50	0.55	-0.05	0.50
51	0.56	-0.05	0.51
52	0.54	-0.05	0.49

Values given in meter.

Table 4.12: Flame height results from burning methanol in a 0.40 m squared burner with 0.55 m ceiling height.

None of the flames from this experiment impinged on the ceiling. Flame height is measured to an average of 0.5 m.

Axis symmetry is good in all tests.

0.65 m ceiling height:

Flame probability plots from burning methanol in a 0.40 m squared burner under a ceiling at 0.55 m height is shown in Figure 4.24.

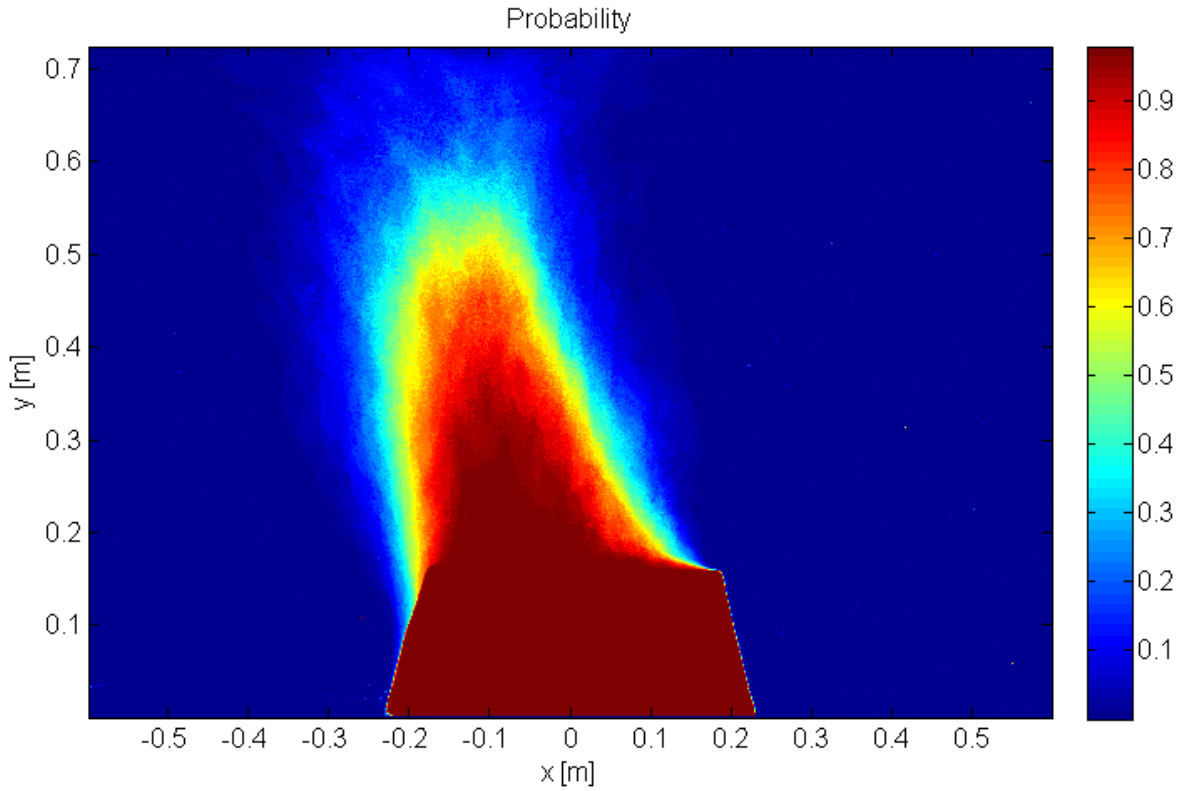

Figure 4.24: Flame probability plot at 0.65 m ceiling height (B40/methanol)

The flame length result from each test are listed in Table 4.13.

Test	Flame height in plot:	Subtraction:	Actual flame height:
53	0.55	-0.07	0.48
54	0.55	-0.07	0.48
55	0.56	-0.07	0.49

Values given in meter.

Table 4.13: Flame height results from burning methanol in a 0.40 m squared burner with ceiling height of 0.65 m.

Flame height is measured to an average of 0.48 m.

Axis symmetry is poor in all tests.

Ceiling height 0.75 and 1.25 m:

Ceiling height 0.75 and 1.25 m give results of flame heights about the same height as the experiment with ceiling height of 0.65 m, which means that the flame height stagnates at this point.

4.3.2. *Liquid and rim temperatures*

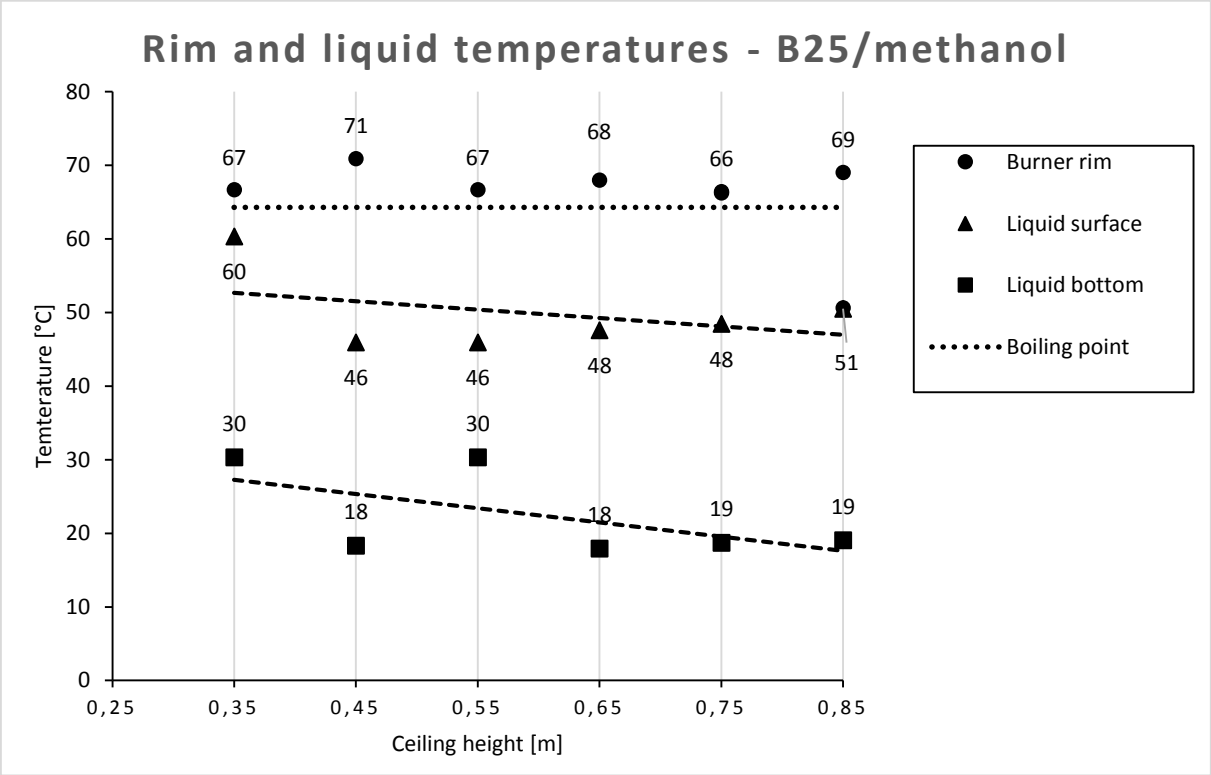

Figure 4.25: Rim temperature when burning methanol in a 40 cm squared burner under various ceiling heights.

4.3.3. *Mass flux*

Figure 4.12 shows result of mass flux, which is the flow rate measured by the flowmeter divided by the liquid surface area

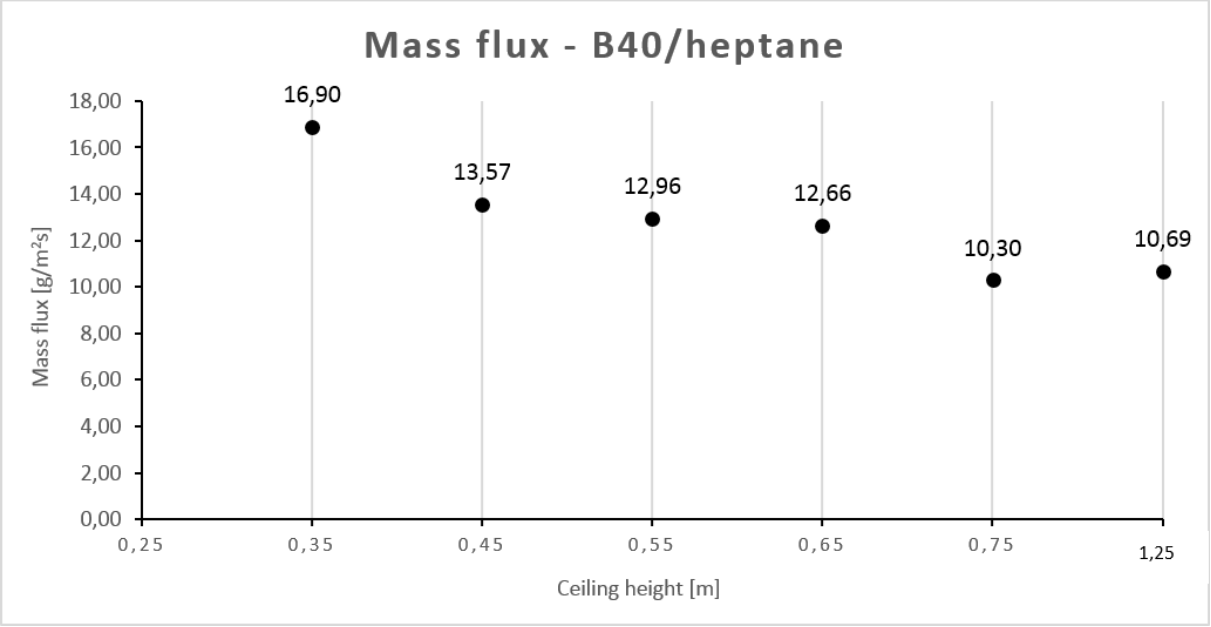

Figure 4.26: Mass flux at different ceiling heights (B25/methanol).

4.3.4. Heat flux

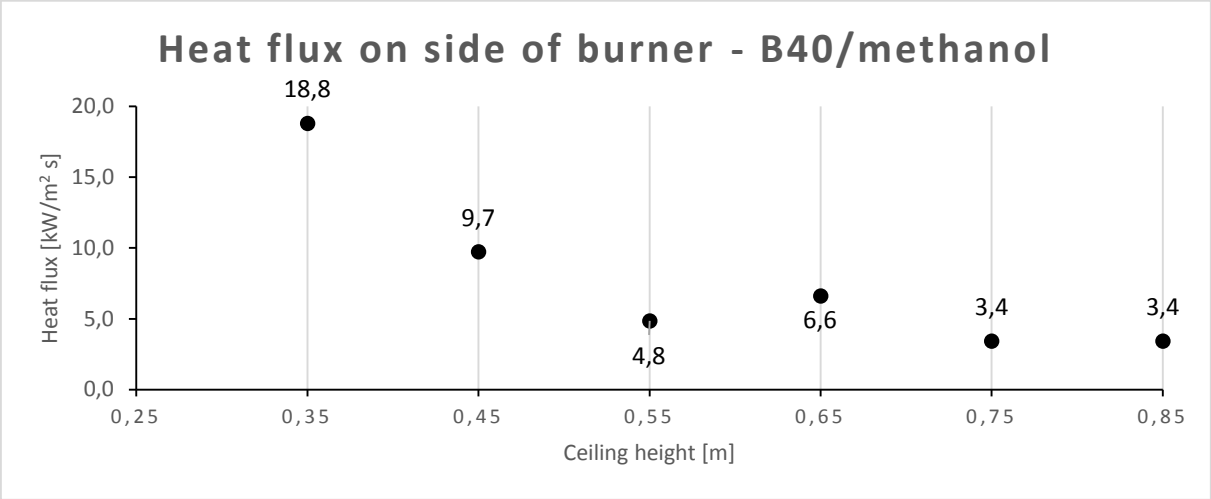

Figure 4.27: Heat flux with various ceiling heights (B40/methanol).

5. Discussion

5.1. Apparatus

The developed apparatus partly achieved the objectives. Some adjustments must be made to the radiative heat flux meter to avoid it from being filled with liquid. When the radiative heat flux meter no longer is useful, the use is wasted. A useless flux meter should be removed instead of displacing liquid surface. Burner sizes used was chosen in order to match combinations of flame height, ceiling length and liquid properties of combustion. The 0.25 m squared burner was perfect for heptane experiments, but too small for methanol. The 0.40 m squared burner was almost wide enough for heptane experiments, but too big for heptane. Only the experiment B25/heptane is considered as successful in this work.

The fuel supply system worked very well and is the main reason to why steady state is achieved in most of the experiments.

5.2. Heat release

The increase of heat release when the liquid surface level drops, was significant. The correlation between heat release and height from the rim to the liquid surface is object for further investigation.

5.3. Length of extending flame

Figure 5.1 shows flame length results from experiment B25/heptane. The horizontal axis represents ceiling height and the vertical axis represents flame length. Big, black dots represent average results from the experiments in this work.

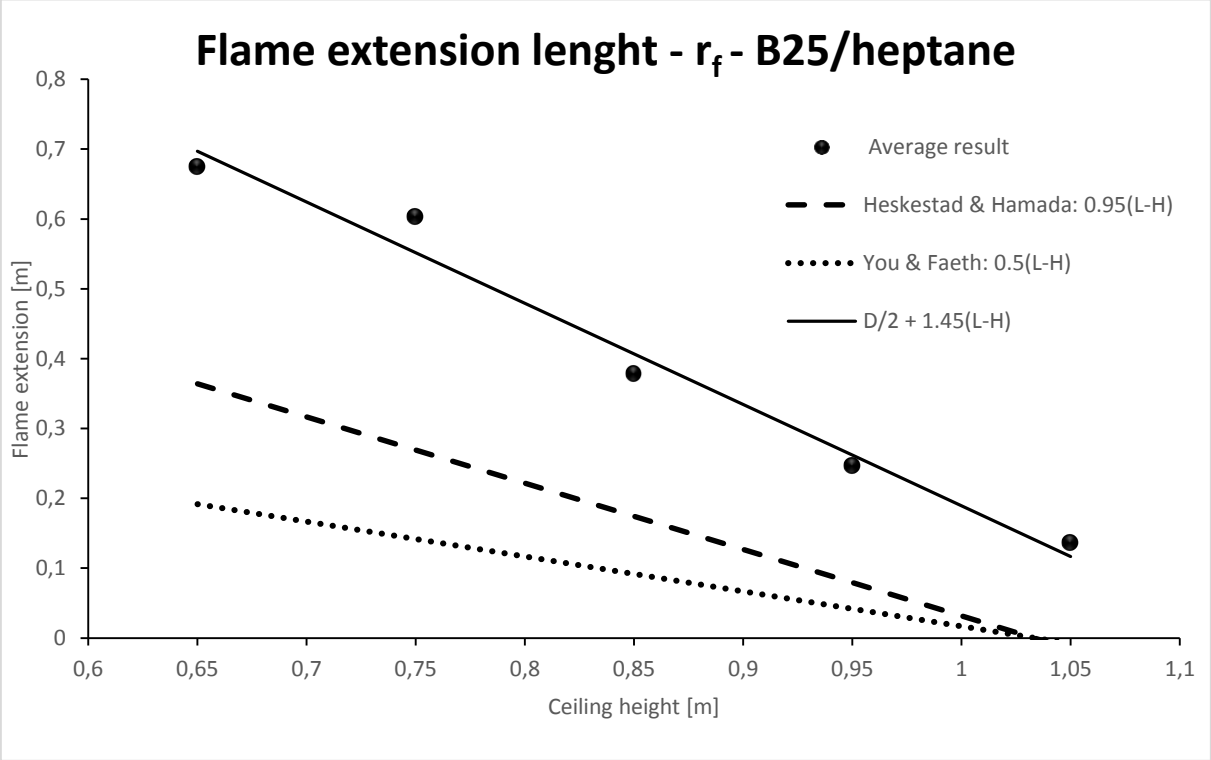

Figure 5.1: Correlation between ceiling height and flame lengths compared with plotted equations developed by Heskestad & Hamada and You & Faeth.

The continuous line represent an empirical equation based on the experiments with heptane in a 25 cm squared burner, given as:

$$r_f = \frac{D}{2} + 1.45(L - H) \qquad \textbf{Eq. 5.1}$$

Where:
D is diameter.
r_f is flame length under the ceiling.
L is free burning flame height.
H is height of the ceiling.

The lower dotted line in Figure 5.1 represent a curve from the empirical equation developed by You & Faeth (see Eq. 2.4 in section 2.2.5). The discontinuous line in the middle represent an empirical equation developed by Heskestad & Hamada (Eq. 2.5 in section 2.2.5).

Figure 5.1 shows that results from the experiments give a greater flame extension length than given by the equation from Heskestad & Hamada, and much greater than the equation from You & Faeth. The main reason is most likely the difference in combustion properties of the fuels used. Both of them used gas as fuel that yields less smoke than heptane pool fires.

The equation for estimating flame height developed by Heskestad (Eq. 2.2 in section 2.2.5), gives a result in flame height of 0.86 m. The equation is dependent of the energy release rate. A consideration points to an inequality in heat release. Higher liquid temperature in the experiments in this work is one possible contribution to the greater heat release.

5.4. Flame heights

Experiment B25/heptane with a 1.25m ceiling height results in a flame height that is greater than from free burning. The 1.25 m ceiling height experiment has a liquid surface temperature of 81 °C while the free burning experiments have a temperature of 66.8 °C. None of the experiments have extending flames. The heat increase must be due to heat radiation to the liquid surface from a ceiling heated by the plume. In addition, the flame height is defined by the time-mean criteria. Flame impinging on the ceiling still occur, but the intermittency (or probability) of the flame is then less than 0.5.

5.5. Temperatures

Gaps in rim and liquid temperature between experiment with ceiling height 1.25 m and without ceiling, was expected. Absence of ceiling result in rim and liquid surface temperature 14 °C lower than with ceiling height of 1.25 m. The liquid bottom temperature was 8 °C lower. This is primarily due to the ceiling is heated by the plume and radiates heat to the fuel bed. However, an uncertainty appeared once the experiment without ceiling became impossible to perform the same day. While dismantling the ceiling, the Board attached to the ceiling frame made cracks and needed repair. Fuel drainage became necessary and takes time. The uncertainty is to whether surroundings are identical. It can occur temperature change in the cooling water by a few degrees that affects the burner and the liquid temperature. With changed liquid temperature follows changed evaporation of fuel. This affects the flame height used in Eq. 2.4 and Eq. 2.5 on page 6.

There are instability within the burner rim temperatures in the experiments, see the early stage of graphs in Figure 5.2.

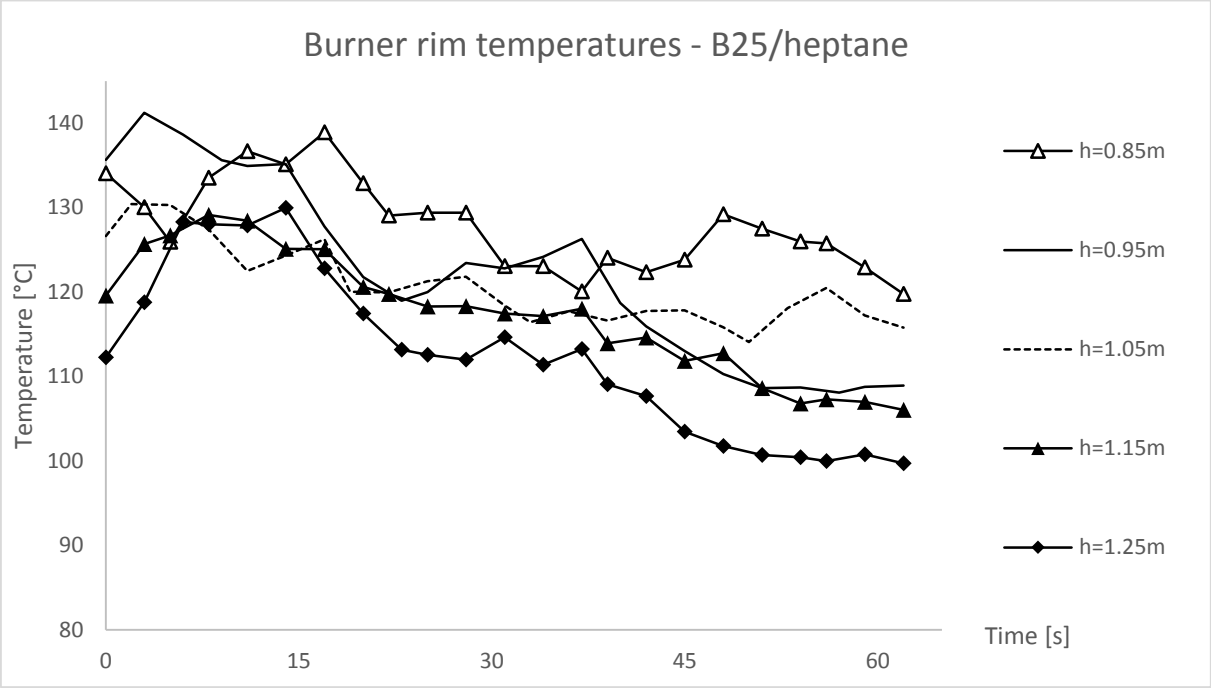

Figure 5.2: Temperature of the rim of the burner over time for selected ceiling heights (B25/heptane).

Experiments with ceiling heights 1.25, 1.15, 0.95 and 0.85 m increases to temperatures between 120 to 140 °C, and reduces after 15 seconds towards steady state. This instability is most likely due to the turbulence in the surrounded air. The flame is touching the outside of the rim where the thermocouples are attached to the steel. Thermocouples gets heated by the flame and do not reflect the realistic temperature of the rim, but a higher. This might be a result from not waiting long enough for air conditions to settle after the extractor fan is off and the vent is closed. The waiting time prior to measurements was set to where the flame was assessed visually as stabilized. It is showed by the temperatures of the rim in Figure 5.2 that the waiting time was inadequate. Waiting time should have been extended by another 30 seconds.

The last seconds shows that these curves have switched places from what is expected.

The last 15 seconds of Figure 5.2 shows temperatures closer to steady state, except the temperature from ceiling heights 0.95 and 1.05 m. Ceiling height 1.05 m give a higher temperature of the rim than from ceiling height 0.95 m. (explain)

6. Conclusions

Experiments performed in this work indicates flame lengths according to an equation gives as:

$$r_f = \frac{D}{2} + 1.45(L - H)$$

Where:
D is diameter.
r_f is flame length under the ceiling.
L is free burning flame height.
H is height of the ceiling.

The equation is based on experiments carried out from only one pool fire size.

Experiments performed indicates that the mass flux increases linearly with reduced ceiling height above a heptane pool fire with a diameter of 0.275 m.

Experiments shows that empirical equations developed by Heskestad & Hamada and You & Faeth with the purpose of estimating the flame length under ceiling, give results of significantly shorter flame lengths than appearing from burning heptane liquid.

7. References

1. **You, H. Z. and Faeth, G. M.** *An investigation of fire impingement on a horizontal ceiling.* University Park, Pennsylvania : Mechanical Engineering Department, Pennsylvania State University, October, 1978. NBS-GCR-79-188.

2. **Björn Karlsson, James G. Quintiere.** *Enclosure Fire Dynamics.* s.l. : CRC Press LLC, 2000. ISBN 0-8493-1300-7.

3. **Hinkley, PL. Wraight H.G.H, and Theobald, C.R.** *The contribution of flames under ceilings to fire spread in compartments. Part 1: Incombustible ceilings.* Fire Research Note 712. : s.n., 1968.

4. **Drysdale, Dougal.** *An introduction to Fire Dynamics, Third edition.* University of Edinburgh, Scotland, UK : John Wiley & Sons, Ltd., 2011. ISBN 978-0-470-319-03-1.

5. **Heskestad, G. and Hamada, T.** *Ceiling Jets of Stron Fire Plumes.* s.l. : Fire Safety Journal, Vol 22, pp. 69-82, 1993.

6. **You, H. Z. and Feath, G. M.** *An investigation on Fire Impingement on a Horizontal Ceiling. NBS-GCR-81-304.* CFR, Gaitherburg, MD : National Bureau of Standards, 1981.

7. **Hamins, A., Kashiwagi, T. and Buch, R.** *Charactersistics of Pool Fire Burning, Fire Resistnce of Industrial Fluids, ASTM STP 1284, Totten and Jurgen Reichel.* Eds. American Society for Testing and Materials. Philadelphia : s.n., 1995.

8. **Beyler, C. L.** Fire Plumes and Ceiling Jets. *Fire Safety Journal, 11 (53-75).* Worcester, MA 01609 (U.S.A) : Center for Fire Safety Studies, Worcester Polytechnic Institute, 1986.

9. **G., Heskestad.** *Fire Plumes.* Quincy, MA : SFPE Handbook of fire protection Engineering, 2nd ed. National Fire Protection Association, 1995.

10. **Hottel, H. C.** *Fire Research Abstracts Reviews (1, 41).* 1959.

11. **McCabe, Warren L., Smith, Julian C. and Harriot, Peter.** *Unit Operations of chemical engineering, 7th edition.* New York : McGraw-Hill, Internal Edition 2005. ISBN 007-124710-6.

12. **Hamins, A., et al.** *Heat Feedback to the Fuel Surface in Pool Fires.* s.l. : Building and Fire Research Laboratory , National Institute of Standards and Technology, Gaithersburg, MD 20899 and School of Mechanical Engineering, Pardue University, West Lafayette, IN 47907., Reprinted from Combustion Scienence and Technology, Vol. 97, No. 1-3, 37-62, 1994.

13. **Burgess, D. and Hertzberg, M.** *In Heat Transfer in Flames, (Eds.: N.H. Afgan and J. M. Beers).* New York (NY) Chapter 27 : John Wiley & Sons, 1974.

14. **Burgess, David, Strasser, Alexander and Grumer, Joseph.** *Diffusive Burning of Liquid Fuels in Open Trays.* Pittsburgh, Pennsylvania : U. S. Department of the Interior, Bureau of Mines, Explosive Research Laboratory, 1961.

15. **Hamins, Anthony, Yang, Jiann C. and Kashiwagi, Takashi.** *A Global Model for Predicting the Burning Rates of Liquid Pool Fires (NISTIR 6381).* Gaithersburg, MD 20899 : National Institute of Standards and Technology, 1999.

16. **Babrauskas, V.** *Burning Rates.* Quincy, MA, USA : National Fire Protection Association, 1995.

17. **Lide, D. R.** *Handbook of chemistry and physics, 74th Edition.* Ohio : Chemical Rubber Company , 1993/1994.

18. **http://www.chemicalbook.com. [Online] Chemicalbook. http://www.chemicalbook.com/ChemicalProductProperty_EN_CB0426554.htm.**

20. Zabetakis, M. G. and Burgess, D. S. ***Research on the hazards associated with the production and handling of liquid hydrogen.*** **RI5707, Pittsburgh, PA. : US Bureau of Mines, 1961.**

8. List of contents

8.1. Figures

8.2. Pictures

8.3. Tables

9. Appendix

Appendix on the following pages.

Appendix 1

Flowmeter correction factor

Actual flow measurement I given by:

$$Q_2 = \frac{(w_1 - w_0)}{\rho \Delta t}$$

Correction factor is given by:

$$C_{corr} = \frac{Q_2}{Q_1}$$

Where:
w_1 is the initial weight of the can used [g].
Q_1 is the value read on the flowmeter scale [l/h].
Δt is the flow duration [h].
w_2 is the weight of the can after [g].
ρ is the density of the fluid [g/cm³].
Q_2 is the actual flow [l/h].

Average correction factor:

$$C_{fluid} = \frac{C_{corr\,1} + C_{corr\,2} + C_{corr\,3}}{3}$$

Fluid densities:

Methanol:	ρ_{met}	0,7918 g/cm³
Heptane:	ρ_{hep}	0,6795 g/cm³

Methanol flow correction:

	Sample 1	**Sample 2**	**Sample 3**
w_1	1107,7 g	1108,1 g	1106,5 g
Q_1	30,5 l/h	42,5 l/h	31,75 l/h
Δt	0,15 h	0,094 h	0,089 h
w_2	5977,1 g	5218,1 g	4023,8 g
$\boldsymbol{Q_2}$	**41,0 l/h**	**55,22 l/h**	**41,40 l/h**
$\boldsymbol{C_{corr}}$	**1,344**	**1,214**	**1,304**

Average correction factor for heptane flow:

$$C_{met} = 1{,}32$$

Heptane flow correction:

	Sample 1	**Sample 2**	**Sample 3**
w_1	1305,5 g	1308,0 g	1312,4 g
Q_1	39,5 l/h	47,5 l/h	35,0 l/h
Δt	0,10 h	0,124 h	0,137 h
w_2	5572,6 g	7420,4 g	6585,6 g
$\boldsymbol{Q_2}$	**62,80 l/h**	**72,54 l/h**	**56,65 l/h**
$\boldsymbol{C_{corr}}$	**1,590**	**1,527**	**1,619**

Average correction factor for heptane flow:

$$C_{hep} = 1{,}587$$

Appendix 2

Additional results from experiment B25/heptane

9.1. Liquid and burner rim temperatures

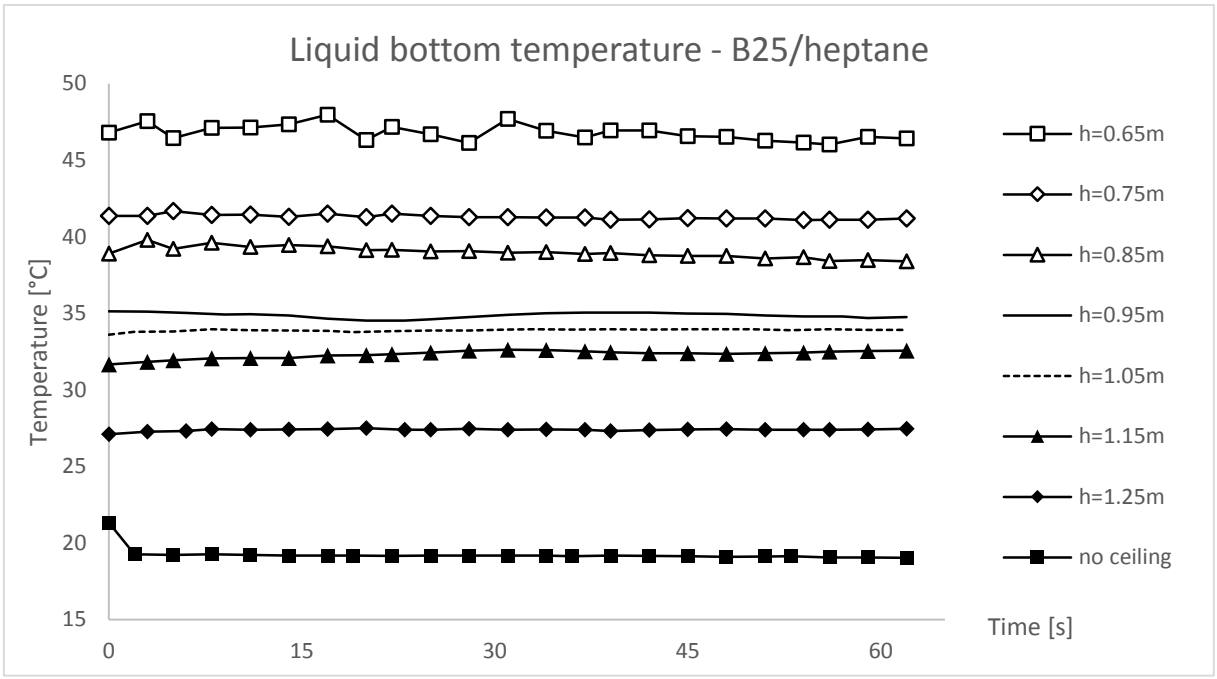

Figure 0.1: Liquid bottom temperatures measured by time, sorted by ceiling height (B25/heptane).

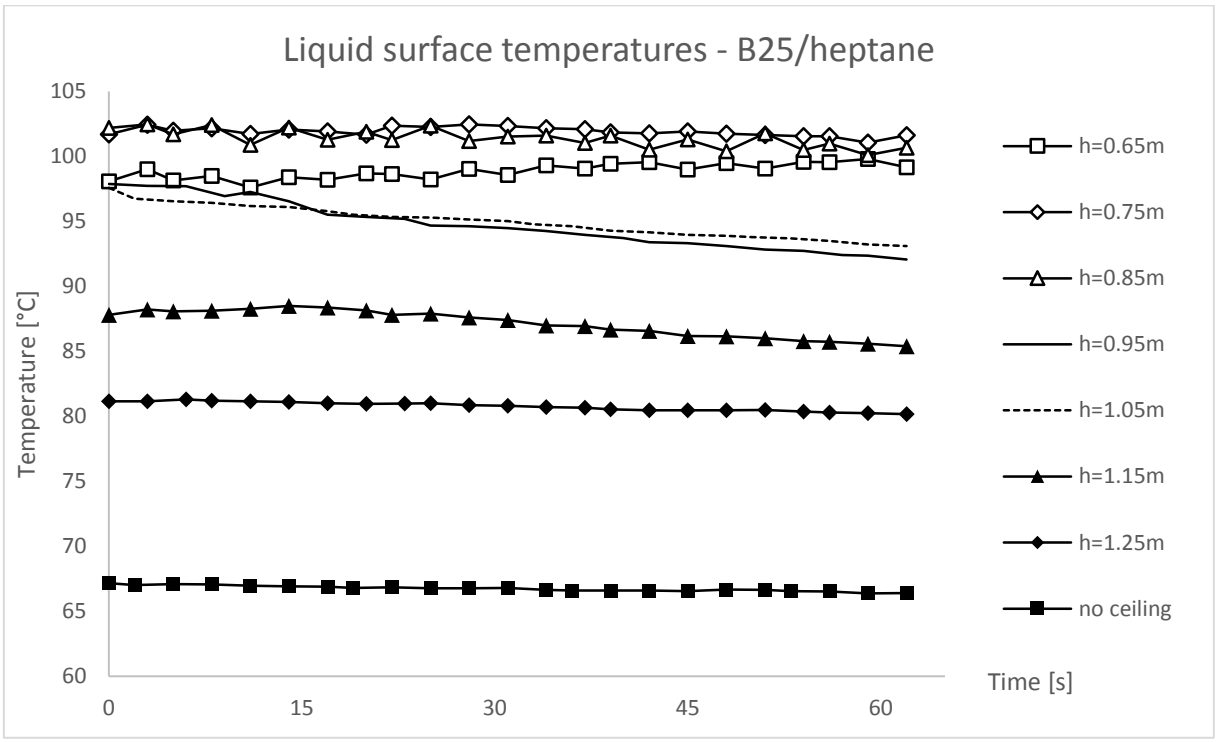

Figure 0.2: Liquid surface temperatures measured by time, sorted by ceiling height (B25/heptane).

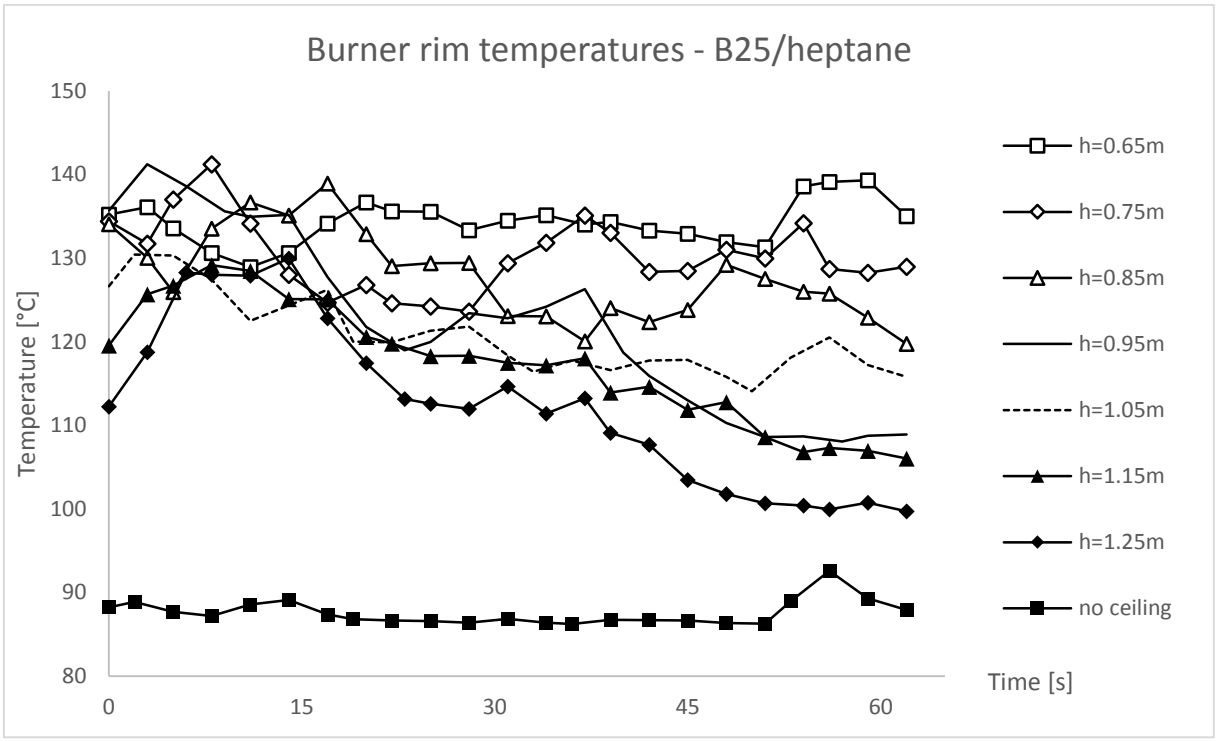

Figure 0.3: Burner rim temperature measured by time, sorted by ceiling height (B25/heptane). Copy of Figure 4.10.

9.2. Mass flux

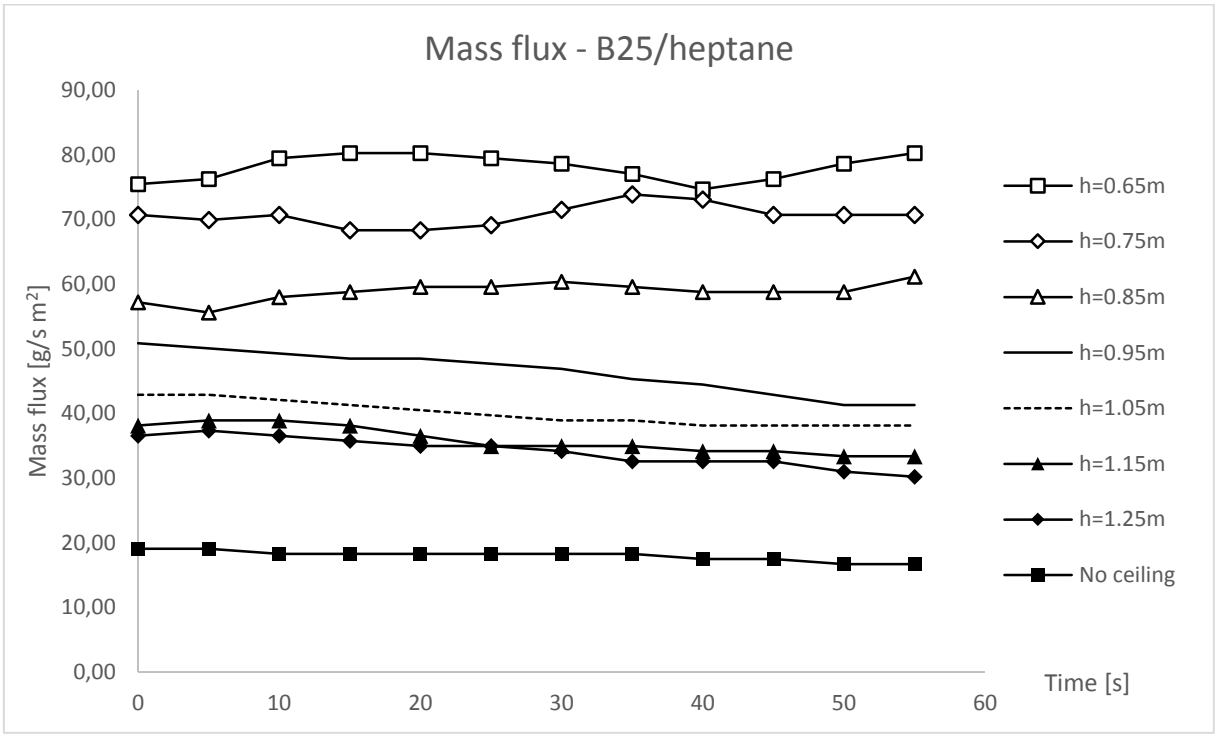

Figure 0.4: Mass flux measured by time (B25/heptane).

9.3.Heat flux

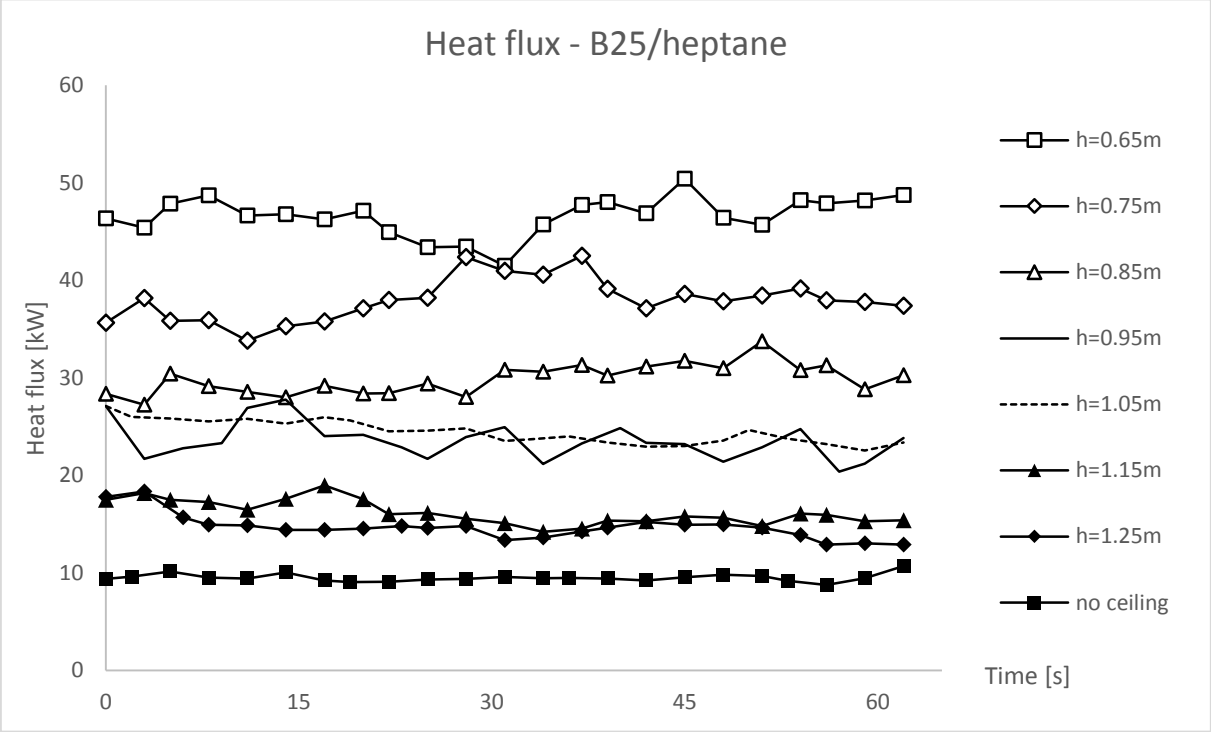

Figure 0.5: Heat flux measured by time on both sides of the burner (B25/heptane)

Appendix 3

MatLab image processor documentation on the next pages.

STORD/HAUGESUND UNIVERSITY COLLEGE

Flame Image Processor

- *Internal Report*

David R U Johansen
21.11.14 Haugesund

Høgskolen Stord/Haugesund
Klingenbergveien 8
5414 Stord

david.johansen@hsh.no
+47 52702728
+47 97179241

Table of Contents

1 Introduction

This document is describing the use of *Flame Image Processor* and program code. The main purpose of the program is to process digital images from fire experiments to filtrate the background of an image where a flame is present. Filtrated images can further be used in Particle Image Velocimetry (PIV) processing. The program can compute various flame characteristics as flame lengths, volume and oscillation frequency. Flame Image Processor is written in MATLAB and uses the Digital Image Processing tool extension.

Flame Image Processor is an open source program and is used at your own risk. The developer takes no responsibility or liability for any use. The author would appreciate feedback and suggestion of how to improve the program, or extensions provided by other contributors.

Flame Image Processor is an in-house program and contains parts from other program. Consequently, due to license restriction the program may not be distributed to other organizations or institutions. The author would like to acknowledge Dr. J. Kristian Sveen, developer of MatPIV[1]. Cross-correlation functions written by Dr. Sveen is implemented in this program.

[1] http://folk.uio.no/jks/matpiv/index2.html

2 Experimental Procedure

Prior and during the experiments the following procedure must be followed:

1) Enable RAW format on the camera.
2) Ensure that the background is properly illuminated.
3) Place calibration plate in the plane of interest, typically on top of the burner. The calibration plate must be close to perpendicular to the sight line of the camera, both with respect to height and radial direction.
4) Take picture of the calibration plate, then remove it.
5) Take picture of the background.
6) Light up the burner and start image sequence on the camera.

The camera must be set on RAW format in order to use pixel information in the image processing. A calibration plate is needed to calculate the magnification factor ([m/pixel]) which is a factor for converting pixel length in to world length. Ensure sufficient contrast between the black square on the calibration plate and the white sheet by illuminating it with an external light source.

The philosophy in the tool is to first filtrate the background from the flame. In order to achieve this, the background must be as similar as possible in the reference image (step 5) and the image sequence of the flame. A sooty flame (which is the case in most natural fires) will illuminate the background. To work around this, the background must be illuminated by an external light source on both the reference image and the image sequence of the flame. In case of a little sooty flames, e.g methanol, an external light source is not necessary. The author recommends an external light source stronger than 10,000 lumen or approximately 500 W halogen lamp. Other recommendation to achieve good-quality images, these tips may be followed:

- Set up the camera with a very short shutter time
- Avoid bright colours, metal or other device that reflect light or even better; place a large piece of black fabric in the background
- Maximize the distance from the flame to the background
- Turn of the light in the room

The user must assess the required frame rate on the camera and the length of the image sequence (in step 6). Due to nature of fires the flame is fluctuating approximately 1-5 Hz. Typically, 10-20 frames per second and a sequence of 10-20 seconds, or in total a sequence of a couple of hundreds images is probably sufficient.

For computation of non-transient variable; flame length and volume the sampling frequency is not crucial. The reason for this is that these variables are computed based on probability of presence of the flame. However, a sufficient number of frames must be processed to achieve sufficient symmetry of the flame.

3 Computing Procedure

A run file for filling in the input data is created to run the program. Before running the code:

1. Create a parent directory. In fig. 2 the directory structure is illustrated.
2. Convert all images to a format supported by MATLAB. The RAW images are typically .CR2 files or similar. These must be converted to a readable format. The author recommends TIF. Conversion may be done in Photoshop of in other photo editing software. If not optimal settings are used on the camera and the arrangement of the experiments optimal, the background is not black and monochrome. This may be fixed by editing the images in photo editing software. Note that a lot time may be spared if tips in listing in sec. 2 are followed.
3. Next, image of the calibration plate must be cropped so that only the calibration plate is visible on the image, as seen in figure 1. Unfortunately, the code is not that sophisticated to trace the calibration plate on an image automatically and is the reason for executing this step. Rename the image of the calibration plate to “caliplate.tif”.

Figure 1: Cropping image of calibration plate.

4. Rename the image of the background or reference image to “background.tif”.
5. Move “caliplate.tif” and “background.tif” into the parent directory created in step 1.
6. Create and move the image sequence in the directory “images_in”. The directory “images_in” must be placed in the parent directory that is created in step 1 (fig. 2). The program is able to automatically read the image sequence. Any special naming of the files are not required except that the numbering must be the same order as the images are recorded.
7. Fill in input data “run_flameIP.m” and run the file. In tab. 1 a description of the input variables are found. Note that the run time may be very long; in order of a couple of hours for approximately a couple hundred images with resolution around a megapixel.

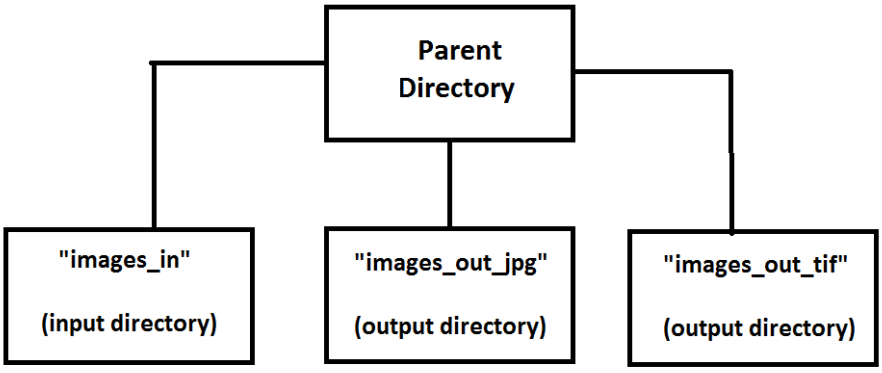

Figure 2: Organization of directories.

Table 1: Description of input variables.

Variable	Description
workingDir	The path to the parent directory, eg.: "*C:\mydirectory*"
dt	Separation time of the image sequence. [c]
fps	Frames per second of the output video. Cannot be less than 3 (reason: unkown).
ss	World square length on the calibration plate in [mm].
n_squares	Number of squares on the calibration plate.
cali_filt	Model constant for filtrating of calibration plate in pixel intensity unit. Recommended: 15-20
bg_filt	Model constant for filtrating of background in pixel intensity unit. Recommended: 15-20
ws	Averaging window size in pixel unit. Recommended: 3 (or 5).
elevate	Elevation of origin in pixel unit.
hori	Mode: Horizontal flame length for investigation of flame lengths under ceilings. [a]
diag	Mode: In case of vertical flame length; diagonal flame length. [a]
lf_crit	Flame length criteria. 0.5 corresponds to 50% presence. Based on probabilistic array. [b]
fv_crit	Flame volume criteria. 0.5 corresponds to 50% presence. Based on probabilistic array. [b]
flame_transient	Mode: Transient flame length. [ac]
flame_lenght	Mode: Flame length based on probabilistic presence. [a b]
flame_volume	Mode: Flame volume based on probabilistic presence. [a b]
flame_oscillation	Mode: Flame oscillation frequency (transient) . [ac]
laminarization_filter	Application for PIV: Filtrating pixels with no changes from frame to frame in order to reduce noise. [ac]

[a] Logical expression: 1==.TRUE. and 0==.FALSE.

[b] Based on probabilistic computation.

[c] Used in transient computation

Finally, verify that the numerical variables in the input file are appropriate. If necessary, change the variables and run the file again. For more information, read in sec. 4 about how the program works. A movie is written in the compressed AVI format. This movie must be opened in software that supports this format. The author recommends Video LAN Client [2] (VLC).

4 Program Code

This section is describing how the program works and is crucial to understand to know the limitations.

4.1 Calibration Plate

1. Converting image to grayscale
2. If pixel intensity is larger than *cali_filt* the pixel intensity is set to black (value 0) else it is set to white (value 1)
3. Grayscale image is converted to a binary file
4. Squares in the image are traced
5. Total pixel area of the square are computed
6. The Maginification factor, *M,* is computeted: *M = physical area/pixel area*

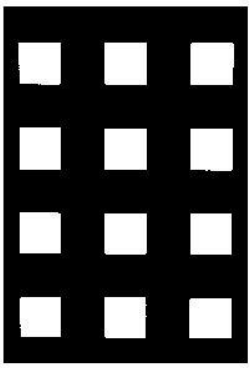

Figure 3: Filtrated image of calibration plate.

4.2 Flame Filtration

The flame filtrating function is removing the background of the images to identify the position of the flame at the specific instances. Filtrated images are used further on in computing the flame characteristics. Procedure of this function is:

1. Converting background image ("background.tif") and the input image. The code is processing one input image completely before starting on the next one.
2. If the pixel intensity difference between the background image and the input image is greater than *bg_filt*, flame is present in that pixel and is set to white (value 1). If it is not, the pixel intensity is set to black (value 0). If the camera is triggered manually (not remotely) the

[2] http://www.videolan.org/vlc/

position might change slightly; a model constant is therefore used for averaging pixel intensity of the background image, as illustrated in fig. 4. Furthermore, *bg_filt* must be decreased if weaker flame areas are desired to consider. However, this might result in not removing certain areas of the background – unless the contrast between the flame and the background is sufficiently large to the flame and the background is monochrome.

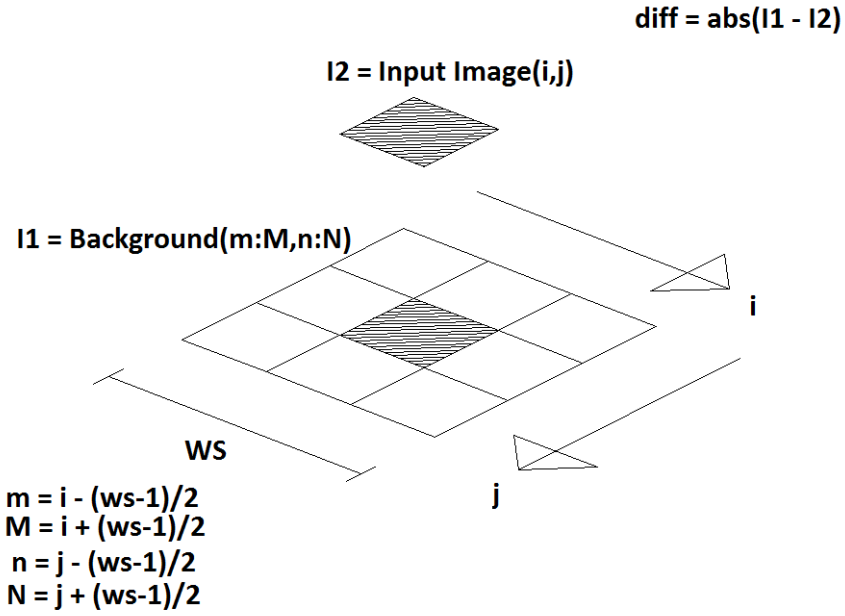

Figure 4: Averaging procedure in flame filtration.

3. Output images I written to the directory "image_tif" in the parent directory. An example of output image is seen in fig. 5.

Figure 5: Input image on left hand side and filtrated image to the right.

4.3 Laminarization Filter

Laminarization filter is doing the same as the flame filter except that *I1* is the image from the previous instance. Large-Scale PIV (Image Correlation Velocimetry (ICV)) is based on tracing

turbulent structures or flamelets instead of particles. The purpose of this function is to remove areas that are laminarized or the velocity is constant from one frame to the next. Statistic computation in PIV processing will give erroneous values if areas where no *tracers* are present are considered.

4.4 Origin

The y-value of origin is defined as the lowest position of the flame. The x-value is found in the mid-point of the flame in height 50 pixels above y-value of origin. The y-value may be elevated with the input value *elevate*, given in pixel unit. Origin is found in the first image of the image sequence. The pitfall in this function is choosing a first image in a sequence where the flame is significantly leaning to any direction or the flame is below the height of the rim of the burner. This is illustrated in fig. 6 where origin is represented by the red dot. The origin is located too far down and towards right on the flame on left hand side. Here, the origin could be elevated by changing the variable *elevate*, but bhe radial position cannot be forced in any direction.

Figure 6: Position of origin on two different flames.

4.5 Transient Flame Length

Transient flame length may be computed in three different ways:

- horizontal direction, seen in fig. 7.
- vertical direction with respect to height, seen in fig. 8.
- vertical direction with respect to diagonal direction or absolute value of the vector from origin to the tip of the flame. This may be used in cross-wind cases (fig. 8).

In fig. 7 and 8 the highest elevated square red dots, in addition to the red line, are representing the limiting area in calculating flame length. The length between the green dots along the green line is the flame length that is computed.

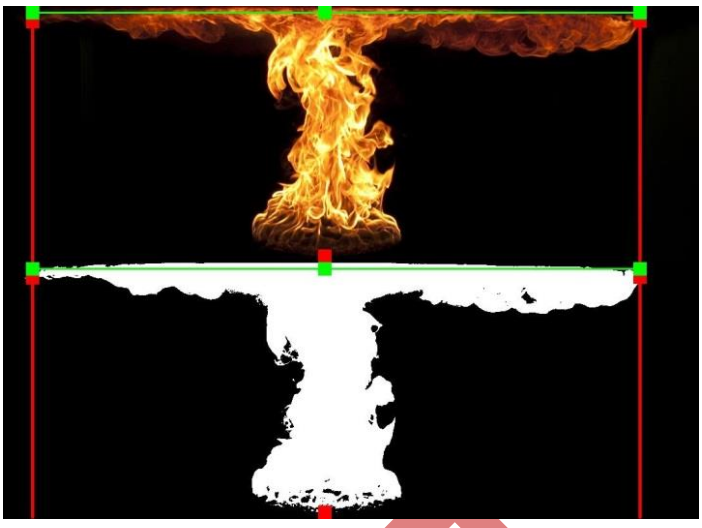

Figure 7: Horizontal flame length under ceiling.

Note that when computing the horizontal flame length the program is only searching in the upper region of the image, equal 15 % of the diameter of the fire. This limitation is chosen so that the flame length is 0, unless the distance from the flame tip to the ceiling is less than 15 % of the fire diameter.

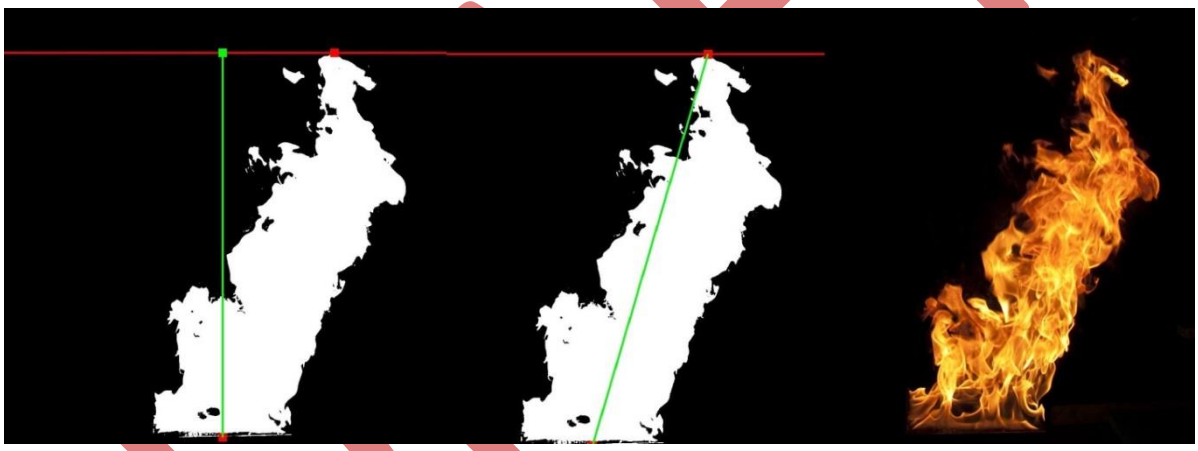

Figure 8: Vertical flame length, with respect to height vs. diagonal length. The green line represents the flame length that is computed.

The flame length is measured by the continuous flame, by definition in fire dynamics. Using functions in the Image Processing toolbox objects in an image can be traced. In this program the continuous flame is defined as the object with the larges area. Search for flame length is still done in the same way. In fig. 9, the flame pocket in top is removed in the image of the on right hand side. The same image is used when searching for the flame length.

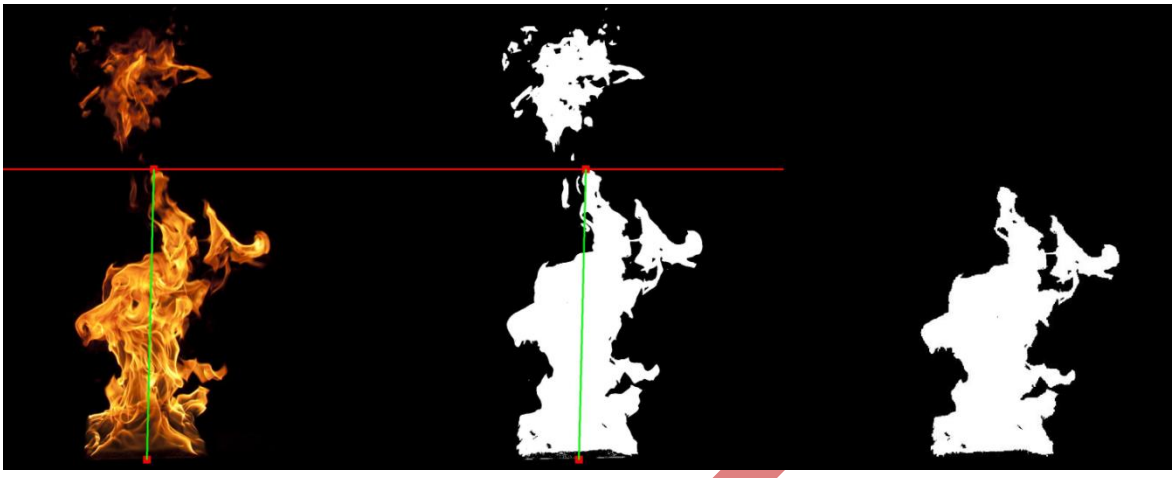

Figure 9: Flame length is defined by the continuous flame, i.e pockets are not accounted for.

4.6 Flame Oscillation Frequency

The flame oscillation function is simply counting the number of times the flame length is crossing the mean flame length and then divided by two. Cycle number one start the first time the flame length is crossing the mean flame length.

4.7 Probability of Flame Presence

A function is computing the probability for the flame being present in a position. This array should be used for computing flame length instead of using the mean transient flame length when the sampling frequency is poor. In fig. 10 an example of a probability plot is presented.

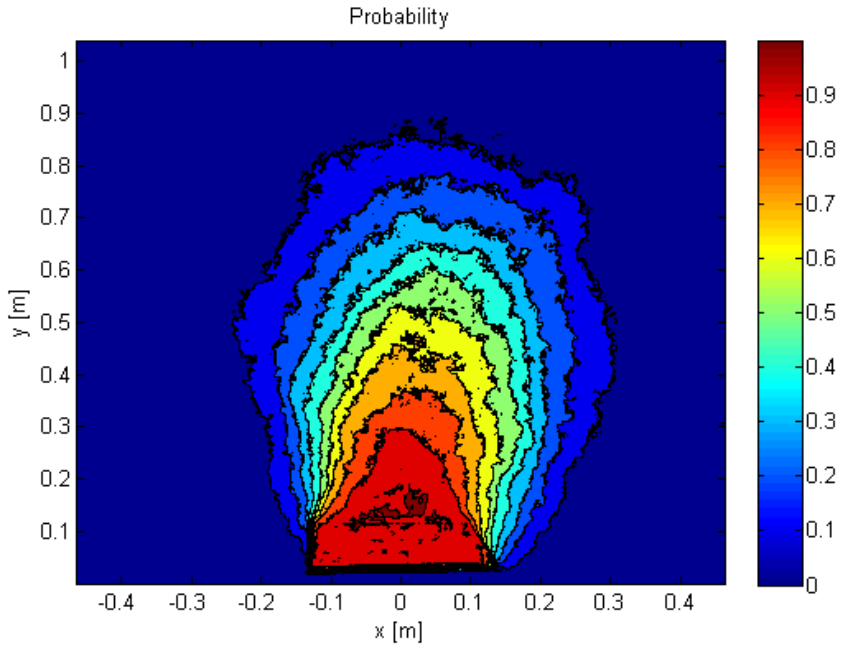

Figure 10: Probability plot of flame presence.

4.8 Probability Flame Length Computation

The probability flame length function is computing the flame length based on the probability array. Input variable *lf_crit* is used as criteria. This function does also support computing the diagonal length.

4.9 Probability Flame Volume Computation

The probability flame volume function is computing the flame volume based on the probability array. This function assumes that the flame is axisymmetric and consists of a disc with thickness 1 pixel and diameter equal the width of the flame at each height. By integrating these volumes with respect to height gives the total volume of the flame.

4.10 Symmetry Check

When doing statistics computations the population, or in this case the number of images, must be large enough. The symmetry function is computing the root mean square across the symmetry axis and is given in percentage. This function should give a number closest possible to 100% in order to give valid results in flame length and flame volume computation based on the probability array.

4.11 Movie Maker

The movie maker function:

- Draw lines in output .jpg images
- Is writing output .jpg images into the directory “images_out_jpg”
- Is writing output AVI movie into the parent director from the .jpg image sequence

Check either the movie, image sequence or both to ensure that input variables are correct.